STUDIES TOWARDS THE PREPARATION OF FUNCTIONALIZED CELLULOSE MICROSPHERES WITH AFFINITIES TOWARDS NEGATIVELY CHARGED BIOMEMBRANES

A THESIS SUBMITTED TO
THE GRADUATE SCHOOL OF NATURAL AND APPLIED SCIENCES
OF
MIDDLE EAST TECHNICAL UNIVERSITY

BY

KAAN DEMİREL

IN PARTIAL FULFILLMENT OF THE REQUIREMENTS
FOR
THE DEGREE OF MASTER OF SCIENCE
IN
CHEMISTRY

JULY 2021

Approval of the thesis

STUDIES TOWARDS THE PREPARATION OF FUNCTIONALIZED CELLULOSE MICROSPHERES WITH AFFINITIES TOWARDS NEGATIVELY CHARGED BIOMEMBRANES

submitted by **KAAN DEMİREL** in partial fulfillment of the requirements for the degree of **Master of Science** i**n Chemistry, Middle East Technical University** by,

Prof. Dr. Halil Kalıpçılar
Dean, Graduate School of **Natural and Applied Sciences** _____

Prof. Dr. Özdemir Doğan
Head of the Department, **Chemistry** _____

Assoc. Prof. Dr. Serhan Türkyılmaz
Supervisor, **Chemistry, METU** _____

Examining Committee Members:

Prof. Dr. Özdemir Doğan
Chemistry, METU _____

Assoc. Prof. Dr. Serhan Türkyılmaz
Chemistry, METU _____

Assoc. Prof. Dr. İrem Erel Göktepe
Chemistry, METU _____

Assist. Prof. Dr. Bilge Baytekin
Chemistry, Bilkent Uni. _____

Assoc. Prof. Dr. Çağdaş Devrim Son
Biology, METU _____

Date: 28.07.2021

I hereby declare that all information in this document has been obtained and presented in accordance with academic rules and ethical conduct. I also declare that, as required by these rules and conduct, I have fully cited and referenced all material and results that are not original to this work.

Name Last Name: Kaan Demirel

Signature:

ABSTRACT

STUDIES TOWARDS THE PREPARATION OF FUNCTIONALIZED CELLULOSE MICROSPHERES WITH AFFINITIES TOWARDS NEGATIVELY CHARGED BIOMEMBRANES

Demirel, Kaan
Master of Science, Chemistry
Supervisor: Assoc. Prof. Dr. Serhan Türkyılmaz

July 2021, 117 pages

Cellulose microspheres (CMs), generally with diameters in the 10-1000 μm range, have been used as stationary phases in chromatography, substrates for ion exchange applications, supports for protein immobilization and solid-phase synthesis, and drug loading and release materials. Furthermore, cellulose and CMs are biocompatible and have been used in many biomedical applications as varied as the dressing of wounds and blood filtration. Targeting of bacterial cells can be achieved using antibodies, antibody fragments, peptides, polycationic dendrimers, antibiotics such as vancomycin, and certain metal complexes. Zinc (II) bisdipicolylamine (Zn_2BDPA) complexes are capable of selectively binding to negatively charged phosphate amphiphiles displayed by bacterial cells. Blood is normally sterile and the presence of bacteria in blood is a condition known as bacteremia. Bacteremia can be caused by burns, injuries, local infections, surgical procedures, and the use of catheters or needles. If undetected and untreated, the immune response to bacteremia can result in sepsis, septic shock, and multiple organ

failure. Septic shock and multiple organ failure as a result of hospital-acquired bacteremia is a leading cause of death in intensive care units.

This study aimed to develop Zn_2BDPA-derivatized CMs as selective sorbents capable of binding to negatively charged liposomes and bacterial cells, with an ultimate goal of obtaining functional materials for the treatment of bacteremia through extracorporeal whole blood filtration. To this end, the preparation of CMs through the thermal regeneration of cellulose from water-in-oil emulsions of viscose has been investigated and the effect of various factors on particle size have been determined. Underivatized (native) CMs were then activated to display aldehyde, amino, carboxylic acid, cyano, and epoxy functionalities. Amine and carboxylic acid bearing BDPA ligands were then coupled with some of these activated CMs. Formation of BDPA-CM conjugates was confirmed using several analytical techniques. Zn_2BDPA complex functionalized CMs were then shown to bind to negatively charged fluorescent liposomes and green fluorescent protein (GFP) expressing bacterial cells through fluorescence spectroscopic measurements and/or fluorescence microscopy. Further development of these materials is likely to lead to effective sorbents for bacterial cells which would have applications in the diagnosis and treatment of bacteremia and in the isolation and preconcentration of bacterial cells from a variety of liquid samples.

Keywords: Cellulose, Cellulose Microspheres, Bacteremia, Bacterial Targeting

ÖZ

NEGATİF YÜKLÜ BİYOMEMBRANLARA AFİNİTESİ OLAN FONKSİYONELLEŞTİRİLMİŞ SELÜLOZ MİKROKÜRELERİN HAZIRLANMASINA YÖNELİK ÇALIŞMALAR

Demirel, Kaan
Yüksek Lisans, Kimya
Tez Yöneticisi: Dr. Öğr. Üyesi Serhan Türkyılmaz

Temmuz 2021, 117 sayfa

Selüloz mikroküreleri (CMler, çap = 10-1000 μm) birçok uygulaması vardır. Selüloz ve CMlerin biyouyumlu olmasının bir sonucu olarak, bu uygulamalar, yaraların pansumanı ve kan filtrasyonu gibi çeşitli biyomedikal uygulamaları da içerir. Bakteri hücrelerinin hedeflenmesi, belirli metal kompleksleri de dahil olmak üzere çeşitli yöntemler kullanılarak gerçekleştirilebilir. Çinko(II) bisdipikolilamin (Zn_2BDPA) kompleksleri, bakteriler tarafından gösterilen negatif yüklü fosfat amfifillerine seçici olarak bağlanma yeteneğine sahiptir. Kan normalde sterildir ve kanda bakteri bulunması bakteriyemi olarak bilinen bir durumdur. Bakteriyemi yanıklar, yaralanmalar, lokal enfeksiyonlar, cerrahi prosedürler ve kateter veya iğne kullanımından kaynaklanabilir. Tespit edilmez ve tedavi edilmezse bakteriyemiye karşı bağışıklık yanıtı sepsis, septik şok ve çoklu organ yetmezliği ile sonuçlanabilir ve hastane kaynaklı bakteriyemi yoğun bakım ünitelerinde önde gelen ölüm nedenidir. Bu çalışma, vücüt dışı tam kan filtrasyonu yoluyla bakteriyemi tedavisi için fonksiyonel materyaller elde etme nihai hedefi ile negatif yüklü lipozomlara ve bakteri hücrelerine bağlanabilen seçici sorbentler olarak Zn_2BDPA

kompleksleriyle türevli CMleri geliştirmeyi amaçladı. Bu amaçla, viskozun yağ-içinde-su (W-O) emülsiyonlarından selülozun termal rejenerasyonu yoluyla CMlerin hazırlanması araştırılmış ve çeşitli faktörlerin parçacık boyutu üzerindeki etkisi belirlenmiştir. Doğal CMler daha sonra çeşitli fonksiyonel gruplarına sahip olacak şekilde aktive edildi. Amin ve karboksilik asit taşıyan BDPA ligandları daha sonra bu aktive edilmiş CMlerin bazıları ile birleştirildi. BDPA-CM konjugatlarının oluşumu birkaç analitik teknik kullanılarak doğrulandı. Zn_2BDPA kompleksi ile işlevselleştirilmiş CMlerin negatif yüklü floresan lipozomlara ve yeşil floresan protein (GFP) ifade eden bakteriyel hücrelere bağlanabildikleri floresans spektroskopisi ve/veya floresans mikroskopisi ile gösterildi.

Anahtar Kelimeler: Selüloz, Selüloz Mikroküre, Bakteriyel Hedefleme

To my family and my friends…

ACKNOWLEDGMENTS

I would like to express my respect and gratitude to Assoc. Prof. Dr. Serhan Türkyılmaz for his guidance and encouragement. He always showed me patience and endless support. I would also like to thank STRG members for their friendship and support.

I would like to thank Prof. Dr. Ali Çırpan, Prof. Dr. Akın Akdağ, Assist. Prof. Dr. Çağatay Dengiz, Prof. Dr. Gülay Ertaş and Assoc. Prof. Dr. İrem Erel Göktepe for their guidance and support.

I would like to thank Şafak Tekir and Oğuzhan Karakurt for their endless support and guidance in my difficult times. We have been in an adamantine friendship since 2015 and I have no doubt that this wonderful friendship will continue.

I would like to thank Gizem Atakan Alkan, Çağdaş Alkan, Nazım Önder Orhan, Sinem Ünlü for the love and support they have shown to me. They are my older brother and older sister, although we are not related by blood.

I would like to thank Doğan Akbulut and Ozan Yılmaz, who are the most enjoyable lab friends to work with, for their friendship and every moment we spend in the lab. Whenever I needed help, they always did their best to help me.

I would like to thank AGM members, Tolgahan Özdemir, Mehmet İkbal Dündar, Mehmet Fatih Bozkurt, Çağrı Can Torun, Atahan Çelik, Alper Kıray, Onur Kıray, Hasan Oğuz Candan, İlkay Karagedik and Burak Albayrak, for the friendship they have shown and for being there during my bad times.

I would like to thank my childhood friends Nihat Efe İşman, Ahmet Utku İşman, Tunahan Çakır, Yılmaz Berkay Demir, Mehmet Fahri Ceyhan, Gönenç Can Altun, Burak Çakıroğlu, Mete Kutay Kutlu, Berat Özbağ, Görkem Ülgen, Yusuf Kenan Bilhan, Kemal Burak Talas, Kuthan Ulusoy, Kemal Canpolat, Batu Elkoca and Umut Sadıkoğlu for the wonderful friendship and good memories we had.

I would like to thank Özgür İlker, Nazlı Ecem Coşkuntürk and Mazlum Usta for their friendship, wonderful conversations, and interesting memories.

I would like to thank Furkan Melih Günay, Hüseyin Kemal Öz, Mehmet Burak Uzun, Ali Ozan Karabüber, İlkay Yıldırım and Cem Maraşlıoğlu for their friendship and good memories.

I would like to thank research assistants Volkan Dolgun and Mehmet Seçkin Kesici for their friendship, interesting memories and being there during my bad times.

I would like to thank DRG members Kübra Erden, Flora Mammadova and Başak Karagöllü for friendship and patience.

I would like to thank Mehmet Can Hüneröz and Emre Koç for their friendship and the good memories. Special thanks to Mehmet Can Hüneröz for the special and beautiful conversations in the arbour in front of Mehmet's house.

I would like to express my gratitude to Şükrü Sinan Aydoğdu, Erdem Besler, Ertürk Besler, Barış Aktaş for the holidays we went and the beautiful memories we had. They are special for me. They always made me feel their support and friendship.

I would like to thank Sıla Polat for the beautiful memories we have had recently and for the wonderful memories we will undoubtedly live after this time. In this short time, she always made me feel her support. She shared my proud moments with me with great joy.

I would like to express my special thanks to my wonderful father and my wonderful mother for all the moral and material support they have shown me. I love these beautiful people who made me become KD.

This study was funded by The Scientific and Technological Research Council of Turkey (TUBITAK) with project number 118Z442. I would also like to thank METU Central Laboratory for HRMS, Mastersizer, SEM, CHNS analysis.

TABLE OF CONTENTS

LIST OF TABLES

LIST OF FIGURES

LIST OF SCHEMES

LIST OF ABBREVIATIONS

ABBREVIATIONS

CM	cellulose microspheres
BDPA	bisdipicolylamine
HLB	hydrophilic-lipophilic balance
HRMS	high resolution mass spectrometry
FTIR	Fourier transform infrared
SEM	scanning electron microscopy
CHNS	elemental analysis
CuEn	bis(ethylenediamine)copper(II) hydroxide
PSTF	Perloza ST Fine
PSTM	Perloza ST Medium
PSTC	Perloza ST Coarse
SEC	size exclusion chromatography
W/O	water-in-oil emulsion

LIST OF SYMBOLS

SYMBOLS

J	coupling constant
δ	chemical shift
η_{rel}	relative viscosity
ν	frequency

CHAPTER 1

INTRODUCTION

Bacteremia is defined presence of viable bacteria in blood. As blood is normally sterile, bacteremia is an abnormality. Bacteremia can result from injury, local infections, surgical procedures, and the use of catheters and needles. Bacteremia causes the spread of infection from one point in the body to other parts. Sepsis, septic shock, and multiple organ failure may be observed when the immune system responds to the presence of bacteria in the bloodstream. Septic shock and multiple organ failure may result in death. The standard method for diagnosing bacteremia and determining the appropriate antibiotic regimen is blood culture. Blood culture takes a relatively long time (2-3 days), which is negative in terms of patient morbidity and mortality. As an alternative to blood culture, various methods have been developed for molecular identification of bacterial cells in a shorter time. Polymerase chain reaction (PCR), which is one of these methods, can be used for the rapid identification of the pathogen by amplification of genetic material, but this method can only be used effectively when bacterial cells are separated from blood components. Various approaches have been developed to separate and concentrate bacterial cells from blood and blood components. The additional advantage of such separation and/or concentration methods is that, if scalable, they could allow for the filtration of whole blood outside the body (extracorporeal blood filtration) for bacteremia treatment. Complementary antibiotic therapy developed with extracorporeal whole blood filtration can be a powerful approach for bacteremia treatment.[1]

1.1 General Properties of Bacteria

Bacteria are prokaryotic microorganisms that can survive in harsh conditions and adapt to different environments. They are well-suited to adapt and thrive in environments as varied as the bodies of organisms, the polar regions, and even radioactive waste. They can be found in the soil, air, and aquatic environments. Cell morphologies are a varied: Rods and cocci being very common, whereas others shapes, such as spiral, budding, and filamentous, are less common. Apart from bacteria involved in the carbon and nitrogen cycle, some bacteria species are capable of photosynthesis and some produce vitamin K in the human intestine. Some bacteria species are frequently used in medicine, agriculture, environmental processes, and various industries. However, some bacteria, called pathogenic bacteria, cause serious diseases like tuberculosis, cholera, or bacteremia.[2]

1.1.1 Differences Between Bacterial and Mammalian Cells

Bacterial cells are much simpler than mammalian cells. Unlike mammalian cells, bacterial cells do not contain a membrane-bound nucleus and internal organelles like mitochondria or endoplasmic reticulum. Interior components of bacterial cells are ribosomes, mesosomes, endospores, chromosomes, or nucleoids, including genetic material. Additional plasmid DNA is also present in bacteria. The cell walls outside of the cell membranes and the outer membranes surrounding them give resistance and shape to bacterial cells. Mammalian cells have organelles surrounded by a phospholipid bilayer and true nuclei where genetic material is stored but do not have a cell wall contributing to their cellular integrity.[3]

When attempting to target pathogenic bacterial cells in the presence of mammalian cells focusing on the differences between mammalian cells and bacterial cells can be beneficial. One of the differences between these two cells is that the cell membranes of bacteria are negatively charged while the cell membranes of healthy mammalian cells are neutral.

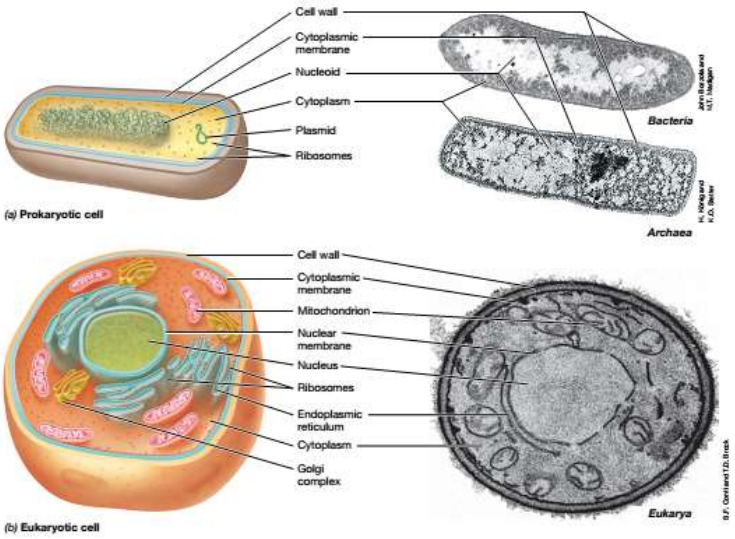

Figure 1.1. Comparison of the structures of prokaryotic and eukaryotic cells.[2]

1.2 Bacterial Targeting Groups

Antibacterial peptides and antibodies,[4,87,88,89] glycodendrimers,[90] antibiotics,[91] and polycationic compounds and polymers[92,93] are some examples of targeting groups that selectively bind to bacteria. While antibodies have remarkable affinities and selectivities towards bacterial cells, they also have significant drawbacks.[4] The size of antibodies is not particularly conducive to their penetration through human tissue and, being proteins, they are liable to degradation by protease enzymes. Certain cationic metal complexes, in particular zinc(II)-bisdipicolylamine complexes, can be used to target negatively charged phosphorylated biomolecules including negatively-charged biomembranes and some of them are suitable for applications in aqueous media.[94,95]

1.2.1 Zinc(II) Bisdipicolyamine (Zn_2BDPA) Complexes

Any bacterial targeting group to be used for bacterial filtration must have a broad-spectrum, that is be capable of binding to many different strains of bacteria, because bacteremia can be caused by many different types of bacteria. Zn_2BDPA complexes are synthetic receptors that bind with high selectivity and somewhat low affinity to cell membranes (necrotic and apoptotic mammalian cells and bacterial cells) that contain negatively charged phosphate amphiphiles (phosphatidylglycerol, phosphatidylserine, lipid A, lipoteichoic acid, and so on) on their outer surfaces (Figure 1.1).[5,6,7,8] Zn_2BDPA complexes have low cytotoxicity, positive pharmacokinetics, and good *in vivo* stability. These complexes are completely synthetic and it is easier to prepare their functional derivatives (with drugs, lipids or peptides, fluorescent dyes, chelating groups for nuclear imaging, and so on) than it is with protein or peptide-based targeting groups. Zn_2BDPA complexes have the potential to be compatible with universal antibacterial approaches because most known bacterial pathogens have negatively charged phosphate amphiphiles in their cell membranes and walls to which these complexes can bind.

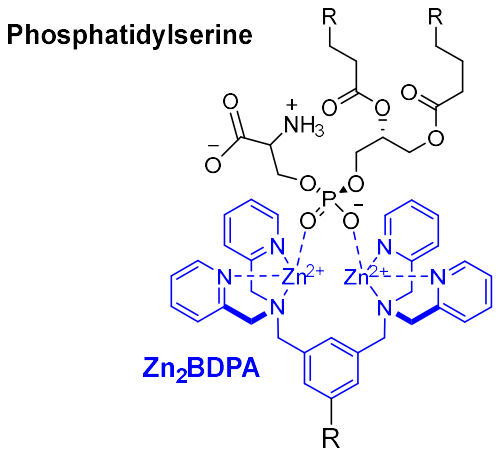

Figure 1.2. Interaction between a Zn_2BDPA complex and the negatively charged phospholipid phosphatidylserine.

Zinc(II) bisdipicolylamine complexes are synthetic receptors suitable for applications where removal of bacterial cells from blood is required. The interaction between Zn_2BDPA complexes and bacterial membranes is based on electrostatics and complex formation between the zinc nuclei and phosphate oxygens of negatively charged phosphate amphiphiles. While certain components of blood (e.g. red blood cells and platelets) have negative zeta potentials in the -10 mV range,[96] the zeta potentials of bacterial cells are significantly larger, being in the -40 mV range.[97] Selective binding of bacterial cells by Zn_2BDPA over blood components can be expected not only based on this significant zeta potential difference, but also based on the fact that the negative charge of bacterial cells is due to the presence of significant amounts of exposed negatively charged amphiphiles on bacterial cell membranes and walls, whereas, for example for red blood cells, the negative membrane charge has its origin in the presence of sialic acid moieties.[98] Compatibility of Zn_2BDPA derivatized systems for *in vivo* applications has been demonstrated by the optical and nuclear imaging of bacterial pathogens in live mice.[5,7] Furthermore, it has been demonstrated that magnetic nanoparticles derivatized with ZnDPA ligands coupled with a microfluidic device can be used to separate bacterial cells from blood on a small scale.[9]

1.3 Bacteremia

Bacteremia is the presence of bacteria in the bloodstream, which can be temporary, intermittent, or continuous, and cause some important health consequences. Fever caused by the passage of bacteria or bacterial toxins into the blood is the name of the clinical picture that progresses with chills, loss of appetite, nausea, vomiting, troubled or fast breathing, fast heart rate, severe sleepiness, and unconsciousness. As a synonym the term septicemia is also used. Bacteria can enter the bloodstream as a serious complication during infection (such as pneumonia or meningitis), during surgery (especially the gastrointestinal tract), or due to foreign

bodies entering the arteries or veins (drug use). Temporary bacteremia can occur after dental procedures or brushing teeth.

Bacteremia can cause some important health consequences. The immune response to bacteria can cause sepsis and septic shock with high mortality. Sepsis is dysregulated response of the immune system to infection and the major cause of sepsis is bacterial infections. Septic shock is another malignant condition that occurs when blood pressure falls below a certain level because of an infection. Bacteria can also spread through the blood to other parts of the body (called hematogenous spread), causing infections. Bacteremia treatment is done with antibiotics and in high-risk cases, antibiotic prophylaxis can be used to prevent it.[10]

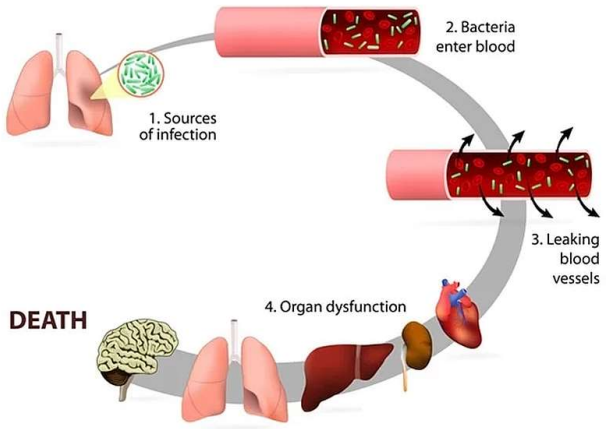

Figure 1.3. Schematic summary of bacteremia and potential consequences.[11]

1.3.1 Treatment of Bacteremia

Many different kinds of bacteria may cause bacteremia and the only known treatment is the use of broad-spectrum antibiotics. An efficient and certain treatment of bacteremia has not been developed yet. Extracorporeal whole blood filtration using bacterial targeting group (such as Zn_2BDPA metal-ligand complexes) derivatized cellulose microspheres as supporting material could be used as a treatment for this potentially fatal disease.

1.3.1.1 Extracorporeal Whole Blood Filtration

Various approaches are being developed to isolate and concentrate bacterial cells from blood and blood components to facilitate the diagnosis of bacteremia.[12] Although the separation of bacterial cells from the blood with magnetic particles derivatized with suitable bacterial binding groups is prominent among these methods, filtration methods also provide bacterial separation on a diagnostic scale.[13,14,15,16,17] In addition to filtration methods, if a scalable technology is used, they can also allow the removal of pathogens from blood by means of extracorporeal whole blood filtration for the treatment of bacteremia. Complementary antibiotic therapy coupled with extracorporeal blood filtration could be a strong approach to treat bacteremia. Cellulose microspheres of certain sizes derivatized with Zn_2BDPA complexes could potentially be used to isolate bacteria from the blood through filtration with high yields. The sizes of particles suitable for extracorporeal whole blood filtration need to be in the 50-250 μm range. Smaller particle sizes would result in blockage of the sorbent column by blood cells and also by formation of excessive back-pressure that would be incompatible with human vasculature. Use of larger particle sizes would end up with a sorbent that does not have a sufficient total surface area suitable for efficient adsorption of pathogenic bacterial cells.

1.4 Cellulose

The cell walls of green plants, most of the algae, and oomycetes contain cellulose. The high cellulose content of cotton makes it an important material to obtain cellulose. Cellulose, a natural D-glucose polymer, is a material with high biocompatibility, low toxicity, and easy to reformulate as a bead, fiber, membrane, or microsphere.[19] There are many approaches especially for the preparation, characterization, and derivatization of cellulose-based microspheres.[18] Cellulose is used as a support material in blood filtration strategies that are being developed for the treatment of many diseases. This approach can be compared to affinity

chromatography: Cellulose microspheres are derivatized with receptors to bind the substrates (proteins, DNA fragments, toxins, and so on) that are desired to be separated from the blood, then whole blood or just the plasma separated by a membrane is filtered from these functional cellulose microspheres and purified from unwanted compounds. Examples of substrates that are separated from blood through functional cellulose microspheres are anti-DNA antibodies, human tumor necrosis factor, and lipopolysaccharide.[20,21]

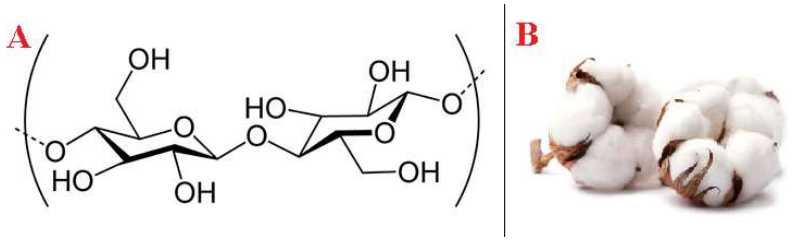

Figure 1.4. Molecular structure of cellulose (a) and image of cotton (b).

1.5 Cellulose Microspheres

Cellulose microspheres have often named as beads, pellets, cellulose gels, pearl cellulose, or beaded cellulose. Cellulose microspheres (CMs, diameters 10-1000 μm) have been used as stationary phases in chromatography, substrates for ion exchange applications, supports for protein immobilization and solid-phase synthesis, and drug loading and release materials.[18] Furthermore CMs are biocompatible and have been used in many biomedical applications as varied as blood filtration[19,20] and the dressing of wounds. They can be defined as spherical particles which are prepared by the dissolution, shaping, and regeneration of cellulose or its derivatives. They are highly comprised of cellulose and shaped by the hydrogen bonding network.

Figure 1.5. Different sizes of cellulose microspheres (a) and commercial cellulose microspheres (b, c).[18]

1.5.1 Shaping of Cellulose into Microspheres

Many starting polysaccharide, solvent and regeneration methods can be applied to obtain cellulose microspheres, but their common feature is the use of the dropping or dispersion techniques.[18]

1.5.1.1 Dropping Technique

Spheres can be formed by dropping the polysaccharide solution as droplets into the nonsolvent coagulation bath. In this method, a certain time is required for the droplets to become spherical. In addition, optimization of the ejection speed, falling height, and the viscosity of the solution play an important role for this technique.[23] On the other hand, a set of devices can also be used to obtain certain size spheres, especially for large batches. For example, spinning disc atomization and spinning drop atomization.[24]

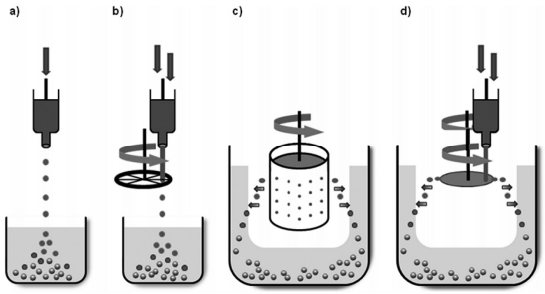

Figure 1.6. Schematic presentation of different ways for the preparation of cellulose microspheres by dropping technique. Dropping (a), jet cutting (b), spinning drop atomization (c), spinning disc atomization (d).[18]

technique	starting material[a]	solvent[b]	additives	dispersion medium	solidification	size[c]
dropping	cellulose	DMA/LiCl			coagulation in water/alcohol	~0.5 mm
		ionic liquids	chitosan		coagulation in water	n.a.
		ionic liquids	lipase + polysaccharides		coagulation in water	~2 mm
		$NaOH_{aq}$			coagulation in water	~1 mm
		$NaOH/urea_{aq}$			coagulation in $HNO_{3\ aq}$	~2 mm
		$NaOH/urea_{aq}$	Fe_2O_3-nanoparticles, active carbon		coagulation in water	~2 mm
		N-ethylpyridinium chloride/dipolar aprotic cosolvent			coagulation in water	~1 mm
		NMMO			solidification at 10 °C, washing with water	~2 mm
		NMMO	chitosan		coagulation in water	n.a.
	CA	acetone/DMSO			coagulation in water, saponification with $NaOH_{aq}$	~1 mm
		DMSO			coagulation in HCl_{aq}, saponification with $NaOH_{aq}$	n.a.
	CXA	$NaOH_{aq}$			coagulation in water, solidification at 90 °C	~2 mm
		$NaOH_{aq}$	$CaCO_3$		coagulation in HCl_{aq}	~4 mm
(jet cutting)	cellulose	ionic liquids			coagulation in water	n.a.
		NMMO			solidification at 10 °C, washing with water/DMSO	50−1000 μm
	CC	$NaOH_{aq}$			coagulation in $H_2SO_{4\ aq}$	~0.5 mm
(spinning drop atomization)	cellulose	$NaOH_{aq}$			coagulation in $H_2SO_{4\ aq}$	~0.5 mm
	cellulose	$NaOH/urea/sulfourea_{aq}$	azodicarbonamide		coagulation in HCl_{aq}	~300 μm
	CXA	$NaOH_{aq}$			coagulation in HCl_{aq}	0.5−1 mm
		$NaOH_{aq}$			coagulation in $H_2SO_{4\ aq}$	~0.5 mm
(spraying)	CA	acetone/organic solvent mixtures			coagulation in water, saponification	~0.5 mm

Figure 1.7. Some examples of cellulose substrates and solvent systems for their dissolution and conditions for regeneration of cellulose using various dropping techniques (CA, cellulose acetate; CC, cellulose carbamate; CXA, cellulose xanthate; NMMO, N-methylmorpholine N-oxide monohydrate).[18]

1.5.1.2 Dispersion Technique

This technique can be described as the stabilization of spherical emulsions which are formed with the dispersion of the cellulose or cellulose derivative solution in a non-miscible solvent under high rotational speed with the help of surfactants. The diameter of the microspheres in the dispersion is determined by the mixing

speed, the type and amount of surfactant, the ratio of hydrophobic solvent to hydrophilic solvent, the dispersion medium, and the viscosity of the cellulose solution.[25,26]

Figure 1.8. Dispersion technique for the preparation of cellulose microspheres.[18]

technique	starting material[a]	solvent[b]	additives	dispersion medium	solidification	size[c]
dispersion	cellulose	caden		benzene	coagulation with acetic $acid_{aq}$	~100 μm
		$Ca(SCN)_{2aq}$		dichlorobenzene	coagulation with methanol	n.a.
		cuoxam		benzene	coagulation with benzoic $acid_{aq}$	~100 μm
		cuoxam		toluene/oil	coagulation with benzoic $acid_{aq}$	~50 μm
		Fe-(II)-tartrate		benzene	coagulation with acetic $acid_{aq}$	~100 μm
		ionic liquids		cyclohexane/oil	coagulation with water	~10 μm
		ionic liquids	tungsten carbide	oil	coagulation with ethanol	100–300 μm
		ionic liquids	bovine serum albumin	poly(propylene glycol)	solidification at 40 °C, washing with alcohol/water	250–1000 μm
		ionic liquids	chitosan, Fe_3O_4 -particles	oil	solidification at 40 °C and by coagulation with ethanol	~200 μm
		$NaOH/urea_{aq}$		oil	coagulation with HCl_{aq}	10–1000 μm
		$NaOH/urea_{aq}$	Fe_3O_4-nanoparticles	oil	coagulation with HCl_{aq}	~10 μm
		$NaOH/urea_{aq}$	Fe_2O_3-nanoparticles	oil	coagulation with HCl_{aq}	~200 μm
		$NaOH/thiourea_{aq}$	konjac glucomannan		coagulation with $CaCl_{2\ aq}$, and HCl_{aq}	~100 μm
		NMMO		oil	solidification at 35 °C, washing with water/alcohol	10–1000 μm
		NMMO		oil	solidification at low temperature	~100 μm
		NMMO	tungsten carbide	oil	solidification at 10 °C, washing with water/alcohol	75–300 μm
	CA	CH_2Cl_2		water	solvent evaporation, saponification with $NaOH_{aq}$	~100 μm
		ethylacetate/methanol mixtures		water	solvent evaporation, saponification with $NaOH_{aq}$	1–10 μm
	CAB	CH_2Cl_2	hydroxyalkyl cellulose	water	coagulation with acetic acid	~100 μm
	CC	$NaOH_{aq}$		chlorobenzene	solidification at 90 °C or coagulation with ethanol/ acid mixture	n.a.
	CXA	$NaOH_{aq}$		benzene	coagulation with acetic acid	~100 μm
		$NaOH_{aq}$		ethylene dichloride	cross-linking and subsequent coagulation with acetic acid	~50 μm
		$NaOH_{aq}$		chlorobenzene	solidification at 90 °C	10–300 μm
		$NaOH_{aq}$		chlorobenzene/ CCl_4	solidification at 90 °C	~100 μm
		$NaOH_{aq}$	ferrite powder	oil	solidification at 90 °C	20–2000 μm
		$NaOH_{aq}$	$CaCO_3$	chlorobenzene	solidification at 90 °C	n.a.
		$NaOH_{aq}$	$CaCO_3$	oil	solidification at 90 °C	~100 μm
		$NaOH_{aq}$	FeOOH	chlorobenzene/oil	solidification at 90 °C	~100 μm
		$NaOH_{aq}$	Ni powder	chlorobenzene/oil	solidification at 95 °C	~100 μm
		$NaOH_{aq}$	starch, tungsten carbid	chlorobenzene/oil	solidification at 95 °C	50–250 μm
		$NaOH_{aq}$	steel powder	oil	solidification at 90 °C	60–180 μm
		$NaOH_{aq}$	TiO_2	chlorobenzene/oil	solidification at 95 °C	n.a.
	TMSC	hexane or CH_2Cl_2		aqueous gelatin solutions	solvent evaporation, desilylation with HCl_{aq}	100–300 μm

Figure 1.9. Solvent systems used for dissolving and regenerating cellulose using the dispersion technique (CA, cellulose acetate; CAB, cellulose acetate butyrate; CC, cellulose carbamate; CXA, cellulose xanthate; TMSC, trimethylsilyl cellulose; Caden, cadmium tris(ethylenediamine) hydroxide; cuoxam, cuprammonium hydroxide; NMMO, N-methylmorpholine N-oxide monohydrate).[18]

1.6 Regeneration and Dissolution of Cellulose

1.6.1 Dissolution of Cellulose

It is well known that cellulose does not dissolve in water or common organic solvents. For this reason, various methods are used to dissolve cellulose. Generally, the following three methods are used.[27] The first of these is the non-derivatizing solvent system. In this method, cellulose dissolves with physical interactions. There is no chemical conversion of the hydroxyl groups. In contrast, in the derivatizing solvent system method, cellulose is temporarily transformed into a cellulose derivative by chemical conversion. Later, the cellulose derivative, which is shaped like spheres, returns to its original state through water or pH change. Another option is to dissolve the stable cellulose derivatives in commonly known organic solvents. However, in this method, unlike the previous one, a chemical transformation is required in the last step to obtain cellulose spheres.[18]

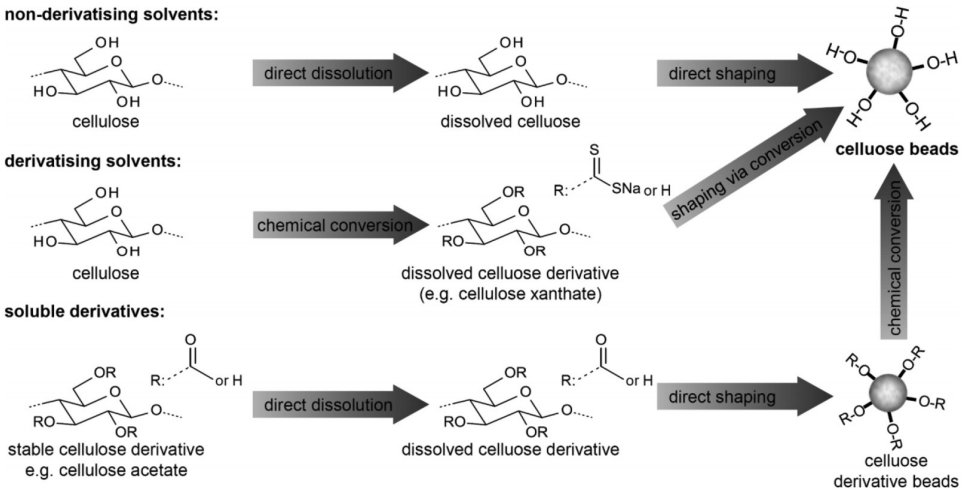

Figure 1.10. Types of cellulose dissolution methods.[18]

1.6.1.1 Derivatizing Cellulose Solvent System

Viscose process can be cited as the most known method for this system. It is the dissolution of cellulose xanthate in NaOH solution, which is formed after alkalization, aging and CS_2 treatment, respectively.[28] Xanthate cannot be separated directly from the reaction solution. Xanthate is detached from the cellulose by acid treatment or increasing the temperature to 95ºC after the desired shape is given to the cellulose. Although there are environmental concerns, the viscose method still plays an important role in obtaining commercial products of cellulose. Nowadays, it is possible to see cellulose spheres prepared by the viscose method commercially (Figure 1.5).

1.6.1.2 Non-derivatizing Cellulose Solvent System

In this system, cellulose is temporarily converted into soluble derivatives and no chemical conversion takes place during this process. Although it gives good results, it requires a lot of effort and produces as much chemical waste. There are many conventionally known non-derivatizing solvent systems to dissolve cellulose. However, the application of these solvents has been strictly limited because of the use of heavy metals.[29] On the other hand, cellulose dissolves in DMA (*N,N*-dimethylacetamide) containing LiCl. With this solvent system, cellulose films, fibers, and highly porous materials can be obtained. In addition, recently, another noteworthy solvent system has been developed.[30] This solvent system, which is obtained with the combination of NaOH solution, contains side substances that prevent gelation. This system has high potential because it contains inexpensive, environmental, and non-toxic compounds. However, if we interpret it thermodynamically, this solvent system is poor to dissolve cellulose. The degree of polymerization and maximum cellulose concentration play a limiting role for this solvent system.

1.6.1.3 Stable Cellulose Derivatives

The most known of the stable cellulose derivatives used to prepare cellulose microspheres is cellulose acetate (CA). Unlike the derivatizing solvent system, CA is a stable cellulose derivative, so it can be isolated directly after preparation of the spheres. In contrast to the xanthate and carbamate groups, the acetyl portion is not cleaved during the regeneration process. CA precipitates as a result of the replacement of organic solvent system with a non-derivatizing solvent system (e.g., water). This means that an additional step is required to convert cellulose-derived spheres into cellulose spheres.[31]

1.7 Stability of Emulsions[32]

There are many water-in-oil (W/O) emulsions products used in the pharmaceutical, cosmetic and food industries. These emulsions show different stability mechanisms compared to oil-in-water emulsions which can be stabilized by electrostatic and steric repulsion. In this case, water-in-oil emulsions are expected to be stable only with steric forces because they have low electrical conductivity in the continuous phase. In fact, many W/O emulsion products exist in solid or semi-solid state. For example, products such as oil and margarine have been stabilized with fat crystals. The reason is that to prevent the sedimentation of the water droplets caused by the three-dimensional network.

However, fluid W/O emulsions generally show low stability. Because the high mobility of water droplets causes sedimentation, coagulation, and coalescence. Most studies generally focus on O/W emulsions, but there are also few studies on W/O emulsions. In order to better understand the relationship between water, oil and emulsifier, it is necessary to focus on the factors affecting fluid W/O emulsion stability.

1.7.1 Hydrophilic-Lipophilic Balance (HLB)[33]

In order to save time in emulsifier selection, in the late 1940s, ICI introduced its systematic scheme for a small number of emulsifiers suitable for any application. It is called the HLB system. The letters of HLB mean "Hydrophilic-Lipophilic Balance". In short, it allows assigning a number to an ingredient or ingredient combination which are desired to emulsify, and then accordingly select an emulsifier or emulsifier mixture with the same number. Although the basic principle of the system depends on this, it is not easy to apply. However, the HLB system is a completely useful guide. A number of questions need to be answered before using the HLB system. What type of emulsion is desired? Is it W/O or O/W? What is the purpose of use? To store or to use? How does it behave in alkaline environments or environments with salt? Do you need it to be non-toxic? These questions are helpful in selecting HLB systems and in eliminating certain types of emulsifiers immediately.

1.7.1.1 HLB Numbers of Emulsifiers[33]

In the HLB system, each emulsifier has its own numerical values, and this is called its HLB. All emulsifiers contain both hydrophilic and lipophilic groups. The HLB value of the emulsifier means the balance of size and strength between hydrophilic and lipophilic groups. If the lipophilic character of an emulsifier is dominant, the HLB value is less than 9.0, but if the hydrophilic character is dominant, the HLB value is greater than 11.0. Emulsifiers with an HLB value between 9-11 are considered as intermediate. If a mixture of two or more emulsifiers is used, it is easy to calculate the HLB value of this mixture. For example, the HLB value of an emulsifier system using 70% TWEEN 80 (HLB = 15.0) and 30% SPAN 80 (HLB = 4.3) can be calculated as follows:

$$HLB_{mixture} = \frac{(HLB_{Tween\,80} \times \%Tween\,80) + (HLB_{Span\,80} \times \%Span\,80)}{100} = 11.8$$

The HLB values obtained as a result of the calculations show which emulsion types the emulsifiers are suitable whether W/O emulsions or O/W emulsions. These HLB values, on the other hand, increase the emulsification efficiency.

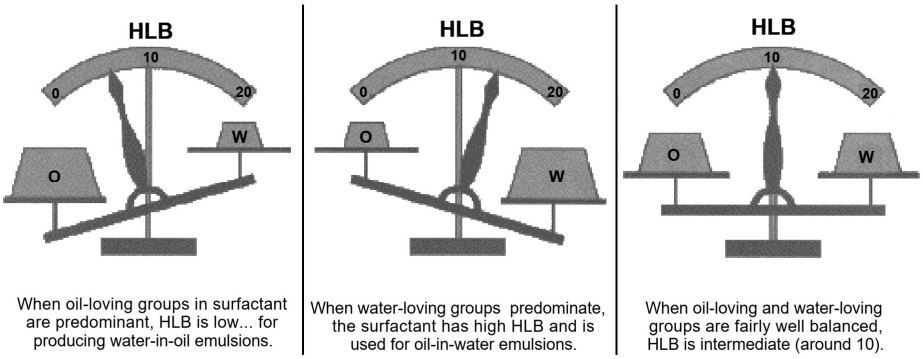

Figure 1.11. The relationship between HLB values and emulsions.[33]

1.7.1.2 Relationship Between Solubility and HLB Value[33]

The HLB value of an emulsifier is related to its solubility. If an emulsifier has a low HLB, it tends to dissolve in oil, but if it is high, it tends to dissolve in water. Although the HLB values are the same, some emulsifiers may show different characteristics. When working with emulsifiers, attention should be paid to the relationship between solubility and behavior. For example, if wanted to create a W/O emulsion, the emulsifier must be oil-soluble.

HLB Range	Use
4-6	W/O emulsifiers
7-9	Wetting agents
8-18	O/W emulsifiers
13-15	Detergents
10-18	Solubilizers

Figure 1.12. HLB values of emulsifiers for various applications.[33]

1.8 Characterization of Cellulose Microspheres[18]

Cellulose microspheres can be used in a number of specific areas depending on their chemical reactions or physical properties such size, morphology, and shape. It is very important to know the physical properties of the microspheres and to know how these properties can be adjusted by changing in the preparation process, in order to use the microspheres in special application areas.

1.8.1 Size and Shape

The size of the cellulose microspheres is decided at the stage of the preparation techniques mentioned earlier (section 1.5.1), and at this stage, the sizes of the spheres can be controlled, and microspheres of different sizes are obtained. Using different analytical tools and additives in dripping and dispersion methods, microspheres from 10 micrometers to 2-3 millimeters can be obtained.[34] It should be known that the dimensions of the microspheres formed are of course not monodisperse, but they are in a fixed range. Generally, a sieve with different mesh spacing is used to determine these ranges, and after this sieving, the microspheres can be separated from each other by weighing. Depending on the mesh range used, the microspheres that passed through the sieving process can roughly give an idea about their distribution. This method is a useful method for large-scale products and is generally used in the dropping method. However, the use of laser light diffraction methods provides more accurate results. Also, laser light diffraction is an ideal technique for the dispersion method.[35]

Beads which are formed after using techniques mentioned earlier (section 1.5.1) behave like perfect spheres. Generally, the shape of the spheres is a little more elliptical. The reason is that the deformation of the droplets after they hit the surface. Using some imaging programs, particle size distribution and shapes can be learned directly by analyzing optical or scanning electron microscopy (SEM) images.[36]

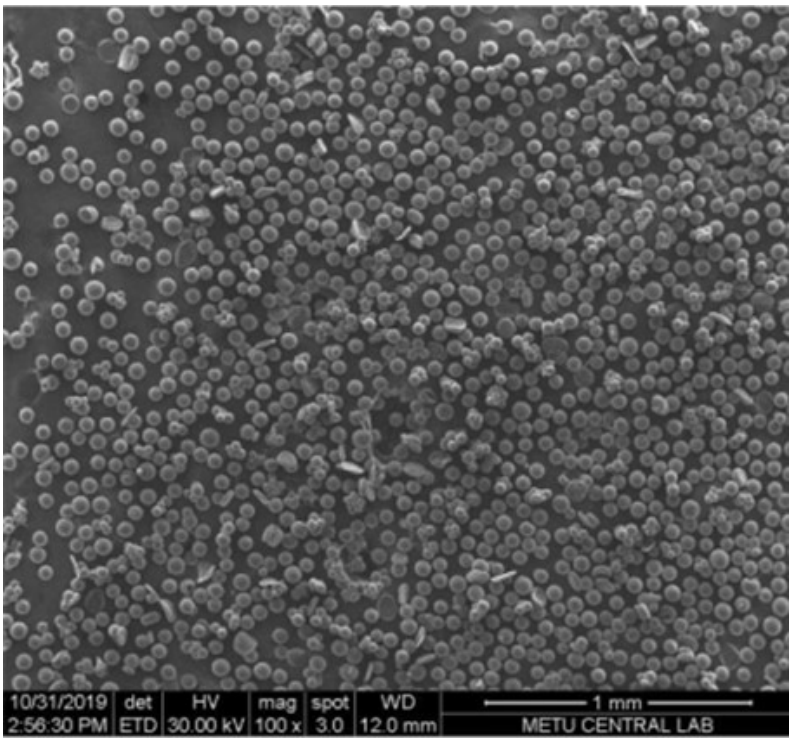

Figure 1.13. An example of a scanning electron microscopy image of cellulose microspheres.

1.8.2 Morphology

Scanning electron microscopy (SEM) is the most common morphology characterization technique for cellulose microspheres. It enables the determination of porous structures on the surface of the spheres, qualitatively.[37] SEM can be used to decide which inorganic materials should or should not be included in the cellulose microspheres. In addition to these, it was mentioned in the previous section that size and shape analysis can be done with SEM.

The cellulose microsphere samples prepared for SEM must undergo appropriate drying processes in order to learn the porous structure and inner surface area. It is not recommended to evaporate the water under vacuum or by heating. Spheres that undergo these processes, are exposed the condition which is called as ‘’hornification’’ and they lose their large porosity and surface area. As freezing water causes an expansion in volume and the formation of ice crystals. It causes damage

to the micro or mesopores, therefore, lyophilization process is one of the techniques that cannot be used. Critical point (CP) drying is an ideal technique for SEM samples.[38] Water replaces first with ethanol, then with acetone, and finally with liquid CO_2. It is finally removed from microspheres under supercritical conditions.

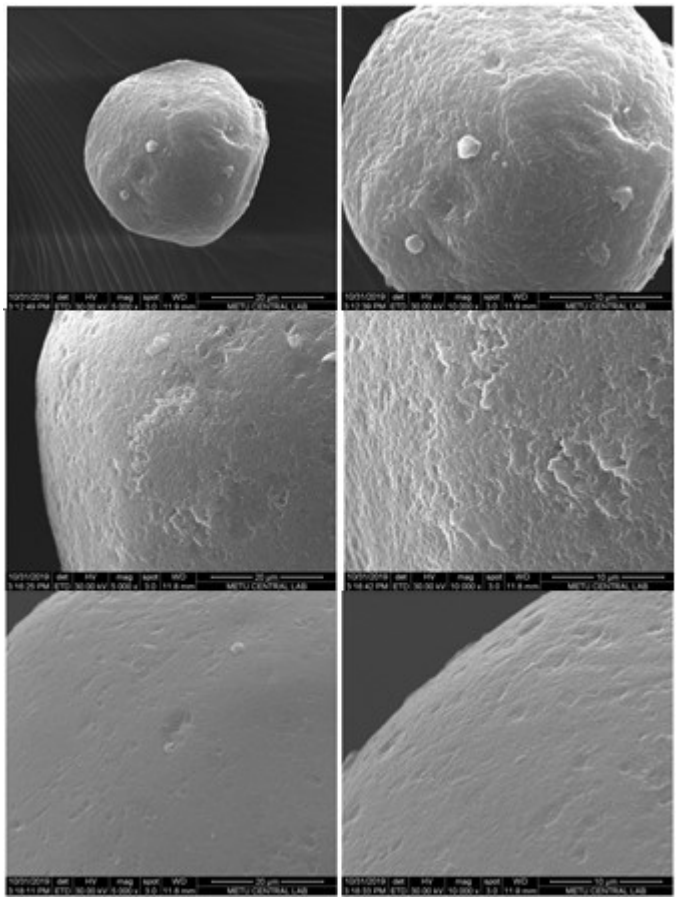

Figure 1.14. Morphology of cellulose microspheres.

The total porosity can be determined by looking at the difference in weight of the non-dried wet spheres and the weight of the dried spheres.[39] In addition, the weight gain by soaking the dry spheres in aqueous solution can be determined. In both cases, the total porosity is indicative of the "free space" in the microspheres but does not correspond exactly to the amount of available pores or the size distribution of those pores.

Using mercury intrusion or nitrogen sorption, the size distribution of the pore as well as the total internal surface area can be measured,[40] which plays a key role

when performing solid-phase synthesis. CP drying is required for both techniques. Liquid nitrogen or mercury is used to fill the pores. During this filling process, pressure is applied to against the surface tension. Especially when applying mercury intrusion, high pressure is applied. As a result of this situation, some pores may disappear, and small pores may close, and it causes false results.

Although CP drying is an ideal method for sample preparation, it affects the morphology of the spheres slightly. Thus, alternative methods have been developed to learn the pore sizes of wet spheres. Using small angle X-ray scattering (SAXS), the pore sizes and surface area of never dried spheres can be determined.[37] The working principle of the technique is based on the electron density difference between the pore wall and the water phase.

Another alternative method used to find the pore size distribution of wet microspheres is the spin echo NMR technique.[41] This method exploits delayed diffusion of water molecules to distant ones compared to those near the pore wall.[42] Interpretation of the results is extremely difficult and literature references are extremely rare. In addition, spin echo NMR measurement does not provide information about surface area unlike other techniques. No special preparation process is required or does not affect the prepared sample for spin echo NMR experiments, as in the case with SAXS measurements.

1.8.3 Mechanical Stability

Mechanical stability plays a very important role in the usage areas of microspheres. For example, they determine the maximum flow rate that can be used in chromatography column applications. At the beginning, the pressure drop increases linearly but when the cellulose spheres begin to crush with increasing flow rate, the pressure drop increases exponentially. [43]

Cellulose spheres are not exactly solid. They have an elastic and compressible structure. Their shape might be deformed permanently after crushes.

However, spheres can be used over and over again in certain applications. It is possible to learn about the mechanical stability of spheres by combining a number of methods. For example, useful information can be obtained from the analysis of centrifugation with microscopic images.

1.8.4 Biocompatibility

Pure cellulose has no known toxic properties and has not been observed to cause any disease.[44] However, in order to use cellulose in biomedical applications, it is necessary to look at some of its properties, such as biocompatibility, cytotoxicity, and other properties related to biomedical applications. Standardized high-level tests must be applied on cellulose microspheres, following the norm procedures. For example, with the help of hemolysis tests, which measures hemoglobin release in ruptured blood cells, and platelet adhesion tests, blood samples can be examined before and after passing through the packed column.[45]

1.9 Functionalization of Cellulose Microspheres

1.9.1 Chemical Modification of Cellulose Microspheres[18]

It is possible to obtain functional microspheres using various chemicals. These functional microspheres are often achieved using heterogeneous modification because of its simplicity. Cellulose contains three reactive hydroxyl groups for each repeating unit. Functional microspheres are obtained by using different chemicals for different application areas.

1.9.1.1 Etherification of Cellulose Microspheres

Cellulose microspheres can be etherified by conversion with halogen or vinyl compounds and oxirane group under alkaline conditions. The advantage of ether

linkages is due to their stability in aqueous solution - despite low or high pH values - compared to ester bonds. For instance, anionic materials, which are formed after functionalization with carboxymethylation, are widely used in ion exchange applications.

For compounds that do not react directly with polysaccharides, cellulose microspheres are etherified with reagents carrying a second reactive group. The most common example of this is the reaction of cellulose microspheres with epichlorohydrin under alkaline conditions. The reaction consists of two steps.[46] First, epoxide undergoes a ring opening reaction with the hydroxyl groups of cellulose microspheres to form a halohydrin. Subsequently, an intramolecular S_N2 reaction results in elimination of HCl and formation of a new oxirane group.

1.9.1.2 Esterification of Cellulose Microspheres

By using inorganic acid derivatives such as phosphorus oxychloride, charged cellulose spheres can be obtained and these obtained spheres can be used in ion exchange or affinity surface absorption chromatography.[47] Cellulose microspheres can be made more available for S_N2 reactions by reacting with tosyl chloride. As is well known, tosyl groups are good leaving groups. Because of the limited stability of ester linkages under alkaline conditions, esterification reactions of cellulose microspheres with carboxylic acid derivatives are rare in the literature.

1.9.1.3 Oxidation of Cellulose Microspheres

One of the methods used to activate cellulose microspheres is oxidation. Usually, $NaIO_4$ is used for this purpose. It selectively breaks the bond between C2 and C3, converting C2 and C3 into reactive aldehyde groups. Additionally, selective oxidation of the primary hydroxyl groups using piperidine oxoammonium salts

(TEMPO) as a catalyst with cooxidants is possible, giving the 6-deoxy-6-carboxy-cellulose derivatives.[48]

1.9.2 Mixing with Other Polysaccharides[18]

Subsequent modification of cellulose microspheres is quite easy and applicable. It should be noted that the particle properties, especially the pore structure, which is as important as the chemical and mechanical stability, will not be changed under harsh reaction conditions such as the use of high temperature or organic solvents. Moreover, while applying the heterogeneous reaction course, it should be taken into account that it affects the distribution of functional groups. Hydroxyl groups on the surface of cellulose microspheres are accessible, but the hydroxyl groups in the inner pores are limited by the diffusion of the reagents into the bead. If it is desired to functionalize the hydroxyl groups in the beads, the density of the functional groups used should be reduced, especially for reagents with high reactivity.

1.10 Applications of Functionalized Cellulose Microspheres

Cellulose microspheres obtained and functionalized by the methods, which are mentioned in the previous chapter, have applications in many fields. Cellulose microspheres can be used easily in many areas due to the fact that they do not have any known toxicity, they are biocompatible, and they are low cost.

1.10.1 Chromatography

Cellulose microspheres are great materials for chromatographic applications due to their spherical shape. They provide less flow resistance than cross-linked

dextran particles and also help eluent flow faster.[49,50] They do not undergo any deformation or breakage. They are easy to handle and simple to pack into columns. Cellulose microspheres are used as stationary phases in many chromatographic applications, for example in the purification of various substances or for the adsorption.

Cellulose spheres with porous structures are generally used in size exclusion chromatography (SEC) and gel filtration.[51] The interaction of the stationary phase and macromolecules with each other is undesirable in SEC. The molecules are specially separated along the porous volume of the cellulose microspheres according to the differences in their hydrodynamic radii, which determines the time it takes to flow.

Unlike SEC, the simple separation mechanism of affinity chromatography is based on the difference of the adsorbed molecules. Generally, unwanted impurities are first eluted and then the desired substances are separated after a delay or with the help of eluent in different compositions. The adsorption capacity of unmodified cellulose spheres is limited by substances that interact with hydroxyl groups. In "dye-ligand chromatography", the interaction between cellulose microspheres derivatized with a specific dye and nucleotide-bound enzymes is used. The affinity ligand interacts with the protein binding site - usually where coenzymes are located - such as NADPH. [52] In addition to dye molecules, a number of high affinity functionalities that bind to biomolecules can be applied on microspheres. Cellulose microspheres derivatized with lysine help separate DNA and endotoxin from biological samples which include blood.

1.10.2 Water Treatment (Metal Ion Exchange)

As it is known, water resources are frequently contaminated with some harmful heavy metals such as lead, cadmium, and mercury that adversely affect human health.[53] Cellulose microspheres functionalized with anionic sulfate,

phosphate, or carboxylate groups are strong, medium, or weak cation exchangers.[54,55] High amounts of metal can be separated from aqueous solutions, depending on the concentration of the functional groups. It is stated in the literature that cellulose microspheres derivatized with carboxyl groups can adsorb large amounts of copper, silver, and lead.[56]

1.10.3 Protein Immobilization[18]

Cellulose microspheres play an important role in the immobilization of enzymes because they can be chemically modified, are biocompatible and sustainable. Because of their spherical shape, porous structure, and large surface area, they are a great option for immobilization of enzymes in column applications. Protein immobilization takes place by the interaction between amino groups found in many amino acid residues of proteins and functionalized cellulose microspheres. In addition, cellulose microspheres containing oxirane or isocyanate groups can interact with amino, thiol, or hydroxyl groups found in the structure of proteins. It has been reported that enzymes immobilized by cellulose microspheres have been used therapeutics in cancer treatment.

1.10.4 Support Material for Solid-Phase Synthesis

Resins based on polystyrene are widely used as reagents in coupling reactions, but their application in polar solvents is limited by their insufficient swelling properties.[57] Functional cellulose microspheres can overcome these difficulties and can be used in solid-phase synthesis. In addition, it has been stated that cellulose microspheres derivatized with amino group can be used in the multiple-step synthesis of peptides according to Merrifield.[58,59]

Functional cellulose microspheres can serve as solid-supported scavengers for electrophiles. Cellulose microspheres derivatized with amino groups are used to

purify amide or urea derivatives from amines.[60] Microspheres bearing allyl groups can be used to remove bromine from the reaction mixture.[57] It has also been suggested that it can act as a scavenger for water treatment, as well as its use in organic synthesis, because they can chemically bind to hazardous compounds.

1.10.5 Drug Loading and Release

Cellulose is used as an approved non-toxic compound in the food and pharmaceutical industry by Europe with the E460 code. Cellulose microspheres provide many advantages over conventional granules. Their inner surface is at least 1 time higher, and it allows the microspheres to be loaded uniformly. In addition, they play an important role in drug release because of their porous structure.[61]

Functional cellulose microspheres can provide significant functionality for specific drug loading through ionic or hydrophobic interactions. For example, microspheres derivatized with carboxymethyl or phosphate groups have been used as tablet matrix for the gradual release of prazosin hydrochloride.[62] Additionally, drug immobilization is possible through covalent bonding. The covalent linkage may be designed to break under certain conditions-for example at a certain pH-allowing for target-specific drug delivery. Despite the high potential of CMs in the drug formulation area, relatively little research has been done and this may be an area of fruitful innovation.

1.11 Aim of the Study

The objective of this study is to develop cellulose-based functional microspheres capable of separating bacterial cells from liquids. This study is intended to be the first step of a research program that aims to develop tools for the diagnosis and treatment of bacteremia through separation of bacterial cells from blood. Cellulose-a natural polymer that is non-toxic, biocompatible, and has already been used for blood filtration applications towards the treatment of various diseases-

was selected as the support material. Numerous processes exist that allow for the preparation of particles of various sizes from cellulose. In order for cellulose-based microspheres to be able to separate bacterial cells from blood, they have to be derivatized with recognition groups that can selectively bind to bacteria. This project aims to utilize zinc(II)-bisdipicolylamine (Zn_2BDPA) coordination complexes, which have been used for bacterial targeting before, as bacterial recognition units. These complexes bind to negatively charged phosphate amphiphiles (eg. Lipid A, DSPG, lipoteichoic acid, and so on) on the outer surfaces of the membranes and walls of bacterial cells, regardless of Gram-type and cell morphology.

In order to reach the objective of this study it is aimed to obtain and characterize cellulose microspheres of various sizes, to activate cellulose microspheres with functional groups that would allow for derivatization with BDPA ligands, to synthesize BDPA ligands capable of conjugation to cellulose microspheres, and to derivatize cellulose microspheres with BDPA ligands. In order to demonstrate that these BDPA-derivatized cellulose microspheres are capable of selectively binding to negatively charged biomembranes, this study also aims to investigate using fluorescence spectroscopy and microscopy the interactions of these functional cellulose microspheres with neutral and negatively charged fluorescent liposomes and GFP-expressing bacterial cells.

CHAPTER 2

EXPERIMENTAL

2.1 General Considerations

Proton (^{1}H NMR) nuclear resonance spectra were recorded on Bruker Spectrospin Avance DPX-400 MHz spectrometers at 400 MHz. The chemical shifts are given in parts per million (ppm) on the delta scale (δ). The solvent peak was used as the reference value. For ^{1}H NMR: $CDCl_3$ = 7.27 ppm. For the proton data: s = singlet; d = doublet, t = triplet; q = quartet; dd = doublet of doublets; dq = doublet of quartets; m = multiplet; b = broad; app = apparent.

Infrared (IR) spectra were collected on an ALPHA PTC-2 spectrometer. Samples for IR were prepared as KBr pellets (KBr). Fluorescence spectra were recorded on a HITACHI F-2500 Fluorescence Spectrophotometer spectrometer and 3 mL 1 cm path length quartz fluorescence cuvettes were used for measurements. A Leica DM4000 B LED microscope equipped with YLP, GFP, and TX-2 fluorescence filters was used for brightfield and fluorescence microscopy. Analytical TLC was performed on E. Merck pre-coated aluminum backed silica gel 60F-254 plates. Analytical TLC visualization was done under UV (254 nm) or using appropriate stains. Flash column chromatography (FCC) was done by using SiliCycle SiliaFlash silica gel (40 - 63 μm, 60 Å) and the procedure developed by Still and coworkers was followed.[63] Solvents used for chromatography or reactions were dried and purified as follows: Ethyl acetate (EtOAc) was distilled from $CaCl_2$. Hexanes were distilled from $CaCl_2$. For reactions reagent grade methylene chloride (CH_2Cl_2) and chloroform ($CHCl_3$) were distilled from CaH_2 prior to use. For chromatography distilled methylene chloride ($CaCl_2$) and analysis grade chloroform were used. For reactions pre-dried dimethylformamide (DMF) and tetrahydrofuran (THF) were used. ACS grade methanol and ethanol were used in chromatography and reactions.

All other chemicals were procured from reputable sources and used as received. GFP-expressing *Escherichia coli* (K12 pSB1C3-GFP) was received as a gift. Perloza ST Fine (PSTF, 50-75 μm), Perloza ST Medium (PSTM, 75-150 μm), and Perloza ST Coarse (PSTC, 150-300 μm) are commercially available cellulose microspheres. They were purchased from PERLOZA S.r.o., Lovosice, Czechia. Bulk density of these commercial spheres is 0.955 g/mL. They are regular spherical particles. They are low porosity dry products with 12% maximum humidity.

2.2 Size Controlled Preparation of Cellulose Microspheres

2.3 Determination of the Molecular Weight of Cotton (Cellulose)[64,65]

i. Preparation of the Copper Hydroxide: 200 g of crystallized copper sulfate was dissolved in 1L of boiling distilled water. The solution was cooled to 45°C. Ammonium hydroxide was slowly added (approximately 100 mL) until the light blue color is turned into blue-violet. An excess amount of ammonium hydroxide should not be added. The formation of greenish precipitate was observed and washed with distilled cold water by filtration until the washings are colorless. The precipitate was transferred into the flask. 640 mL of 8% (w/w) NaOH was added dropwise while stirring in an ice-bath. It was allowed to stand for 10 min. The copper hydroxide precipitate was washed with distilled water until some drops of $BaCl_2$ solution does not lead to the formation of a precipitate of $BaSO_4$ in the washing residue. Then, it was washed with 100 mL of acetone and allowed to dry in a vacuum.

ii. Determination of the Copper Content: 2 g of copper hydroxide was dissolved in 200 mL of 1M HCl. 25 mL of the solution was transferred into a titration flask. 25 mL of 10% potassium iodide solution was added. Titration was done with 0.05 M of sodium thiosulfate solution. The starch solution was used as the indicator. The indicator was added when the titration is nearing to the end. (the color of violet disappears)

iii. Determination of Ethylene-Diamine Content: 10 mL of ethylene-diamine was transferred into a 100 mL volumetric flask. It was filled up to the mark with distilled water. 20 mL of the solution was taken and titrated with 0.5 M sulfuric acid solution using methyl orange as the indicator. 64.75 mL (average) of 0.5 M sulfuric acid solution was used.

iv. Preparation of the Cupriethylene-Diamine (CuEn) Solution: 63.5 g of copper hydroxide was dissolved in 50 mL of distilled water 1-L of volumetric flask. 120 g (133.3 mL) of ethylene-diamine was added. The solution was filled up to the mark with distilled water. It was allowed to stand for 24 h, then filtered and filled up to the mark again.

v. Determination of the Molecular Weight of Cellulose (Cotton): 3 different concentrations of cotton solution in CuEn were prepared (0.1, 0.2 and 0.4 in g/100 mL). Intrinsic viscosity was determined using a Ubbelohde capillary viscometer. The relative viscosity (η_{rel}) was determined by dividing the flow time of polymer solution through a capillary by that of pure solution. $ln(\eta_{rel})/c$ was plotted against c (e.g. concentration of polymer solution). According to Kraemer Equation, the intercept of the graph gives intrinsic viscosity. The average viscometric degree of polymerization was calculated by multiplying intrinsic viscosity with 190 (the Mark-Houwink-Sakurada equation was applied). The molecular weight of anhydroglucose monomer was taken as 162 g/mol.

2.4 Attempts at Preparation of CMs Using a Non-Derivatizing Solvent System

Following a procedure by Zhang and coworkers,[66] attempts were made to dissolve cotton in a solution comprised of 7/1/81(w/w/w) NaOH/urea/water. The mixture was agitated using a mechanical stirrer at 1000 rpm at a temperature of -11°C. Dissolution of cotton, which would have been evidenced by formation of a

transparent solution, was not observed after 30 minutes. Increasing the time or rotor speed (1200-2000 rpm) did not change the outcome. Numerous other conditions reported for the NaOH/urea/water system were also explored, but none yielded satisfactory cotton solutions.

2.5 Preparation of CMs Through Thermal Regeneration of Cellulose from Water-in-Oil Emulsions of Viscose

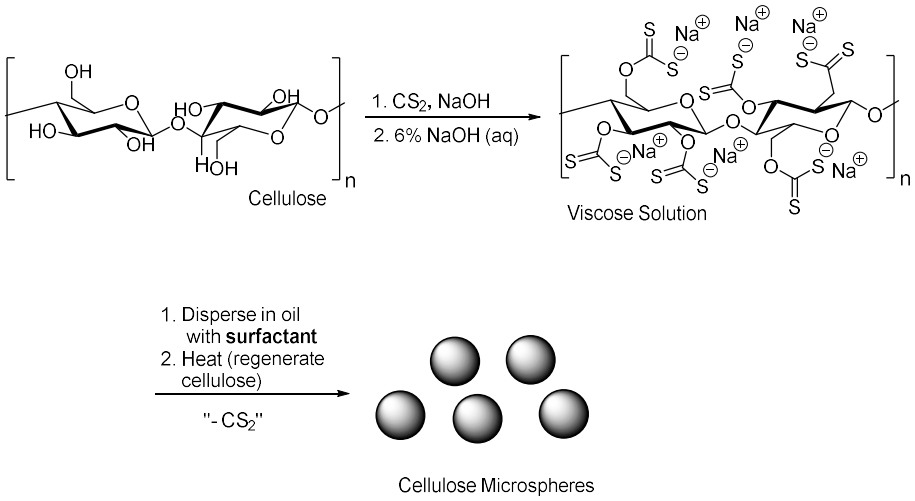

i. NaOH Treatment of Cotton: To 2 g of cotton which was dried overnight in a vacuum oven at 55^{o}C was added 20 ml of 20% NaOH solution (w/w). After 2 hours, excess NaOH solution was removed by pressing the cotton against a clean surface and the alkali-treated cotton was shredded into small pieces. The shredded alkali-treated cotton was placed in a 100 ml Erlenmeyer and was allowed to age at room temperature for 48 hours.

ii. Preparation of Cellulose Xanthate: The pretreated cotton was placed in a 50 mL Falcon tube and 2.5 mL CS_2 was added dropwise in 5 aliquots (0.5 mL each) and the tube was vortexed vigorously after the addition of each aliquot. The tube was sealed and allowed to stand at room temperature overnight.

iii. Preparation of Viscose Solution: 20 mL of 6% NaOH solution (w/w) was added to cellulose xanthate in two aliquots. After each addition, the mixture was stirred vigorously using a glass rod to aid in the dissolution of cellulose xanthate. The Falcon tube was resealed and was placed in a shaking incubator at room temperature at 250 rpm overnight. The viscose solution had a volume of about 25 mL and was obtained as an opaque orange-brown thick liquid.

iv. Preparation of Regenerated Cellulose Microspheres: Viscose solutions thus prepared were employed in the preparation of CMs through thermal regeneration of cellulose from water-in-oil emulsions of viscose. The viscose solution was centrifuged at 8000 rpm to precipitate any undissolved cotton fibers and the supernatant (approximately 25 mL) was placed in a syringe. The syringe was placed in a syringe pump and droplet size was adjusted via pipette tips attached to the end of a narrow plastic tube attached to the syringe. The viscose solution was added dropwise over 45 minutes into a mechanically stirred solution of 240 mL paraffin oil and a small amount of surfactant. When the addition was completed, the mixture was mechanically stirred at set rpm value for an additional hour at room temperature after which, while still being stirred, it was heated to 95°C in 30 minutes and kept at that temperature for an additional 2.5 hours. Upon completion of cellulose regeneration, as evidenced by the formation of white particles, the reaction mixture was cooled using an ice bath and agitation was ceased. To the reaction mixture was added 150 mL DI water and the mixture was poured into a separatory funnel. The aqueous phase along with the CMs was separated from the oil layer. The CMs were separated from the aqueous layer through vacuum filtration and the CMs were washed, in sequence, with 3x50 mL DI, 2x25 mL ethanol 2x50 mL DI water again, 1x25 mL ethanol, and finally with 3x25 mL acetone. The CMs were then air-dried. Further drying, when needed, was done under high vacuum or using lyophilization. This method typically gave CMs in approximately 60% yield based on the starting cellulose weight. The obtained dry CMs were then passed through test sieves (500, 320, 150, and 40 μm) and the fractions were weighed to obtain a weight-based size distribution. The fractions were then recombined, and size analysis was

done using a Mastersizer particle size analyzer. A small aliquot of CMs was stained using aqueous Congo red solution, dried, and the dyed CMs were examined through brightfield micrography.

2.6 Activation of CMs

2.6.1 Epoxidation of CMs and Determination of Their Epoxy Content

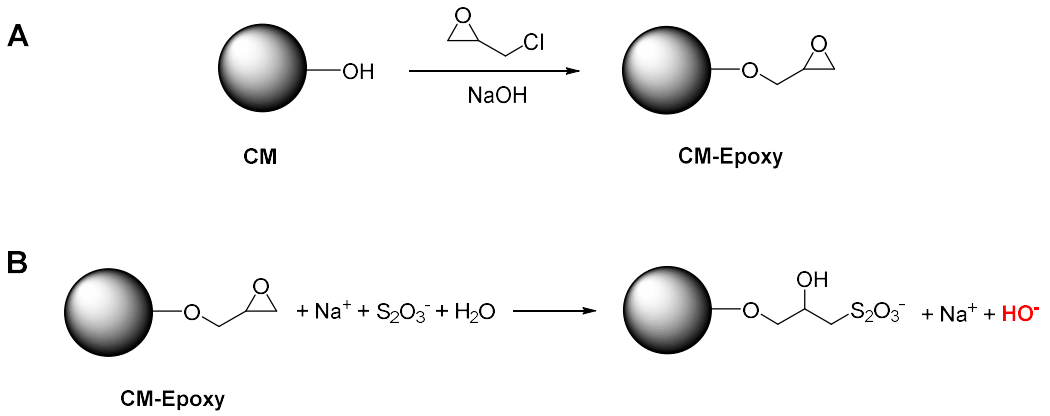

To 500 mg of CMs was added 0.5 mL epichlorohydrin and 1.5 mL 2.5 M NaOH (aq). The reaction was agitated at 250 rpm in a shaking incubator at 40°C for 2.5 hours after which the CMs were separated through filtration and washed with DI water and acetone. After air-drying the CMs were lyophilized. Oxirane group in CM-Epoxy was determined as follows. 26 mg of oxirane-containing CM-Epoxy was added to 10 ml of 1.3 M neutralized sodium thiosulphate solution and then wait 30 min for equilibrium. Then, pH was kept at 7 by adding 1 M HCl. The amount of oxirane present in CM-Epoxy was calculated from the amount of HCl needed to maintain neutral. FTIR (KBr) ν 1580, 1237, 1022, 896, 796.7 cm^{-1}.

2.6.2 Amine Functionalization of CMs

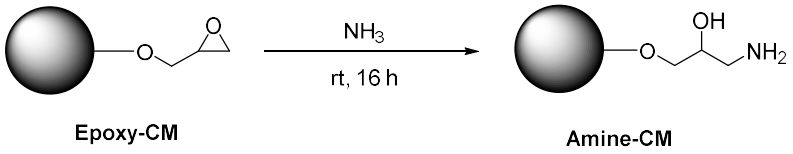

Epoxy-CM Amine-CM

To 100 mg epoxy-CMs in a test tube was added 1 ml 25% NH_4OH solution and the tube was sealed. The reaction was placed in a shaking incubator and agitated at 150 rpm at room temperature. were put into a test tube. The mixture was stirred at 150 rpm at room temperature for overnight. The CMs were recovered by filtration, washed with DI water and acetone, and air-dried. Lyophilized samples were subjected to CHNS analysis and amine content was found to be in the 257-421 μmol/g range. FTIR (KBr) ν 1427, 1050 cm^{-1}.

2.6.3 Cyanoethylation of CMs

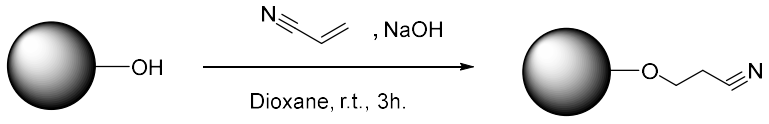

CM Cyano-CM

A 2 g sample of CMs was treated twice with 10 mL 0.5 M NaOH solution and the alkali treated CMs were recovered using vacuum filtration. The moist beads were transferred to a test tube containing a mixture of 4 mL dioxane and 8 mL acrylonitrile. The reaction was agitated at room temperature in a shaking incubator at 150 rpm for 3 hours. The derivatized CMs were washed with acetone, water, and acetone again. Air-dried CMs were analyzed using FTIR. FTIR (KBr) ν 3440, 2251, 1700, 894 cm^{-1}.

2.6.4 Preparation of Bisaldehyde-CMs and Determination of Their Aldehyde Content[67,68]

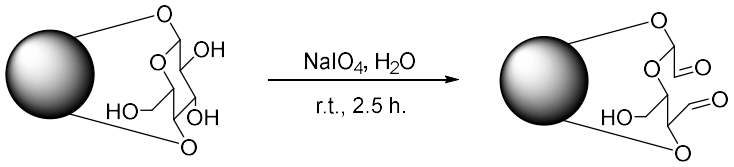

CM Bisaldehyde-CM

To a sample of 488.1 mg of CMs was added 1.5 mL of an aqueous solution of 0.20 M $NaIO_4$ and the reaction was incubated in the dark at 25 °C in a shaking incubator at 250 rpm. The CMs were recovered by vacuum filtration. The CMs were washed five times with DI water to remove excess periodate and kept at 4°C until further use. An aliquot of dialdehyde-CMs was lyophilized and the aldehyde content was determined as follows. 60 mg of dialdehyde-CMs were placed in a vial and 4 mL of 0.25 N NaOH was added. Solution was stirred for 10 seconds and then was heated to 70 ºC for 1 min. Then, solution was cooled by swirling in an ice-bath for 1 min. Then, 6 mL of 0.25 N H_2SO_4 was added to the solution. The solution was titrated by using 0.25 N NaOH to pH=7 (repeated 2 times). Aldehyde content was found to be in the 5.79-12.87 mmol/g range. FTIR ν 1681, 894 cm^{-1}.

2.6.5 Preparation of Dicarboxy-CMs and Determination of Carboxyl Group Content[69]

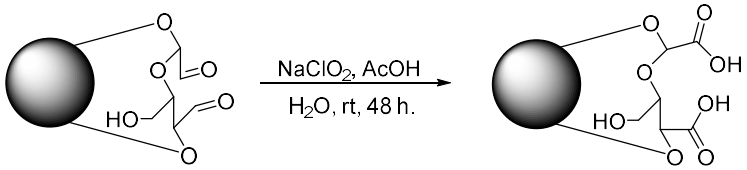

Bisaldehyde-CM Biscarboxyl-CM

A 6 mL volume of bisaldehyde-CMs suspension containing 300 mg solid was mixed with 6 mL of 0.4M $NaClO_2$ in 2 M acetic acid. The reaction was incubated at 20 ºC for 48 hours in a shaking incubator at 250 RPM. The CMs were washed with

DI water. The carboxyl group content was determined as follows. 60 mg of biscarboxy-CMs were weighted and put into 9 mL DI water and 1 mL of 0.1M NaCl was added into this solution. pH was measured and after it comes to the equilibrium. Then, the solution was titrated with 0.1M NaOH (repeated 2 times). Carboxyl group content was found to be 0.233 mmol/g. FTIR ν 1730, 894 cm^{-1}.

2.6.6 Preparation of Carboxyl-CMs[70]

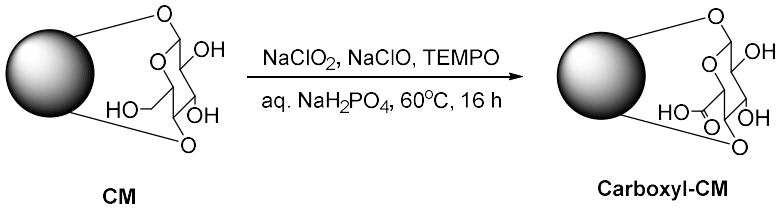

In a 25 ml flask, 1 g (18.5 mmol, anhydrous glucopyronase unit) were placed in 9 ml (50 mmol) NaH_2PO_4 solution. Then, 1.112 g (12.3 mmol) of $NaClO_2$ and 31 mg (0.2 mmol) of TEMPO were added sequentially followed by addition of 45 mg (0.6 mmol) NaClO. After the addition of NaClO, the flask was left open, as evolution of chlorine gas was expected. The reaction was stirred at 60 ºC overnight. The reaction was cooled to room temperature and pH of final reaction was measured and found, as expected, to be 5. Oxidized beads were washed with 3x30 mL of 1M HCl, 3x30 mL of DI water, and 10 mL of acetone. 60 mg of dried carboxyl-CMs were weighed and put into 9 mL DI water and 1 mL of 0.1M NaCl was added into this solution. pH was measured after equilibrated. Then the solution was titrated with 0.1M NaOH (repeated 2 times). Carboxyl group content was found to be 0.367 mmol/g. FTIR ν 1731, 894 cm^{-1}.

2.7 Preparation of BDPA Ligands

2.7.1 Preparation of BDPA-Acid (6)[71]

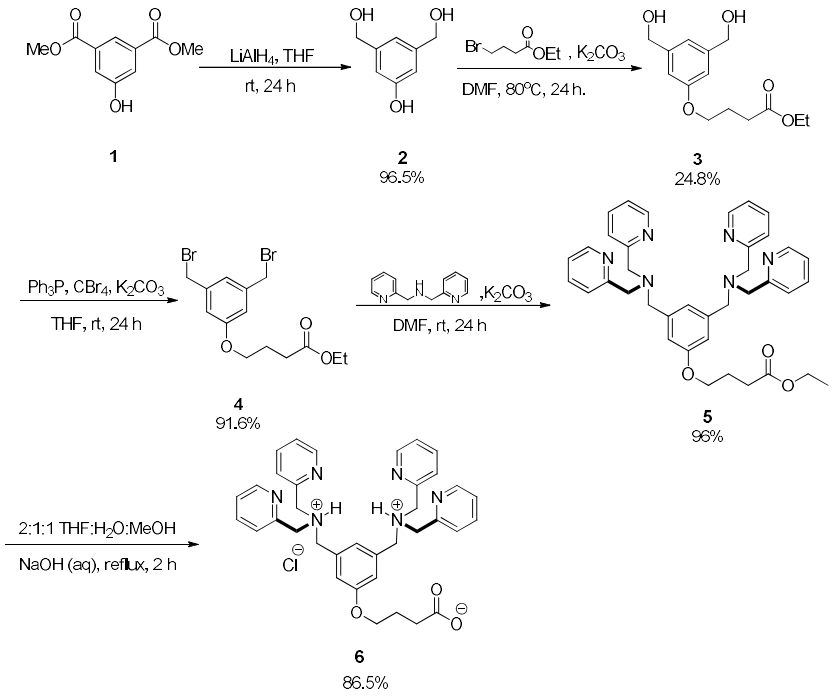

Scheme 2.1. Preparation of BDPA-acid **6**.

2.7.1.1 Reduction of 5-Hydroxyisophthalate (2)

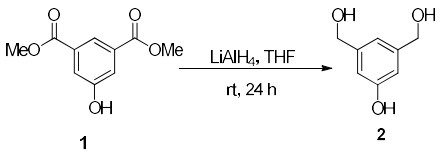

Into a dispersion of 1 g (26.35 mmol) of lithium aluminum hydride ($LiAlH_4$) in 40 mL anhydrous THF under N_2 atmosphere was added dropwise a solution of 3 g (14.27 mmol) of 5-hydroxyisophthalate (**1**). The reaction was magnetically stirred under N_2 atmosphere for 24 hours at room temperature. After that the reaction was cooled to 0°C in an ice bath and then quenched with dropwise addition of 20 mL 10% H_2SO_4. The solvent was removed *in vacuo*. The residue was partitioned

between 100 ml saturated brine and 100 ml EtOAc. The aqueous phase was extracted an additional 5 times with 50 ml EtOAc each. The combined organic phase was dried with Mg_2SO_4 and the solvent was removed *in vacuo*. 2.116 g (96.5% yield) of **2** was obtained as a crystalline white solid. R_f: 0.35 (SiO_2, EtOAc). ^1H NMR (400 MHz, CD_3OD) δ ppm 4.53 (s, 4 H) 6.70 (s, 2 H) 6.80 (s, 1 H).

2.7.1.2 Ethyl 4-(3,5-bis(hydroxymethyl)phenoxy)butanoate (3)

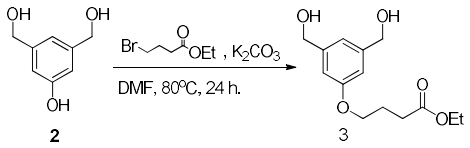

1.259 g (0.924 mL, 6 mmol) Ethyl 4-bromobutyrate, 500 mg (3 mmol) of **2**, and 2.23 g (16 mmol) of potassium carbonate (K_2CO_3) in 10 mL anhydrous DMF was magnetically stirred under N_2 atmosphere for 24 hours at 80˚C. Upon completion of the reaction, the solvent was removed *in vacuo*. The residue was partitioned between 25 mL each of EtOAc and H_2O. The extraction was repeated twice more, After the extraction, the organic phases were combined, dried with Mg_2SO_4, and the solvent was removed *in vacuo* to give a pale yellow oily material. The material was subjected to FCC (SiO_2, EtOAc). 0.200 g (24.8% yield) of **3** was obtained as a yellow viscous oil. R_f: 0.40 (SiO_2, EtOAc). ^1H NMR (400 MHz, $CDCl_3$) δ ppm 1.27 (t, J=7.15 Hz, 3 H) 2.07 - 2.21 (m, 2 H) 2.47 - 2.56 (m, 2 H) 4.03 (t, J=6.02 Hz, 2 H) 4.09 - 4.23 (m, 2H) 4.61 - 4.74 (m, 4 H) 6.84 (s, 2 H) 6.94 (s, 1 H). HRMS (ESI+) calculated for $C_{14}H_{20}O_5$ ($[M+H]^+$): 269.1344, founded: 269.0115.

2.7.1.3 Ethyl 4-(3,5-bis(bromomethyl)phenoxy)butanoate (4)

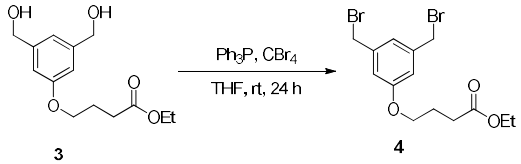

A solution of 1.235 g (3.72 mmol) of carbon tetrabromide (CBr_4) in 2 mL anhydrous THF was added dropwise into a mixture of 400 mg (1.49 mmol) of **3**, 975 mg (3.7 mmol) of triphenylphosphine (PPh_3), and 824 mg (5.96 mmol) of potassium carbonate (K_2CO_3) in 4 mL anhydrous THF under N_2 atmosphere. The reaction was magnetically stirred under N_2 atmosphere for 24 hours at room temperature. Upon completion of the reaction the solvent was removed *in vacuo*. The residue was dissolved in EtOAc, the undissolved K_2CO_3 was removed by filtration, and the solvent was removed *in vacuo* to give and orange oil. This material was subjected to FCC (SiO_2, 1:1 EtOAc, Hexane) give 0.538 g (1.3 mmol, 91.6% yield) product **4** as a yellow viscous oil. R_f: 0.67 (SiO_2, 1:1 EtOAc, Hexane). ^1H NMR (400 MHz, $CDCl_3$) δ ppm 1.27 (t, J=7.15 Hz, 3 H) 2.08 - 2.19 (m, 2 H) 2.52 (t, J=7.28 Hz, 2 H) 4.03 (t, J=6.15 Hz, 2 H) 4.16 (q, J=7.28 Hz, 2 H) 4.43 (s, 4 H) 6.74 - 6.88 (m, 2 H) 7.00 (s, 1 H). HRMS (ESI+) calculated for $C_{14}H_{18}Br_2O_3$ ($[M+H]^+$): 394.9679, founded: 394.9680.

2.7.1.4 Ethyl 4-(3,5-Bis(pyridine-2-ylmethyl)amino)methyl)phenoxy)butanoate (5)

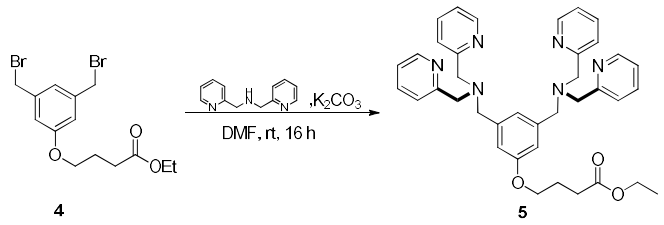

4 5

To a mixture of 538 mg (1.26 mmol) **4** and potassium carbonate (K_2CO_3) in 19.1 mL DMF under N_2 atmosphere was added dropwise a solution of 556 mg (501 μL, 2.79 mmol) dipicolylamine. The reaction was magnetically stirred under N_2 atmosphere overnight at room temperature. The solvent was removed *in vacuo*. The residue was partitioned between 50 mL each of H_2O and $CHCl_3$. The aqueous phase was extracted with 3 more times with 50 mL $CHCl_3$. The organic phases were combined, washed with 50 mL saturated brine, and dried with Na_2SO_4. The solvent

was removed *in vacuo* give a dark orange/brown oil which was subjected to FCC (SiO_2, 10:1:0.1 $CHCl_3$:MeOH:NH_4OH). 190 mg (0.3 mmol, 96% yield) of product was purified. R_f: 0.68 (SiO_2, 10:1:0.1 $CHCl_3$:MeOH:NH_4OH). ^1H NMR (400 MHz, $CDCl_3$) δ ppm 1.24 - 1.27 (t, 3 H) 2.11 (t, J=6.53 Hz, 2 H) 2.52 (t, J=7.40 Hz, 3 H) 3.65 (s, 4 H) 3.81 (s, 8 H) 3.99 (t, J=6.02 Hz, 2 H) 4.14 (d, J=7.03 Hz, 2 H) 6.86 (s, 2 H) 7.07 (s, 1 H) 7.12 - 7.15 (m, 4 H) 7.60 - 7.66 (m, 8 H) 8.51 (d, J=4.77 Hz, 4 H). HRMS (ESI+) calculated for $C_{38}H_{42}N_6O_3$ ($[M+H]^+$): 631.3397, found: 631.3397.

2.7.1.5 4-(3,5-Bis((bis(pyridin-2-ylmethyl)ammonio)methyl)phenoxy)butanoate chloride (6)

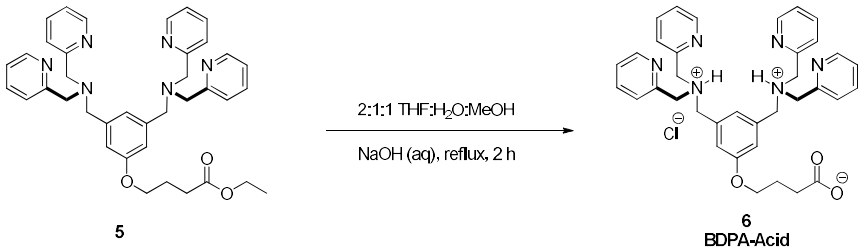

5 6
BDPA-Acid

To a solution of 190 mg (0.3 mmol) of **5** in 3 ml of THF, 1.5 ml of H_2O, and 1.5 ml of MeOH, 148 µl of 20% NaOH solution (w/w) was added dropwise. The reaction was refluxed for 2.5 hours. Upon completion the reaction was carefully neutralized (pH 7, using pH paper) with 1 M HCl after which volatiles were removed *in vacuo*. 10 ml $CHCl_3$ was the residue, and the product was dissolved, leaving NaCl crystals. The $CHCl_3$ solution was removed, and this "liquid-solid" extraction was repeated twice more. The combined organic phase was dried with Na_2SO_4 and the solvent was removed *in vacuo*. 140 mg (0.2 mmol, 86.5% yield) of **6** was obtained as a dark yellow/brown viscous oil. ^1H NMR (400 MHz, $CDCl_3$) δ ppm 1.17 - 1.31 (m, 4 H) 2.11 (quin, J=6.65 Hz, 2 H) 2.52 (t, J=7.40 Hz, 2 H) 3.65 (s, 4 H) 3.81 (s, 8 H) 3.99 (t, J=6.02 Hz, 2 H) 4.14 (q, J=7.19 Hz, 3 H) 6.86 (s, 2 H) 7.07 (s, 1 H) 7.10 - 7.19 (m, 4 H) 7.53 - 7.70 (m, 8 H) 8.51 (d, J=4.77 Hz, 4 H). HRMS (ESI+) calculated for $C_{36}H_{39}ClN_6O_3$ ($[M+H]^+$): 603.3084, found: 603.3084.

2.7.2 Preparation of BDPA-Amine (10)[72]

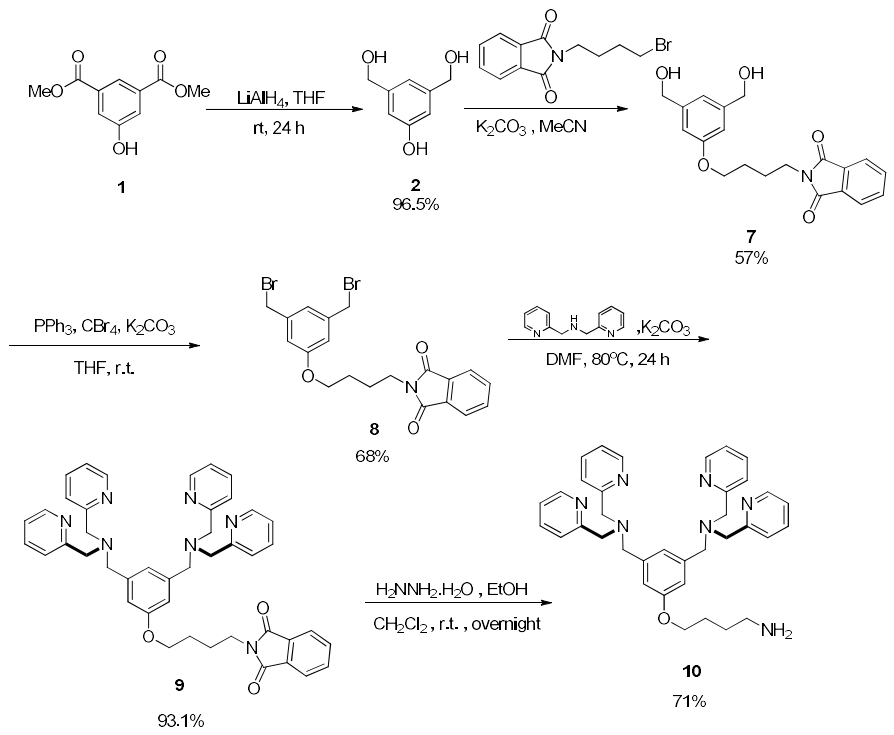

Scheme 2.2. Preparation of BDPA-amine **10**.

2.7.2.1 2-(4-(3,5-Bis(hydroxymethyl)phenoxy)butyl)isoindoline-1,3-dione (7)

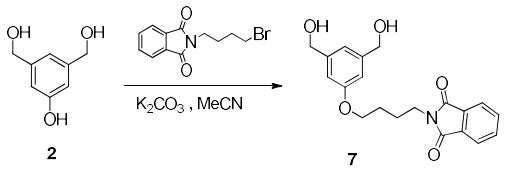

To a stirred mixture of 500 mg (3.24 mmol) of **2** and 3 g (22 mmol) of potassium carbonate (K_2CO_3) in MeCN was added dropwise a solution of 1.10 g (3.89 mmol) N-(4-bromobutyl)phthalimide in 10 mL MeCN. The reaction was refluxed overnight using a reflux condenser equipped with a drying tube ($CaCl_2$). Upon completion of the reaction the solvent was removed *in vacuo*. The residue was partitioned between 20 ml $CHCl_3$ and 20 ml H_2O. The aqueous phase was extracted twice more with 20 ml of $CHCl_3$. The organic phases were combined, dried with

Na_2SO_4 and the solvent was removed *in vacuo*. The residue was subjected to FCC (SiO_2, EtOAc). 672 mg (57% yield) white crystal solid material was obtained. R_f: 0.38 (SiO_2, EtOAc). ^1H NMR (400 MHz, $CDCl_3$) δ ppm 1.87 (br. s., 4 H) 3.76 (t, J=6.78 Hz, 2 H) 4.02 (t, J=5.90 Hz, 2 H) 4.64 (s, 4 H) 6.82 (s, 2 H) 6.91 (s, 1 H) 7.68 - 7.75 (m, 2 H) 7.82 - 7.87 (m, 2 H). HRMS (ESI+) calculated for $C_{20}H_{21}NO_5$ ($[M+H]^+$): 356.1498, found: 356.1498.

2.7.2.2 2-(4-(3,5-Bis(bromomethyl)phenoxy)butyl)isoindoline-1,3-dione (8)

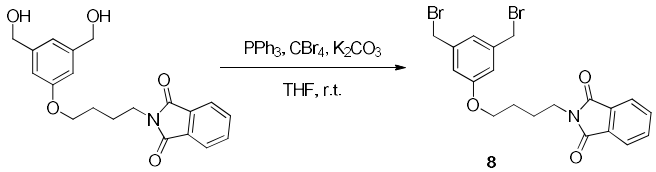

A solution of 0.930 g (2.8 mmol) of carbon tetrabromide (CBr_4) in 4 mL anhydrous THF was added into a mixture of 397 mg (1.12 mmol) of **7**, 736 mg (2.8 mmol) of triphenylphosphine (PPh_3), and 775 mg (5.6 mmol) of potassium carbonate (K_2CO_3) in 4 mL anhydrous THF under a N_2 atmosphere. The reaction was magnetically stirred under a N_2 atmosphere for 24 hours at room temperature. Upon completion of the reaction 7 mL of THF was added to the reaction, potassium carbonate was removed by filtration, and the solvent was removed *in vacuo* to give a yellow viscous oil. This material was subjected to FCC (SiO_2, 1:1 EtOAc, Hexane). 354 mg (0.7 mmol, 68% yield) **8** was obtained as a yellow viscous oil. R_f: 0.65 (SiO_2, 1:1 EtOAc, Hexane). ^1H NMR (400 MHz, $CDCl_3$) δ ppm 1.83 - 1.92 (m, 4 H) 3.78 (t, J=6.65 Hz, 2 H) 4.01 (t, J=5.77 Hz, 2 H) 4.42 (s, 4 H) 6.84 (d, J=1.25 Hz, 2 H) 6.99 (s, 1 H) 7.71 - 7.75 (m, 2 H) 7.83 - 7.89 (m, 2 H). HRMS (ESI+) calculated for $C_{20}H_{19}Br_2NO_3$ ($[M+H]^+$): 481.9810, found: 481.9789.

2.7.2.3 2-(4-(3,5-Bis((bis(pyridin-2-ylmethyl)amino)methyl)phenoxy)-butyl)isoindoline-1,3-dione (9)

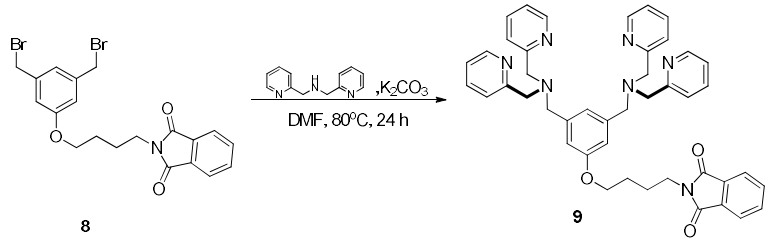

8 9

To a mixture of 333 mg (0.69 mmol) **8** and 960 mg (6.96 mmol) potassium carbonate (K_2CO_3) in 20 mL anhydrous DMF under a N_2 atmosphere was added dropwise 275 µl (304 mg, 1.5 mmol) of dipicolylamine. The reaction was stirred under N_2 at room temperature for 24 hours. Upon completion of the reaction the solvent was removed *in vacuo* and the residue was partitioned between 25 mL each of H_2O and $CHCl_3$. The aqueous phase was extracted twice more with 25 mL $CHCl_3$. The organic phases were combined, washed with 50 mL saturated brine, dried with Na_2SO_4 and the solvent was removed *in vacuo*. The dark orange/brown residue was subjected to FCC (SiO_2, 8:1:0.1 $CHCl_3$:MeOH:Et_3N). 465 mg (0.6 mmol, 93.1% yield) of **9** was obtained as a dark orange/brown oily material. ^{1}H NMR (400 MHz, $CDCl_3$) δ ppm 1.83 - 1.93 (m, 4 H) 2.81 (br. s., 2 H) 3.63 (s, 4 H) 3.80 (s, 8 H) 3.98 (t, J=5.90 Hz, 2 H) 6.85 (s, 2 H) 7.05 (s,1 H) 7.13 (td, J=5.90, 1.51 Hz, 4 H) 7.59 - 7.66 (m, 8 H) 7.70 - 7.73 (m, 2 H) 7.83 - 7.86 (m, 2 H) 8.50 (d, J=4.77 Hz, 4 H). HRMS (ESI+) calculated for $C_{44}H_{43}N_7O_3$ ($[M+H]^+$): 718.3505, found: 718.3506.

2.7.2.4 N,N'-((5-(4-Aminobutoxy)-1,3-phenylene)bis(methylene))bis(1-(pyridin-2-yl)-N-(pyridin-2-ylmethyl)methanamine)

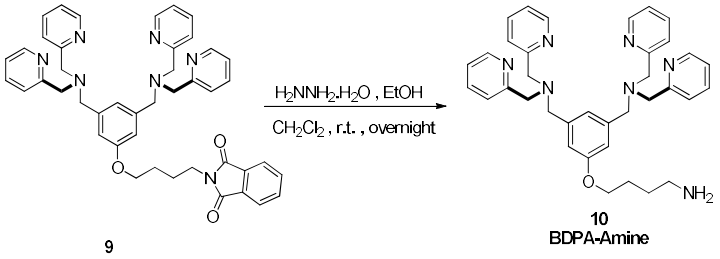

9 10 BDPA-Amine

245 mg (3.96 mmol) of **9** was dissolved in 7.4 ml of EtOH and 2 ml of DCM and 538 µl (554 mg, 11.1 mmol) of hydrazine monohydrate was added dropwise to this solution under a N_2 atmosphere. The reaction was magnetically stirred overnight under a N_2 atmosphere at room temperature. The reaction was diluted with 15 mL DCM, filtered, and the solvent was removed *in vacuo*. The residue was purified via gradient FCC (SiO_2, $CHCl_3$ to 8:2:0.2, $CHCl_3$:MeOH:Et_3N). 142 mg (71% yield) yellow oily material was obtained. R_f: 0.47 (SiO_2, $CHCl_3$ to 8:2:0.2, $CHCl_3$:MeOH:Et_3N). ^{1}H NMR (400 MHz, $CDCl_3$) δ ppm 1.84 - 1.93 (m, 4 H) 3.01 (t, J=6.53 Hz, 2 H) 3.60 (s, 4 H) 3.78 (s, 10 H) 3.96 (t, J=5.40 Hz, 2 H) 6.76 - 6.80 (m, 2 H) 6.95 (s, 1 H) 7.12 (dd, J=6.65, 5.65 Hz, 4 H) 7.52 - 7.65 (m, 8 H) 8.51 (d, J=4.77 Hz, 4 H). HRMS (ESI+) calculated for $C_{36}H_{41}N_7O$ ($[M+H]^+$): 588.3455, found: 588.3451.

2.8 Preparation of BDPA Ligand Bearing CMs

2.8.1 Coupling of BDPA-Acid (6) with Amine-CMs

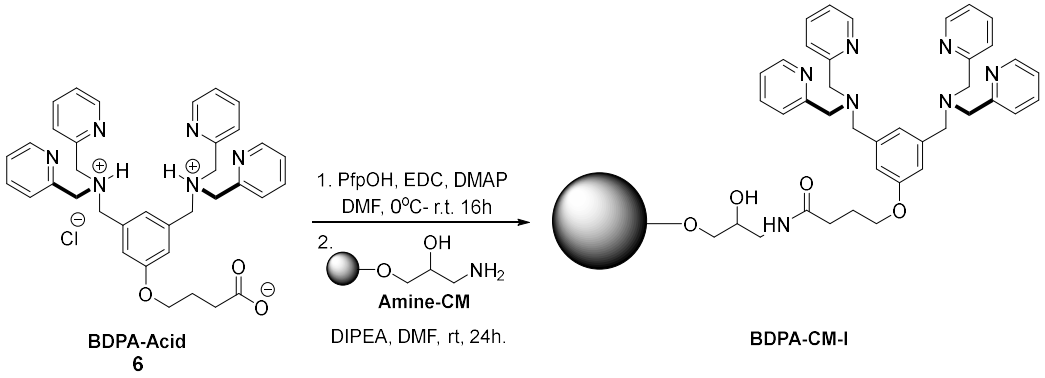

To 25 mg of BDPA-acid **(6)** in 2.5 ml DMF at 0ºC was added sequentially 7.19 mg (0.039 mmol) of PfpOH, 7.47 mg (0.039 mmol) of EDC, 1 mg (0.007 mmol) of DMAP. The reaction was stirred at 0ºC for 10 min and allowed to heat room temperature. The reaction was allowed to proceed overnight. A solution of 5.05 mg (6.81 µL, 0.039 mmol) DIPEA in 0.5 mL DMF was added to the reaction. Then 35 mg (343 µmol/g amine) of amine-CMs were added to the reaction. The reaction was stirred at room temperature under a N_2 atmosphere overnight. The solvent was removed *in vacuo*. BDPA-CM-I were washed with 3x25 mL DI water and 1x25 mL ethanol. The CMs were dried under vacuum. Lyophilized samples were subjected to CHNS analysis and BDPA content was found to be 0.123 µmol/mg. FTIR ν 1651, 1061, 894, 766 cm^{-1}.

2.8.2 Coupling of BDPA-Amine (10) with Bisaldehyde-CMs

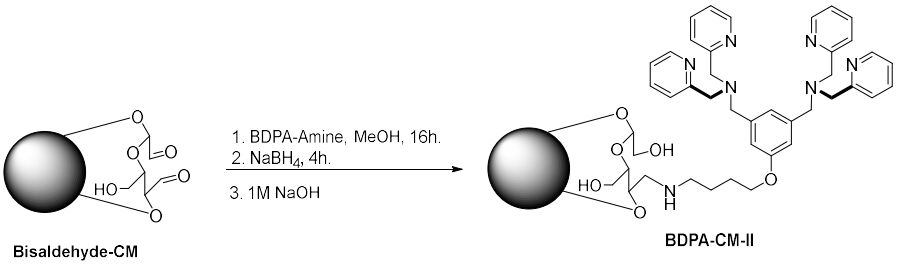

100 mg (0.2 mmol) of BDPA-Amine (**10**) was dissolved in 5 ml of MeOH. To this solution was added 100 mg (1.3 mmol aldehyde-content) bisaldehyde-CMs. The reaction was placed in a shaking incubator and agitated at 250 rpm overnight. 38.6 mg (1 mmol) of $NaBH_4$ was added to this solution. After giving sufficient time, the reaction was washed with 5 mL of 1 M NaOH then washed with 3x25 mL DI water and 1x25 mL ethanol. BDPA-CM-II manifested itself as yellow beads. Dried samples were subjected to CHNS analysis and BDPA content was found to be 0.070 µmol/mg. FTIR ν 1592, 1156, 1026, 894, 798 cm^{-1}.

2.8.3 Coupling of BDPA-Amine (10) with Epoxy-CMs

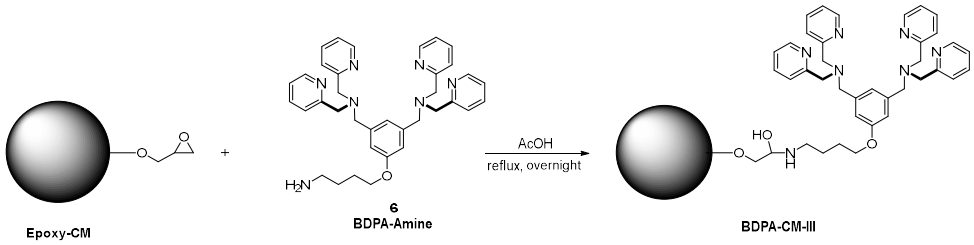

To a dispersion of 100 mg (83.8 µmol, epoxy content) CM-Epoxy and 1 ml of acetic acid, 50 mg (83.8 µmol) BDPA-Amine (**6**) was added. Then, the reaction was refluxed under N_2 atmosphere overnight. The reaction was washed with 20 mL of ethanol, 10 mL of 0.1 M HCl, 10 mL of 0.1 M NaOH, and 10 mL of DI water. Lyophilized samples were subjected to CHNS analysis and BDPA content was found to be 0.020 µmol/mg. FTIR ν 1596, 1157, 1023, 796 cm^{-1}.

2.9 Investigation of the Affinities of Neutral and Negatively Charged Biomembranes Towards Zn_2BDPA-Complex Bearing CMs

2.9.1 Investigation of the Affinities of Neutral and Negatively Charged Liposomes Towards Various Functionalized Cellulose Microspheres

i. Liposome Formation: Stock liposome dispersions (1 mL) with 3.32 mM total lipid were desired. Lipid solutions (compositions given in Table 2.1 and 2.2) were prepared in 13x100 mm test tubes and the solvent was removed by gently blowing nitrogen over them. The lipid films thus formed were dried under vacuum overnight. Lipid films were hydrated with 1000 µL pH 7.4 HEPES buffer (10 mM HEPES, 137 mM NaCl, 3.2 mM KCl, 2 mM NaN_3, 0.1 M $Zn(NO_3)_2$). The hydrated films were subjected to 6x freeze-thaw cycles (40°C ↔ liquid N_2) after which the formed MLVs were subjected to 21 passes through a 200 nm Nucleopore filter to give liposomes.

Table 2.1. Lipid composition for **neutral** liposomes containing **2 mol% DiO**, 3.32 µmol total lipid.

	$[Lipid]_{stock}$ (mM)	Volume (µL)	Moles (µmol)	Mol %
DiO*	0.50	132	0.066	2
POPC	16.45	137.3	2.258	68
Cholesterol	16.45	60.8	1.00	30

*(2Z)-3-octadecyl-2-[(E)-3-(3-octadecyl-1,3-benzoxazol-3-ium-2-yl)prop-2-enylidene]-1,3-benzoxazole perchlorate

Table 2.2. Lipid composition for **negatively charged** liposomes containing **10 mol% POPG-Na** and **2 mol% DiD**, 3.32 µmol total lipid.

	$[Lipid]_{stock}$ (mM)	Volume (µL)	Moles (µmol)	Mol %
DiD*	0.50	132	0.066	2
POPG-Na	1.30	255	0.332	10
POPC	16.45	117.1	1.926	58
Cholesterol	16.45	60.8	1.00	30

*1,1′-dioctadecyl-3,3,3′,3′-tetramethylindodicarbocyanine 4-chlorobenzenesulfonate salt

ii. DLS and Zeta Potential Measurements: 125 μL aliquots of liposomal dispersions were diluted with 875 μL pH 7.4 HEPES buffer and subjected to DLS analysis using a Zetasizer Nano ZS particle sizer. The following settings were used: 173.1° backscatter angle, material used was defined as DPPC, RI = 1.489, absorbance = 0, dispersant H_2O, temperature 25°C. For each sample 3 runs with 11 scans, each scan lasting 10 seconds, was performed (1 sample takes ~6 min to run). Data are reported for intensity particle size distribution results (Intensity PSD). Zeta potentials were measured using the Smoluchowski method.

iii. Preparation of Fluorescence Calibration Graphs: Stock liposomal dispersions prepared as described above were diluted with pH 7.4 HEPES buffer to give liposomal dispersions with dye concentrations of 0.066, 0.132, 0.198, 0.264, 0.330, and 0.660 μM. Fluorescence measurements were taken in at least triplicate at room temperature in a 3 mL quartz cuvette with 1 cm path length. For DiO liposomes (neutral) $\lambda_{excitation}$ was 484 nm and $\lambda_{emission}$ was 501 nm. For DiD liposomes (negatively charged) $\lambda_{excitation}$ was 644 nm and $\lambda_{emission}$ was 663 nm. For all measurements excitation slit width was set to 5 nm and emission slit width to 10 nm.

iv. Determination of the Affinities of Neutral and Negatively Charged Liposomes to Various Functionalized Cellulose Microspheres: 2 mL liposomal dispersions containing 0.132 μM of either dye were mixed with 25 mg each of the six functionalized CMs investigated in this study. The mixtures were incubated at room temperature for 45 minutes in an orbital shaker at 200 rpm. The mixtures were then decanted into fluorescence cuvettes and fluorescence measurements were carried out as described above. Comparison of the fluorescence values obtained through binding experiments with fluorescence values of liposomal dispersions containing 0.132 μM of either dye gave the extend of binding of neutral and negatively charged liposomes to various functionalized CMs. These binding experiments were done at least in triplicate. Student's t-test (one-tailed, 95% probability level) was used to determine whether binding differences were significant or not.

v. Micrographic Investigation of Affinities of Negatively Charged Liposomes to Various Functionalized Cellulose Microspheres: 2 mL negatively charged liposomal dispersions containing 0.132 μM of DiD were mixed with 25 mg each of the six functionalized CMs investigated in this study. The mixtures were incubated at room temperature for 45 minutes in an orbital shaker at 200 rpm. Following incubation, the liquid was decanted and the CMs were washed 4 times using 1000 μL 10 mM pH 7.4 HEPES buffer containing 0.1 mM $Zn(NO_3)_2$. After the final decantation, the CMs were placed on microscopy slides and brightfield and fluorescence (using a TX-2 filter) micrographs were recorded.

2.9.2 Investigation of the Affinities of *Escherichia coli* Cells to Various Functionalized Cellulose Microspheres

i. Preparation of Stock Bacterial Dispersion: 5 mL sterile Lysogeny broth (LB) was inoculated from a frozen bacterial stock dispersion of GFP-expressing *Escherichia coli* (K12 pSB1C3-GFP) and the broth culture was grown in a shaking incubator at 37ºC at 200 rpm overnight. Bacterial cells were pelleted through centrifugation at 3000 rpm for 2 minutes. The bacterial pellet was resuspended in 1 mL of 10 mM pH 7.4 HEPES buffer and pelleted through centrifugation using the aforementioned parameters. The supernatant was removed and bacterial pellets were resuspended in 1 mL of 10 mM pH 7.4 HEPES again. This washing procedure was repeated 3 more times. The pelleted bacterial cells were finally resuspended in 1 mL of 10 mM pH 7.4 HEPES buffer. A bacterial dispersion of $1x10^8$ CFU/mL (CFU = colony forming units) in 10 mM pH 7.4 HEPES buffer containing 0.1 mM $Zn(NO_3)_2$ was prepared through adjustment of the optical density (OD) measured at 600 nm of the washed dispersion obtained above.

ii. Micrographic Investigation of Affinities of *Escherichia coli* Cells to Various Functionalized Cellulose Microspheres: The bacterial stock dispersion was diluted to 10^6 CFU/ml using 10 mM pH 7.4 HEPES buffer containing 0.1 mM $Zn(NO_3)_2$. To 5 mg each of the functionalized CMs of interest in 500 μL PCR vials

was added 250 μL each of the diluted bacterial dispersion and the mixtures were incubated at room temperature in a shaking incubator for 30 min at 250 rpm. Following incubation, the liquid was decanted and the CMs were washed 4 times using 250 μL 10 mM pH 7.4 HEPES buffer containing 0.1 mM $Zn(NO_3)_2$. After the final decantation, the CMs were placed on microscopy slides and brightfield and fluorescence (using a GFP filter) micrographs were recorded.

CHAPTER 3

RESULT AND DISCUSSION

3.1 Studies Towards the Size-Controlled Preparation of CMs

3.1.1 Determination of the Average Molecular Weight of the Cotton Used in This Study

The molecular weight of the cellulose (cotton) used in this work was determined by dissolving differing amounts of celluose in a solution of bis(ethylenediamine)copper(II) hydroxide (CuEn solution) and measuring the viscosities of these cellulose solutions.[73] CuEn is an easier to prepare and more stable version of Schweizer's reagent, ($[Cu(NH_3)_4(H_2O)_2](OH)_2$), which was used in the past for the production of rayon and cellophane from cellulose. Schweizer's reagent (and hence CuEn) reacts with the vicinal diols (on C2 and C3) of the glucose subunits of cellulose to form a complex and as a result renders cellulose soluble in water (Figure 3.1).

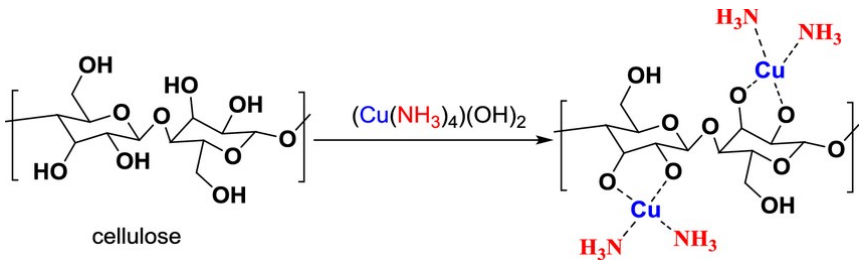

Figure 3.1. Reaction of Schweizer's reagent with cellulose.[74]

To determine the molecular weight of cotton, 3 different concentrations of cotton solution in CuEn were prepared (0.1, 0.2 and 0.4 in g/100 mL). Intrinsic

viscosity was determined using an Ubbelohde capillary viscometer. The relative viscosity (η_{rel}) was determined by dividing the flow time of polymer solution through a capillary by that of pure solution:

$$\eta_{rel} = \eta / \eta_0$$

$$\eta_{rel} = t_{solution} / t_{solvent}$$

where η is the viscosity of solution , η_0 is the viscosity of pure solvent, and η_{rel} is relative viscosity. $t_{solvent}$ was found to be 350 seconds. The data obtained for viscosity measurements are given in Table 3.1.

Table 3.1. Viscosity measurement for the detemination of cellulose molecular weight.

c **(g/ 100 mL)**	$t_{solution}$ **(s)**	$t_{solution} / t_{solvent}$	$\ln(\eta_{rel})$	$\ln(\eta_{rel})/c$
0.1	597	1.705714286	0.533984	5.33984
0.2	899	2.568571429	0.94335	4.716749
0.4	1591	4.545714286	1.514185	3.785462

$ln(\eta_{rel})/c$ was plotted againts c (i.e. concentration) (Figure 3.2). According to the Kraemer equation,

$$\frac{ln(\eta_{rel})}{c} = [\eta] - k_K[\eta]^2 c$$

the intercept of the graph gave the intrinsic viscosity, [η], as 5.805 cm^3/g. The average viscometric degree of polymerization was then calculated by multiplying the intrinsic viscosity with 190 according to the Mark-Houwink-Sakurada equation.[65] The degree of polymerization for the cotton used was found to be 1103. The molecular weight of anhydroglucose monomer was taken as 162 g/mol. Therefore, the molecular weight of the cotton used in this study was found to be about 179 kDa.

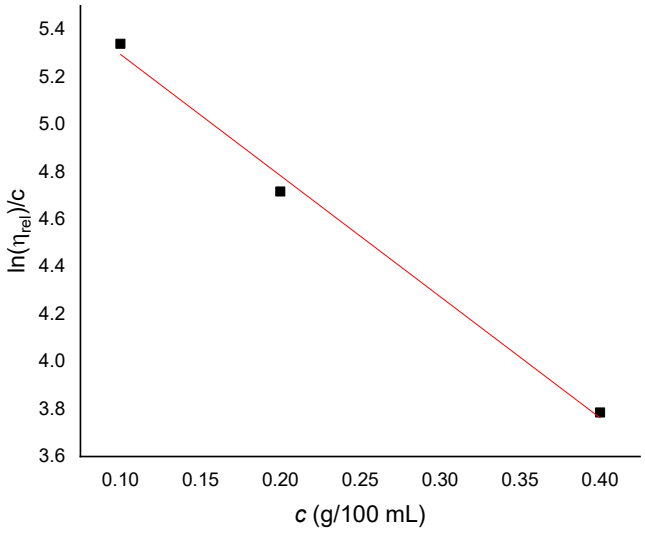

Figure 3.2. *ln(*η_{rel}*)/c* versus *c* (i.e. concentration) plot (Slope = -5.106, intercept = 5.805, R^2 = 0.9942).

3.1.2 Attempts at Preparation of CMs Using a Non-Derivatizing Solvent System

Following a procedure by Zhang and coworkers,[66] attempts were made to dissolve cotton in a solution comprised of 7/12/81(w/w/w) NaOH/urea/water. The mixture was agitated using a mechanical stirrer at 1000 rpm at a temperature of -11°C. Dissolution of cotton, which would have been evidenced by formation of a transparent solution, was not observed after 30 minutes. Increasing the dissolution time or rotor speed (1200-2000 rpm) did not change the outcome. Numerous other conditions reported for the NaOH/urea/water system were also explored, but none yielded satisfactory cellulose solutions (Table 3.1). Zhang herself underscores the need for improvements to the solvent system by stating "The NaOH/urea system requires further investigation to enhance the dissolving capacity and the stability of the cellulose solution."[75]

Table 3.2. Attempts at dissolving cellulose using the NaOH/urea/H_2O non-derivatizing solvent system.

Solvent System	Rotor Speed (rpm)	Time (min)	Temperature (°C)	Source of Cellulose
7 / 12 / 81 NaOH/Urea/H_2O	800	15-60	-10	Medical Cotton
	1000	30-60	-12	Cosmetic Cotton
	1200	45-60	-14	High Quality
	1400	60	-16	Ashless Filter
	1600	60	-20	Paper
	1800	30-60	-20	A4 Paper
	2000	30-60	-20	A4 Paper
8 / 6 / 86 NaOH/Urea/H_2O	2000	30-60	-16	Medical and Cosmetic Cotton
6 / 8 / 86 NaOH/Urea/H_2O	2000	30-60	-16	Medical and Cosmetic Cotton

3.1.3 Preparation of CMs Through the Thermal Regeneration of Cellulose from Water-in-Oil Emulsions of Viscose

Since the NaOH/urea/H_2O system did not give the desired results, the more well-established method of obtaining a viscose solution from cellulose, dispersion of viscose in oil, and thermal cellulose regeneration was tried.[45,75] In the method developed on this basis, cotton was first kept in a 20% NaOH solution, squeezed and aged for 2 days. Then, an appropriate amount of carbon disulfide (CS_2) was added to this processed cotton and cellulose xanthate was allowed to form overnight. After cellulose xanthate was formed, a viscose solution was prepared using 6% aqueous NaOH solution. The viscose solution had a viscosity of 16.101 Pa·s at 25°C and 7.227 Pa·s at 50°C. The viscose solution was dispersed into paraffin oil (viscosity 0.029, 0.018, and 0.012 Pa·s at 25, 35, and 48°C respectively), and which contained a certain amount of surfactant (for example, Span 80), and then this emulsion was heated to 95°C and regenerated cellulose microspheres were obtained (Scheme 3.1). The microspheres were washed (water, EtOH, hexane, acetone) and freed from

paraffin. The product was sieved to separate the microspheres from large cellulose particles and aggregates.

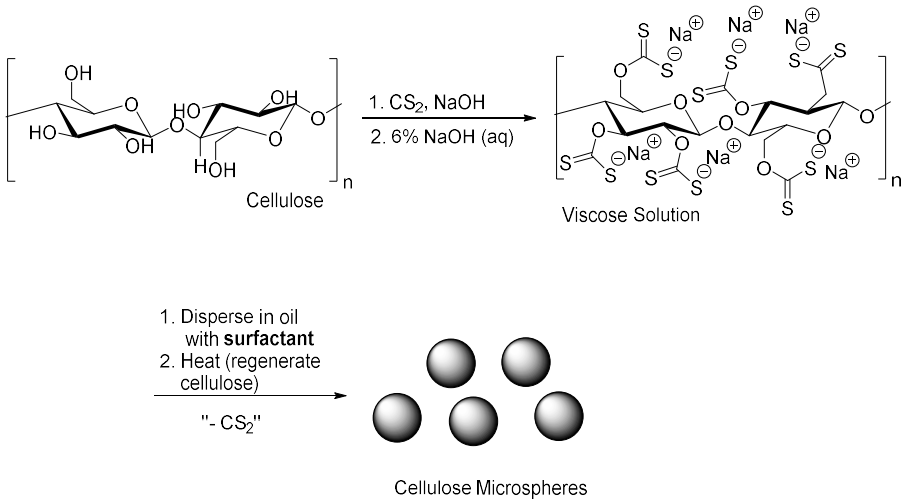

Scheme 3.1. Formation of CMs through the thermal regeneration of cellulose from water-in-oil emulsions of viscose.

3.2 Some Initial Results for CM Formation

Numerous experiments have been carried out to obtain microspheres using this method. Details of some of these experiments are given in Table 3.4. The microsphere diameters given here were found by light microscopy. SEM images for CM-I, CM-III, and CM-IV are given in Figure 3.3. In Table 3.4, data for commercial products Perloza ST Fine (PSTF, 50-75 m), Perloza ST Medium (PSTM, 75-150 μm), and Perloza ST Coarse (PSTC, 150-300 μm) are given as well. SEM images for the commercial CMs are given in Figure 3.4. SEM images indicate that the CMs obtained in this study have smoother surfaces and are likely to be less porous than the comercial oners. The initial results indicated that the method developed in these early experiments allowed for the preparation of CMs with diameters in the 40-250 μm range in a controlled manner.

Table 3.3. Some initial results for CM formation.

Microspheres	*Surfactant Type*	*Surfactant Weight (mg)*	*Rotor Speed (rpm)*	*Proper Microspheres?*	*Diameter*
CM-I	Span 80	660	1000	Yes	39.3 ± 10.0
CM-II	Span 80	660	750	Yes	84.8 ± 27.3
CM-III	Span 80	330	500	Yes	107.0 ± 24.1
CM-IV	Span 80	165	500	Yes	168.2 ± 50.6
CM-V	Span 80	80	500	Partial	>250
Perloza-Fine	NA	NA	NA	Yes	62.6 ± 6.8
Perloza-Medium	NA	NA	NA	Yes	141.5 ± 39.4
Perloza-Coarse	NA	NA	NA	Yes	250.1 ± 56.2

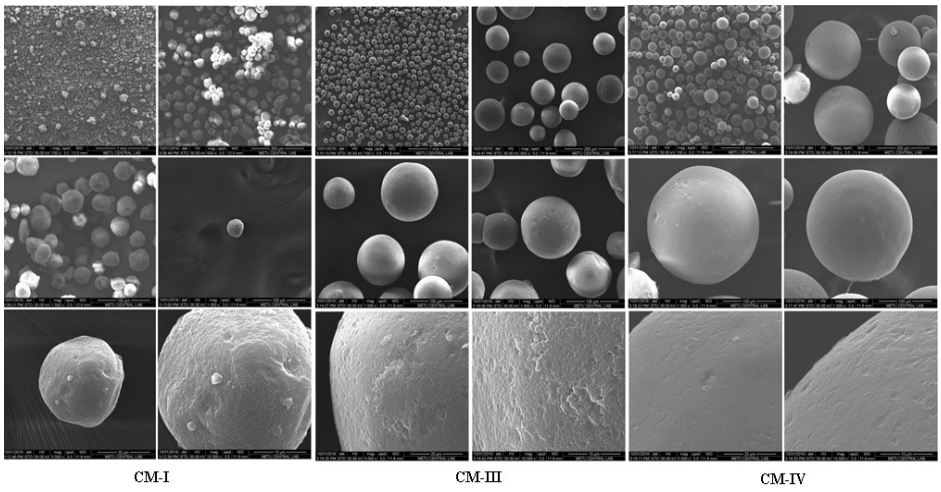

Figure 3.3. SEM images of CM-I, CM-III, and CM-IV.

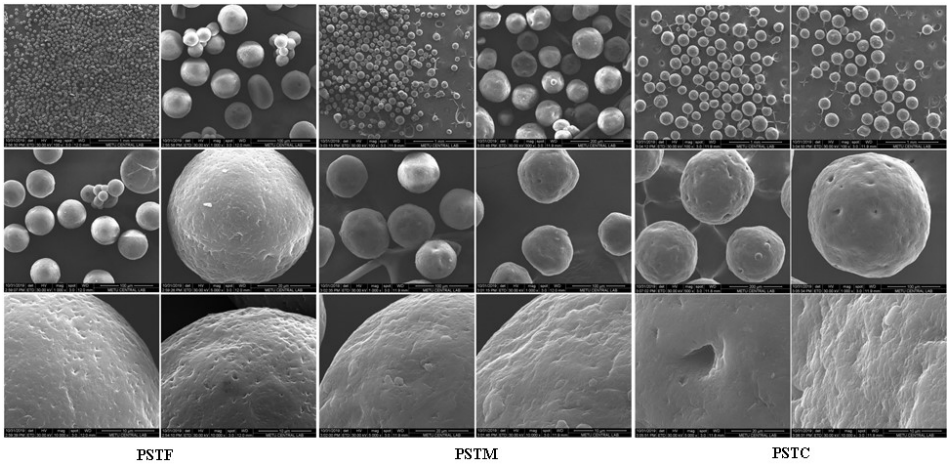

Figure 3.4. SEM images of PSTF, PSTM, and PSTC.

These CMs were further analyzed using FTIR (KBr). The bands at 897, 1106, 1159, 1427 cm^{-1} (Figure 3.5) correspond to asymmetric stretching of the ring, asymmetric stretching of C-O-C, and symmetric bending vibration of CH_2 for native cellulose.[2] The weak band at 898 cm^{-1}, which is characteristic of native cellulose (Cellulose I), is replaced by a stronger band at 894 cm^{-1}, which is characteristic of regenerated cellulose (Cellulose II) in PSTF. Additionally, the peak at 1427 cm^{-1} dissappeared and a peak at 1366 cm^{-1} appeared when cellulose was regenerated. Furthermore, commercial PSTF (and also PSTM and PSTC, data not shown) CMs and the CMs obtained in this study have almost identical FTIR spectra (Figure 3.6).

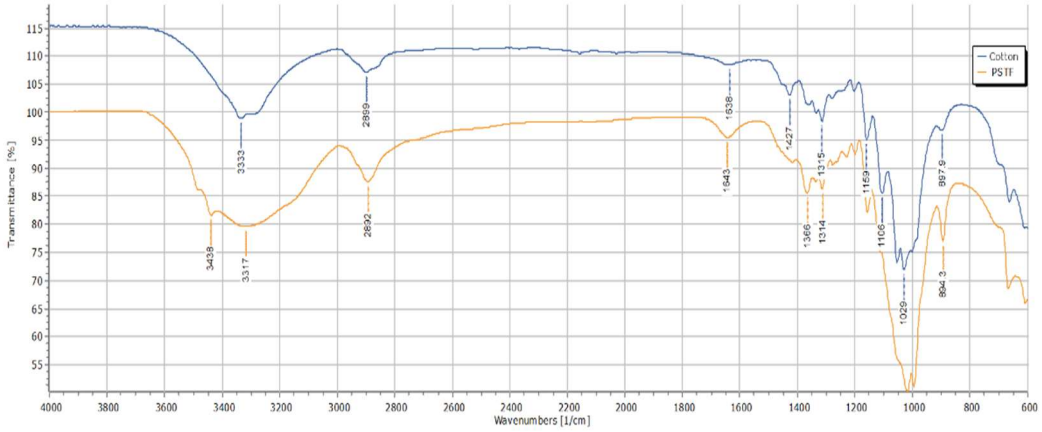

Figure 3.5. FTIR spectra of cotton and PSTF commercial CMs.

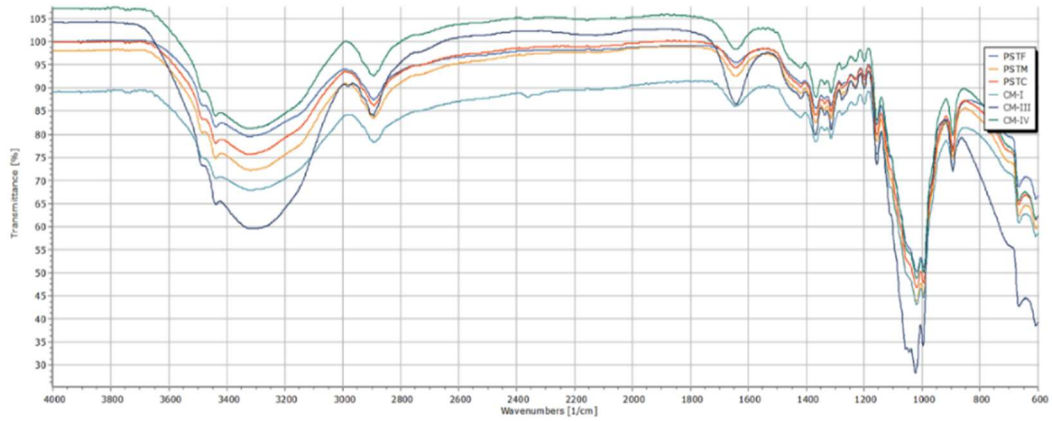

Figure 3.6. FTIR spectra for PSTF CMs and CMs (CM-I, CM-II, CM-IV) obtained in this study.

3.3 Investigation of the Factors Affecting the Particle Size of CMs Obtained Through the Thermal Regeneration of Cellulose from Water-in-Oil Emulsions of Viscose

With the initial success in CM formation, it was decided to further investigate the factors that might affect the particle sizes of the CMs obtained through the thermal regeneration of cellulose from water-in-oil emulsions of viscose. The following factors were investigated in this study: i. Amount of surfactant; ii. Type of surfactant; iii. Viscose droplet size, iv. Rotor speed (rpm), v. Rotor size. Other factors such as viscose solution concentration and aqueous/organic phase ratio were not investigated in this study. Before this study the viscose production process was optimized so that the concentration of cellulose did not vary from experiment to experiment. Also, in order to improve reproducibility, a syringe pump was employed to deliver the viscose solution to the paraffin oil at reproducible rates.

3.3.1 Reference Microspheres

In order to determine the effect of the above factors on the size of CMs, it is necessary to select reference CMs. The reference CMs were obtained by adding dropwise (approximately 17.8 µL drop volume) 25 mL viscose solution (0.08 g/ml cellulose) into 240 ml liquid paraffin which is containing 330 mg Span 80 over 45 minutes with a rotor speed of 500 rpm. After the addition was completed. The dispersion was stirred for an additional 1 hour at room temperature, after which the temperature was raised to 95°C over half an hour and kept at that temperature for 2.5 hours. The CMs were isolated as described in the experimental section. The CMs (CM-Ref) were obtained as a result of three experiments were passed through 4 different analysis sieves and their weight distribution was determined according to the size range (Table 3.4). The mean diameter of the CM-Ref was measured as 174.78 µm using a Mastersizer particle sizer (Figure 3.7). After staining the same

spheres with Congo red, micrographs were taken with 100x magnification (Figure 3.8).

Table 3.4. Sieving data for reference CMs.

CM	*Surfactant Type*	*Surfactant Quantity (mg)*	*Rotor Speed (rpm)*	*42-150 µm Weight (%)*	*150-320 µm Weight (%)*	*320-500 µm Weight (%)*
CM-REF	Span 80	330	500	56.77	38.12	5.11

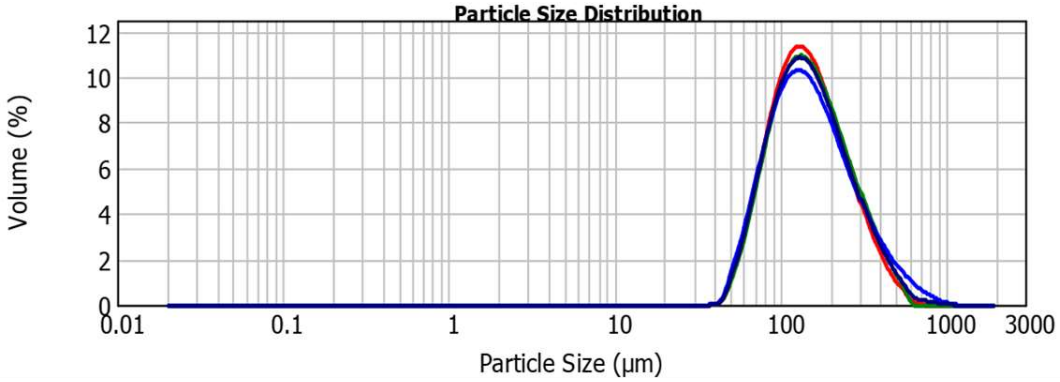

Figure 3.7. Mastersizer analysis of reference CMs.

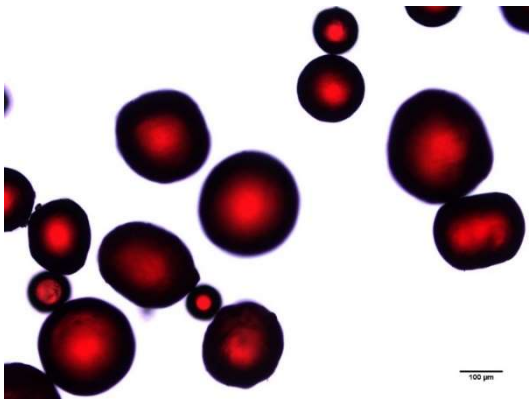

Figure 3.8. Light micrography (Congo red staining) of reference CMs.

3.3.2 Effect of Viscose Solution Droplet Size on CM Diameter

In this study, the effect of droplet volume on the diameters of the final CMs during the transfer of viscose solutions to the paraffin phase was investigated. Three

different droplet sizes were studied: i. 12.5 µL (CM-A) was the small size; ii. 17.8 µL (CM-REF) was the medium size; and iii. 46.6 µL was the large (CM-B). The transfer of the viscose to the liquid paraffin phase was done with a syringe pump within 45 minutes, after which the system was continued to be mixed at 500 rpm for an additional hour at room temperature to equilibrate, then the thermal cellulose regeneration step was started. The morphologies of the formed CMs were examined by light micrography analysis (Figure 3.10). It has been shown through the use analysis sieves (Table 3.5) and Mastersizer particle size analysis (Figure 3.9 and Table 3.6) that the diameters of the CMs increase as the droplet size increases.

Table 3.5. Sieving data for the study investigating the effect of viscose droplet size on CM diameter.

Microspheres	*Droplet Volume (µL)*	*42-150 µm Weight (%)*	*150-320 µm Weight (%)*	*320-500 µm Weight (%)*
CM-A	12.5	72.74	27.26	0
CM-REF	17.8	56.77	38.12	5.11
CM-B	46.6	30.33	50.11	19.56

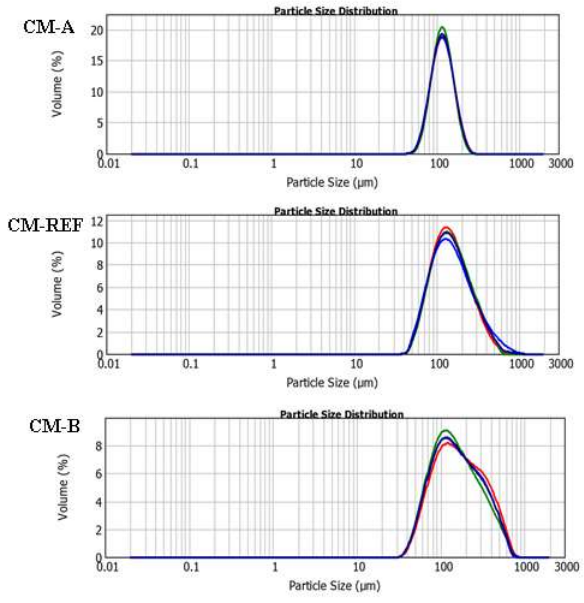

Figure 3.9. Mastersizer analysis of effect of viscose droplet size on CM diameter.

Table 3.6. Average diameter of CM-A, CM-Ref, CM-B (Mastersizer).

Microspheres	*Droplet Volume (µL)*	*CM Diameter (µm)*
CM-A	12.5	122.89
CM-REF	17.8	174.78
CM-B	46.6	193.00

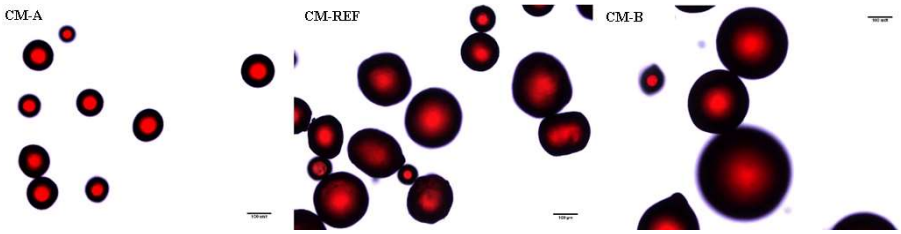

Figure 3.10. Light micrography (Congo red staining) of CM-A, CM-Ref, and CM-B.

3.3.3 Effect of Quantity of Surfactant (Span 80)

In this study, the effect of the amount of Span 80 used as surfactant on the diameters of the obtained CMs was investigated. The amount of Span 80 was tested as 80, 165, 330 and 660 mg, while the viscose volume was 25 ml, the liquid paraffin volume was 240 ml, the rotor speed was 500 rpm, and the viscose droplet volume was 17.8 µL. The morphologies of the obtained CMs were examined by light micrograph analysis (Figure 3.12). It is shown by using analysis sieve (Table 3.7) and Mastersizer particle size analysis (Figure 3.11 and Table 3.8) that the diameters of the obtained CMs decrease as the amount of Span 80 increases. The surfactant stabilizes water droplets (i.e. viscose solution) in the oil phase by forming monolayers around them, therefore it is reasonable to assume that an increase in surfactant concentration would allow for the stabilization of smaller water droplets.

Table 3.7. Sieving data for the investigation of the effect of the quantity of surfactant on CM diameter.

Microspheres	*Quantity of Span 80 (mg)*	*42-150 µm Weight (%)*	*150-320 µm Weight (%)*	*320-500 µm Weight (%)*
CM-C	80	12.73	74.16	13.12
CM-D	165	31.10	59.64	9.27
CM-REF	330	56.77	38.12	5.11
CM-E	660	83.66	16.34	0

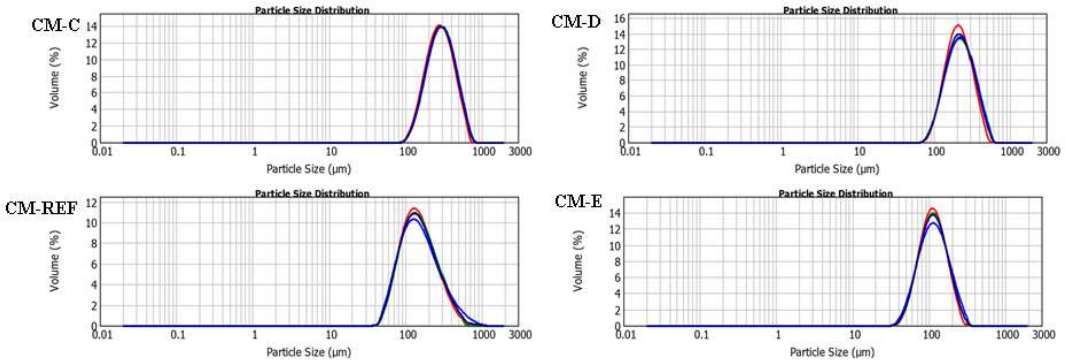

Figure 3.11. Mastersizer analysis of effect of quantity of Span 80 on CM diameter.

Table 3.8. Average diameter of CM-C, CM-D, CM-Ref, CM-E (Mastersizer).

Microspheres	*Quantity of Span 80 (mg)*	*CM Diameter (µm)*
CM-C	80	312.87
CM-D	165	236.69
CM-REF	330	174.78
CM-E	660	123.54

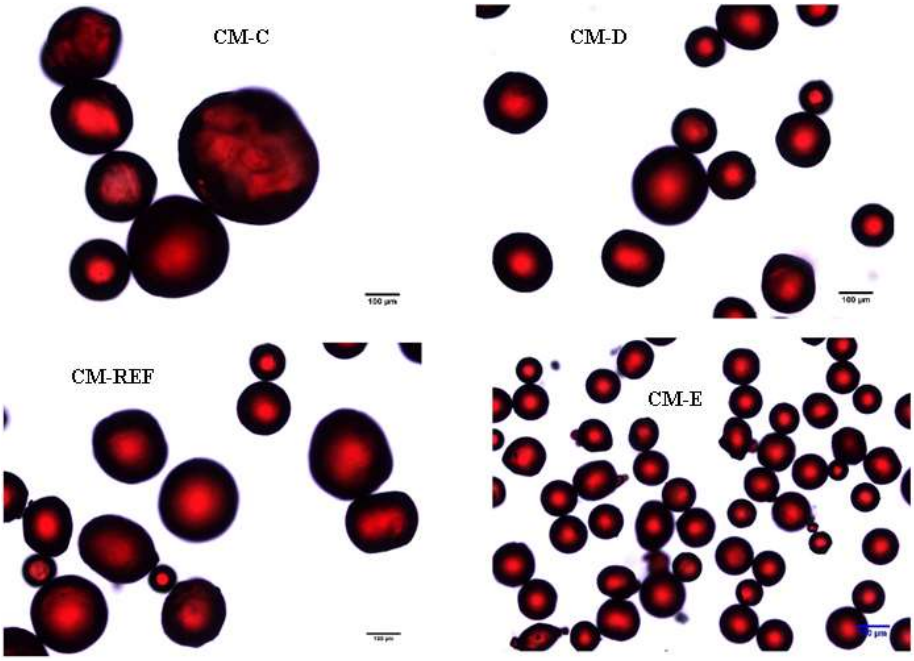

Figure 3.12. Light micrography of CM-C, CM-D, CM-Ref, and CM-E.

3.3.4 Effect of the Type of Surfactant on CM Diameter

In this study, surfactant mole number was kept constant to be equal to the number of moles of 330 mg Span 80 and surfactant type was changed. Span 80, Span 85, oleic acid, Tween 40, and Tween 80 were used as surfactants (Figure 3.13). The viscose volume was 25 ml, the liquid paraffin volume was 240 ml, the rotor speed was 500 rpm, and the viscose droplet volume was kept constant at 17.8 µL. The size-diameter distribution of the CMs were determined using analysis sieves (Table 3.9). The diameter of the CMs increased with decrease of HLB value. Tween 40 and Tween 80, which are generally used for stabilization of oil-in-water emulsions, did not allow for the preparation CMs under these conditions.

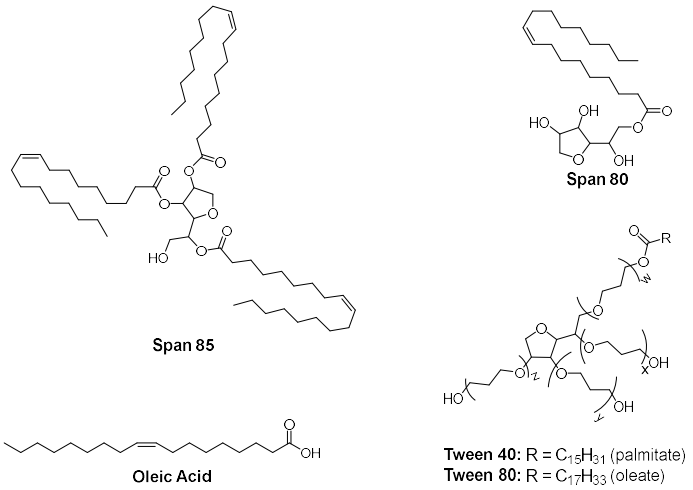

Figure 3.13. Surfactants used in this study.

Table 3.9 Sieving data for effect of surfactant type on CM size.

Microspheres	*Surfactant Type and Quantity (mg)*	*42-150 µm Weight (%)*	*150-320 µm Weight (%)*	*320-500 µm Weight (%)*	*HLB Value*
CM-REF	Span 80 (330 mg)	56.77	38.12	5.11	4.3
CM-F	Span 85 (737 mg)	26.40	34.44	39.17	1.8
CM-G	Oleic Acid (217 mg)	25.00	75.00	0	1.6
CM-H	Tween 40 (988 mg)	-	-	-	15.6
CM-I	Tween 80 (1009 mg)	-	-	-	15

3.3.5 Effect of the Rotor Speed (rpm) on CM Diameter

In this study, the effect of rotor rotation speed (rpm) on the diameters of CMs was investigated. Rotor rotation speeds were selected as 250, 500, 750 and 1000 rpms. In these experiments, the Span 80 amount was kept constant at 330 mg, viscose volume was 25 ml, liquid paraffin volume was 240 ml, and viscose droplet volume was 17.8 µL. The morphologies of the obtained CMs were examined by light micrography (Figure 3.15). It is shown through analysis sieve (Table 3.10) and Mastersizer particle size analysis (Figure 3.14 and Table 3.11) that the diameters of

the obtained CMs decrease as the rotor speed increases. CMs could not be obtained when 250 rpm rotor rotation speed was used. As the speed of the rotor increases the shear forces that result cause the formation of finer water droplets, therefore larger rotor speeds result in smaller CMs. Viscose emulsions in paraffin oil are not thermodynamically stable, therefore when agitation drops below a certain limit, as demonstrated in the experiment where the rotor speed was 250 rpm (CM-J, Table 3.10), viscose droplets coalesce and do not form CMs.

Table 3.10. Sieving data for the effect of rotor speed (rpm) on CM size.

Microspheres	*Rotor Speed (RPM)*	*42-150 µm Weight (%)*	*150-320 µm Weight (%)*	*320-500 µm Weight (%)*
CM-J	250	-	-	-
CM-REF	500	56.77	38.12	5.11
CM-K	750	69.43	30.57	0
CM-L	1000	87.68	12.32	0

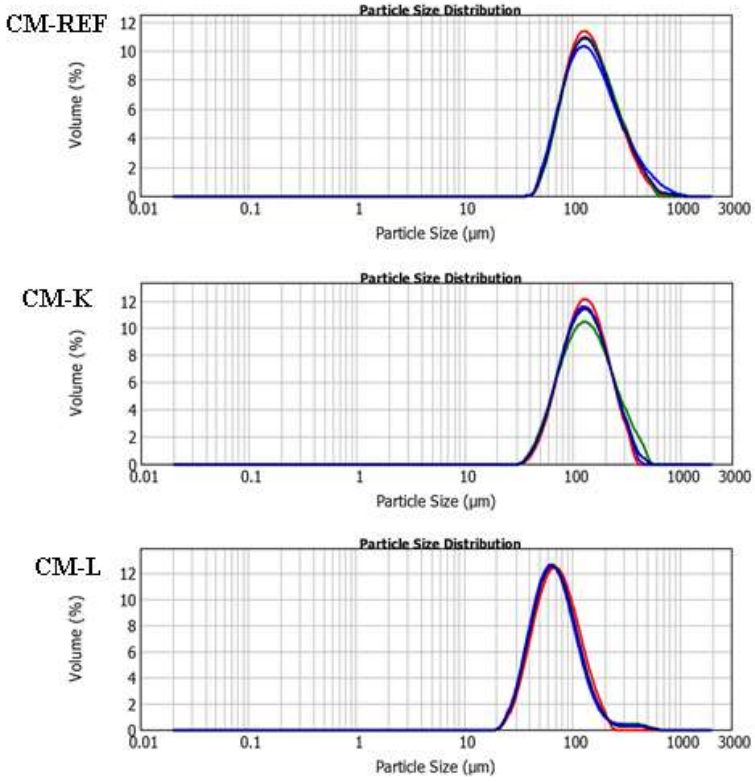

Figure 3.14. Mastersizer analysis for the effect of rotor speed (rpm) on CM diameter.

Table 3.11. Average diameters of CM-J, CM-Ref, CM-K, and CM-L (Mastersizer).

Microspheres	*Rotor Speed (rpm)*	*CM Diameter (µm)*
CM-J	250	-
CM-REF	500	174.78
CM-K	750	148.07
CM-L	1000	80.25

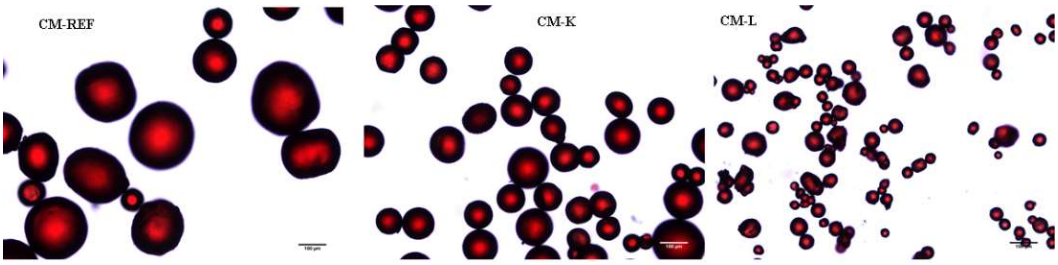

Figure 3.15. Light micrography (Congo red staining) of CM-Ref, CM-K, and CM-L.

3.3.6 Effect of the Rotor Size on CM Diameter

In this study, the effect of two different rotors (Figure 3.16; Rotor A 1x3.1 cm; Rotor B 1.5x5.8 cm) on the diameters of CMs was investigated. Rotor A was used in all previous studies. In these experiments, Span 80 amount was kept constant at 330 mg, viscose volume was 25 mL, liquid paraffin volume 240 ml, rotor speed was 500 rpm, and viscose droplet volume was 17.8 µL. The morphologies of the obtained CMs were examined by light micrography (Figure 3.18). It is shown by using analysis sieves (Table 3.12) and Mastersizer particle size analysis (Figure 3.17 and Table 3.13) that the diameters of the CMs were smaller when the rotor with larger dimensions was employed. The mechanical stirrer used in this study regulates the torque delivered to the solution in order to maintain the rotor speed at the set value, therefore the force applied to the dispersion is larger for the rotor with larger dimensions. Larger forces would result in larger shear forces experienced by the water droplets, which in turn would result in smaller CMs.

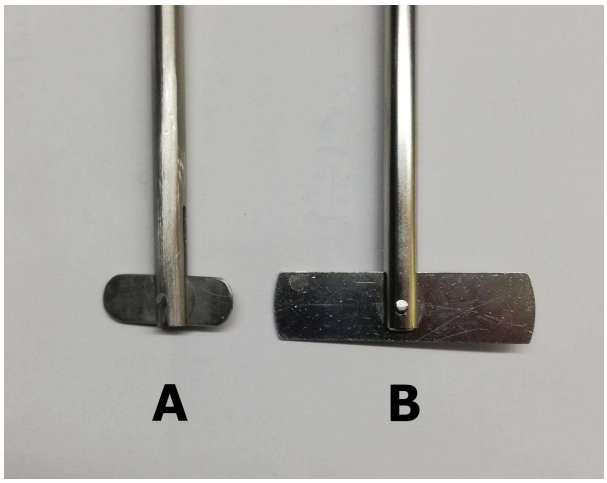

Figure 3.16. Rotors: Rotor A (*1x3.1 cm*), Rotor B (*1.5x5.8 cm*)

Table 3.12. Sieving data for the investigation of the effect of rotor size on CM diameter.

Microspheres	***Rotor***	***42-150 µm Weight (%)***	***150-320 µm Weight (%)***	***320-500 µm Weight (%)***
CM-REF	Rotor A (1x3.1 cm)	56.77	38.12	5.11
CM-M	Rotor B (1.5x5.8 cm)	95.73	4.27	0

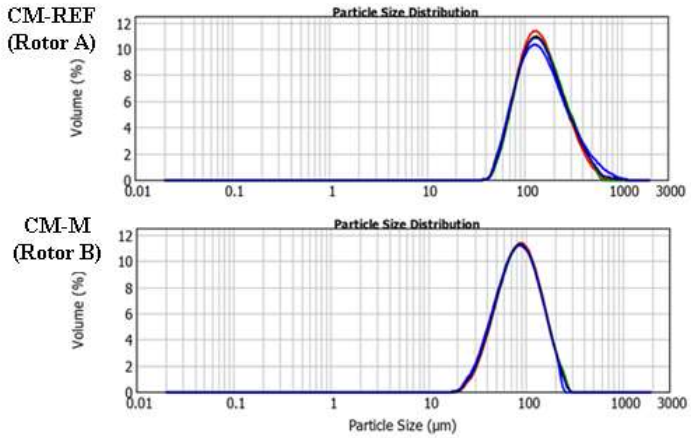

Figure 3.17. Mastersizer particle size analysis of the effect of rotor size on CM particle size.

Table 3.13. Average diameters of CM-Ref and CM-M.

Microspheres	*Rotor*	*CM Diameter (µm)*
CM-REF	Rotor A (1x3.1 cm)	174.78
CM-M	Rotor B (1.5x5.8 cm)	95.16

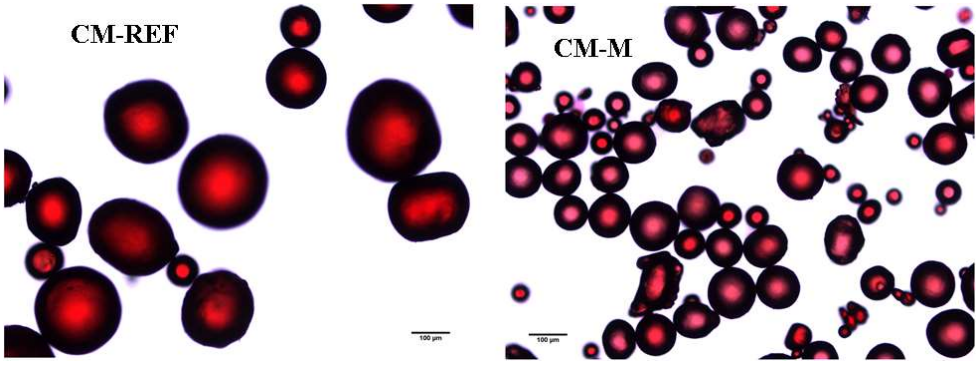

Figure 3.18. Light micrography of CM-Ref (Rotor A) and CM-M (Rotor B).

3.3.7 Studies Towards the Determination of the Maximum and Minimum Size CMs Obtainable Using this Method

In this study the maximum and minimum size CMs attainable using this method was investigated. To make large CMs a mixture of Span 80 and Tween 80 as surfactants was used. The Span 80 amount was 292 mg, the Tween 80 amount was 100 mg, the viscose volume was 25 mL, liquid paraffin volume was 240 mL, rotor speed was 500 rpm, and the viscose droplet volume was 46.6 µL. Weight based size distribution results from analysis sieves are given in Table 3.14. Mastersizer particle size analysis indicates an average diameter of 689 µm for CM-N (large CMs), compared to 175 µm for CM-Ref. Based on the previously tested parameters, preparation of minimum sized cellulose microspheres was also attempted. The Span 80 amount was 660 mg, viscose volume was 25 mL, liquid paraffin volume was 240 mL, rotor speed was 1250 rpm, and viscose droplet volume was 12.5 µL. Weight based size distribution results from analysis sieves for the minimum sized CMs (CM-O) are given in Table 3.14.

Table 3.14. Sieving data for the determination of maximum and minimum size CMs.

Microspheres	*Droplet Volume (µL)*	*<42 µm Weight (%)*	*42-150 µm Weight (%)*	*150-320 µm Weight (%)*	*320-500 µm Weight (%)*	*500> µm Weight (%)*
CM-N	12.5	82.28	17.72	0	0	0
CM-REF	17.8	0	56.77	38.12	5.11	0
CM-O	46.6	0	30.33	9.01	63.06	27.93

3.4 Activation of Cellulose Microspheres

For all activation studies reported here the principal CMs employed were PSTF-CMs. CMs prepared in this work were subjected to some of the activation reactions to demonstrate similar reactivity as commercial CMs.

3.4.1 Epoxy Functionalized CMs

Epoxidation of CMs has been attempted because it is a relatively common and easy method for CM activation. Furthermore, BDPA-CMs can be obtained by reacting epoxy-CMs with BDPA-amine ligand **10**. To this end PSTF, PSTM, PSTC, and CM-III were reacted with epichlorohydrin in aqueous NaOH at 40°C (Scheme 3.2). After washing with copious amounts of water and acetone, the epoxy-CMs were air-dried and then lyophilized. After lyophilization, the epoxy content of CMs was found by titration of the hydroxide ions, which are released by their reaction with sodium thiosulfate, with HCl.[76] The results obtained are given in Table 3.15.

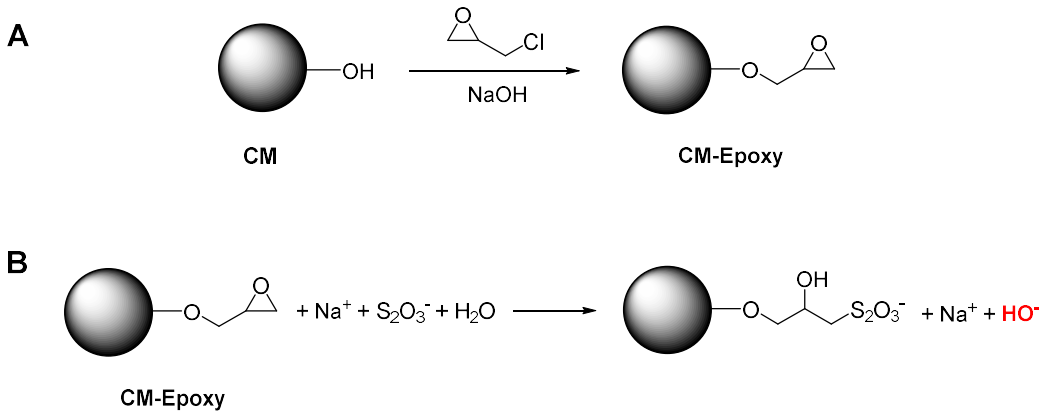

Scheme 3.2. Formation of epoxy-CMs by reaction of CMs with epichlorohydrin (A) and titration of epoxy groups on epoxy-CMs using sodium thiosulphate (B).

Table 3.15. Epoxy content of various epoxy-CMs based on thiosulphate titration.

Epoxy	*Epoxy Content (µmol/g)*
Epoxy-PSTF	735
Epoxy-PSTM	750
Epoxy-PSTC	734
Epoxy-CM-III	648

3.4.2 Amine Functionalized Cellulose Microspheres

BDPA-CMs could also be prepared by coupling of BDPA-acid ligand **6** with amine-bearing CMs through amide bond formation. For this purpose, amine-CMs were obtained by treating epoxy-CMs with ammonia solution (Scheme 3.3).[77] The amine group concentrations in amine-CMs were determined through CHNS analysis (Table 3.16). FTIR spectra of epoxy-CM and amine-CM are given in Figure 3.19. The peaks at 1580, 1237, and 797 cm^{-1} are indicative of epoxy functionality and disappear upon treatment with ammonia solution.[78]

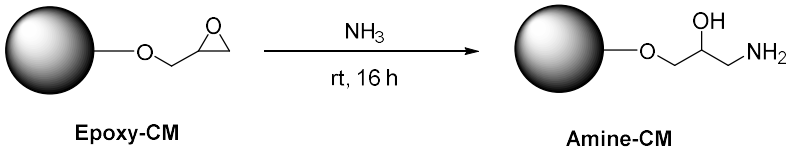

Scheme 3.3. Preparation of amine-CM by reaction of epoxy-CM with ammonia solution.

Table 3.16. Nitrogen content of various amine-CMs determined through CHNS analysis.

Amine-CM	*Amine Content (µmol/g)*
Amine-PSTF	421
Amine-PSTM	343
Amine-PSTC	414
Amine-CM-III	257

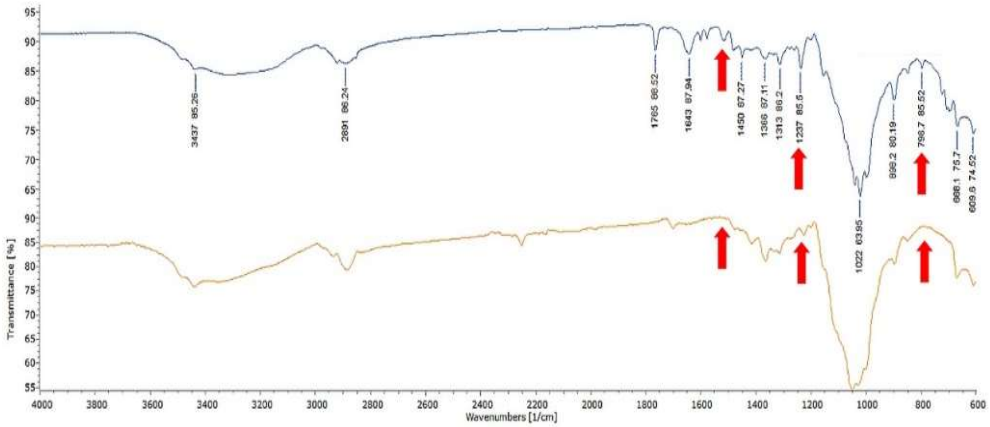

Figure 3.19. FTIR spectra for epoxy-CM (upper spectrum) and amine-CM (lower spectrum).

3.4.3 Cyano Functionalized Cellulose Microspheres

Cyano functionalized CMs could be reduced to give alternative amine-CMs. Therefore, studies have been conducted on the cyanoethylation of CMs with acrylonitrile. Briefly, CMs were first treated with a 0.5 M NaOH solution, then mixed with acrylonitrile in dioxane at room temperature while agitating and 150 rpm for 3 hours (Scheme 3.4). After the reaction, derivatized CMs were washed with

water and acetone and dried. It can be seen from the FTIR spectrum that cyano-CM has a new sharp peak at about 2251 cm^{-1}, indicative of the presence of cyano functional group (Figure 3.20). It is the characteristic band for stretching vibration of C≡N.[79] Furthermore, stretching vibration of OH groups were shifted from 3400 to 3440 cm^{-1} and new absorption band was observed at 1700 cm^{-1}.[80] A number of reactions were carried out to reduce the cyano functionality (Scheme 3.5). First, cyano-CMs were reacted with a solution of $NaBH_4$ in diglyme followed by addition of $BF_3{\cdot}OEt$. After washing with water and ethanol, the CMs obtained were air-dried and then lyophilized. FTIR spectra of these CMs showed that there was no change in peak at 2251 cm^{-1}. Therefore, it was concluded that the reaction was not successful (Method A). Secondly, cyano-CMs were added to a solution of $LiAlH_4$ in THF. After the reaction, the CMs were washed with water and ethanol. FTIR spectra of these CMs showed that there was no change in the peak at 2251 cm^{-1} (Method B). Finally, to a dispersion of cyano-CMs in THF, 1 M $BH_3{\cdot}THF$ was added dropwise and then the reaction was refluxed under a N_2 atmosphere for 5 hours. After that methanol was added to the reaction to destroy excess borane complex. The slurry was refluxed for 1h. After the reaction, the CMs were washed with water and ethanol. The reaction apparently did not go to completion and the peak at 2251 cm^{-1} was observed again in the FTIR spectrum of the product (Method C).

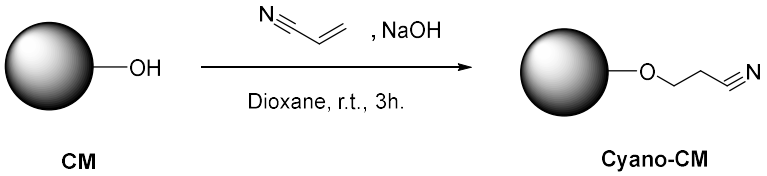

Scheme 3.4. Preparation of cyano-CM by cyanoethylation of CMs.

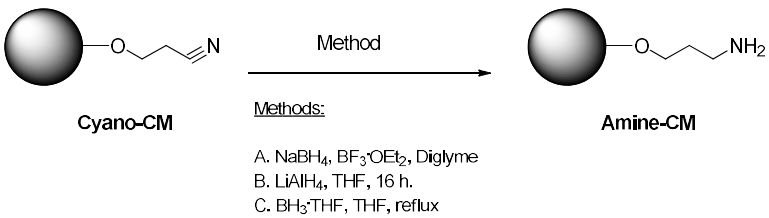

Scheme 3.5. Attempts at the reduction of the cyano functionality.

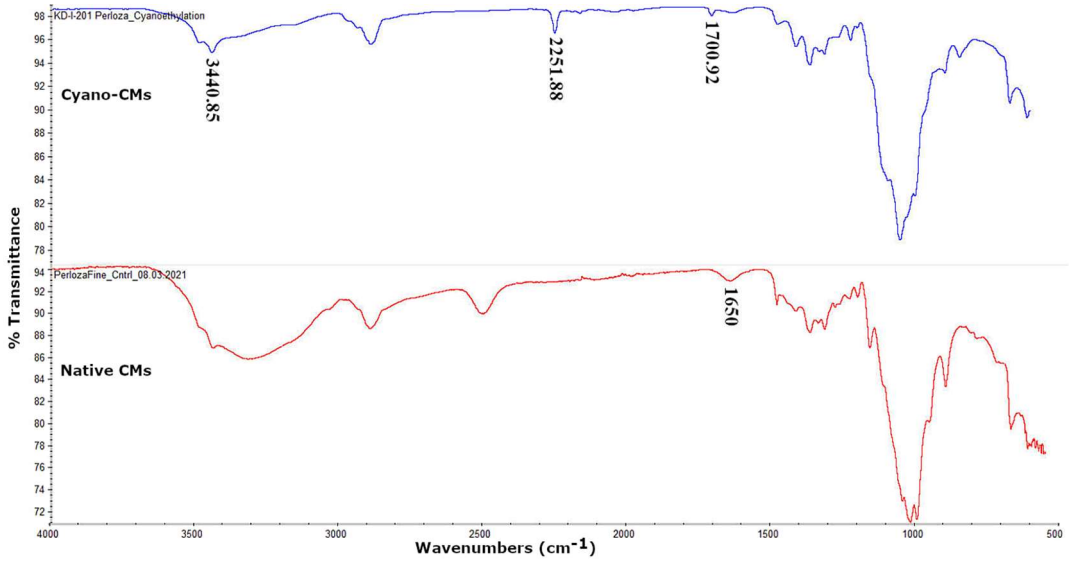

Figure 3.20. FTIR spectra of cyano-CM (upper spectrum) and native CMs (lower spectrum).

3.4.4 Bisaldehyde Functionalized Cellulose Microspheres

BDPA-CMs could also be prepared through a reductive amination reaction between BDPA-amine ligand **10** to aldehyde functional group bearing CMs. Therefore, studies were conducted to obtain bisaldehyde-CMs through oxidation of CMs with $NaIO_4$ (Scheme 3.6).[67] Several batches of bisaldehyde-CMs were prepared and aldehyde concentrations were found to be in the 5.79 – 12.87 mmol/g range by titration.[68] The carbonyl peak expected at 1720 cm^{-1} for the aldehyde group in cellulose dialdehyde products is often seen at 1640 cm^{-1} due to water adsorption.[81] A similar peak is observed in our FTIR measurements (Figure 3.21, lower spectrum). Lyophilization resulted in a shift of the carbonyl peak to around 1698 cm^{-1} (Figure 3.21, upper spectrum)

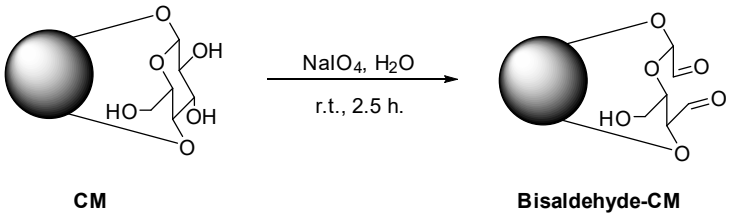

Scheme 3.6. Preparation of bisaldehyde-CMs through oxidation of CMs.

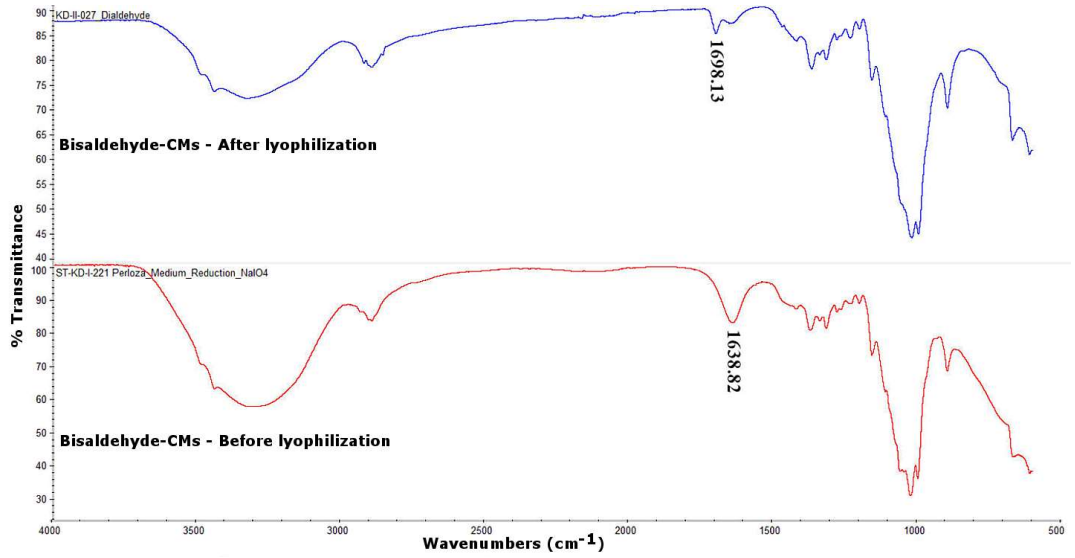

Figure 3.21. FTIR spectra of bisaldehyde-CMs before (lower spectrum) and after lyophilization (upper spectrum).

3.4.5 Biscarboxyl Functionalized Cellulose Microspheres

It is possible to further oxidize bisaldehyde-CMs to dicarboxylic acid derivatives. biscarboxyl-CMs could then be coupled with BDPA-amine ligand **10** through amide bond formation. Conversion of bisaldehyde-CMs to biscarboxyl-CMs using $NaClO_2$ was attempted (Scheme 3.7).[69] A decrease in the aldehyde peak and a weak peak formation were observed in the 1710 cm^{-1} region (Figure 3.22, upper spectrum). The reaction did not go to completion. Presumably, the biscarboxyl derivative was formed with low efficiency. Carboxyl group concentration was determined by titration as 0.233 mmol/g.

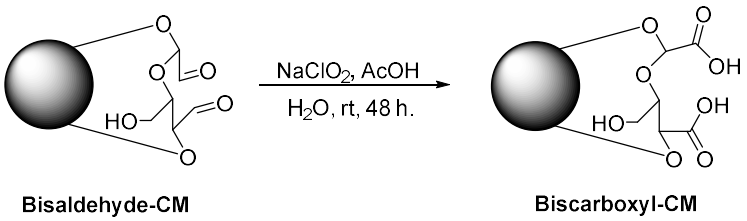

Scheme 3.7. Attempted preparation of biscarboxyl-CMs from bisaldehyde-CMs.

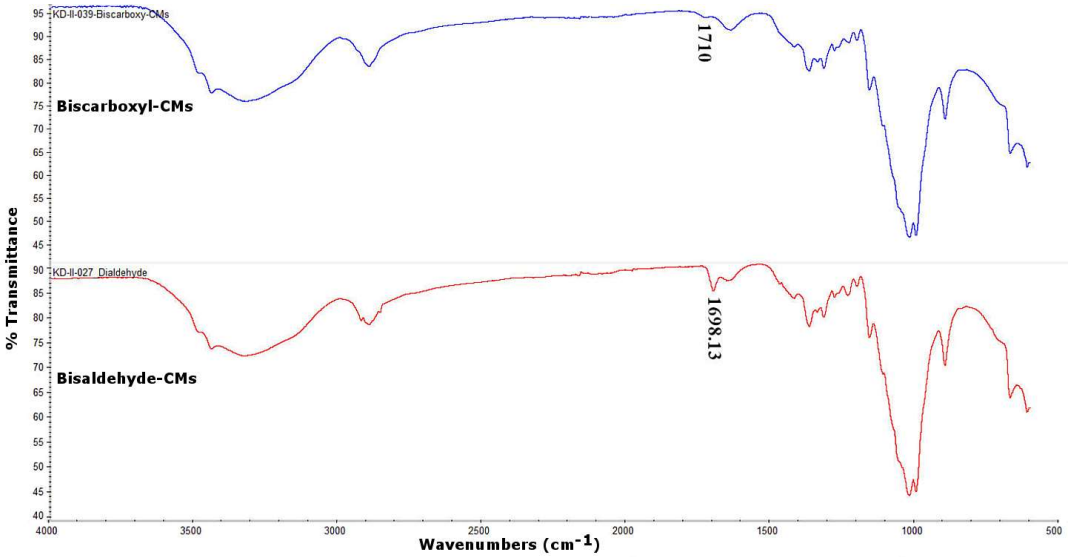

Figure 3.22. FTIR spectra of biscarboxyl-CMs (upper spectrum) and bisaldehyde-CMs (lower spectrum).

3.4.6 Preparation of Carboxyl-CMs

In order to obtain carboxyl-CMs, studies were conducted towards the oxidation of C6 on the glucose subunits of cellulose. To this end CMs were oxidized using $NaClO_2$, NaClO, and TEMPO (Scheme 3.8).[82] Formation of carboxyl functional group was confirmed via FTIR (Figure 3.23) as a new peak appearing at 1731 cm^{-1}. Carboxyl group concentration was determined by titration as 0.367 mmol/g.

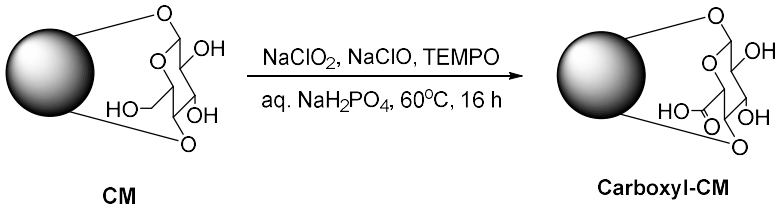

Scheme 3.8. Preparation of carboxyl-CMs from CMs through oxidation.

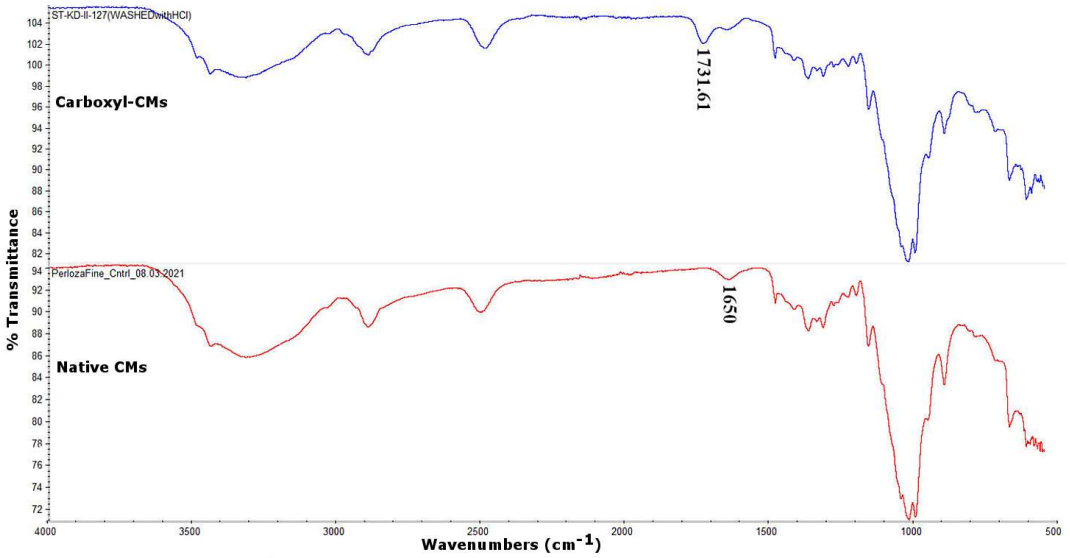

Figure 3.23. FTIR spectra of carboxyl-CMs (upper spectrum) and native CMs (lower spectrum).

3.5 Preparation of BDPA-Ligands

3.5.1 Preparation of BDPA-Acid Ligand 6

BDPA-acid ligand **6** can be used to derivatize amine-CMs. **6** was prepared according to a literature report and the synthetic sequence is summarized in Figure 3.32.[71] Dimethyl-5-hydroxyisophthalate (**1**) was reduced to the corresponding dialcohol (**2**) which was converted to the ether **3** through reaction with ethyl 4-bromobutyrate. **3** was converted through an Appel reaction[83] to the dibromo compound **4**, which in turn was reacted with dipicolylamine to give the BDPA-ester **5**. Basic hydrolysis followed by careful work-up gave the desired BDPA-acid **6**. The identity of all intermediates and final product was confirmed by ^{1}H NMR and HRMS.

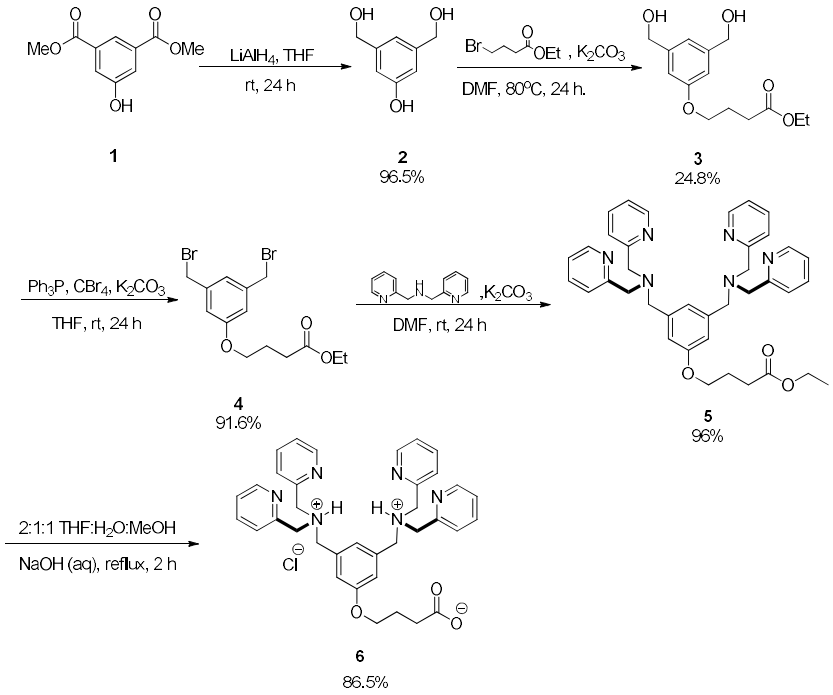

Scheme 3.9. Preparation of BDPA-acid **6**.

3.5.2 Preparation of BDPA-Amine Ligand 10

BDPA-amine ligand **10** can be used to derivatize epoxy-CMs, bisaldehyde-CMs, and carboxyl-CMs. **10** was prepared according to a literature report and the synthetic sequence is summarized in Figure 3.33.[72] Dimethyl-5-hydroxyisophthalate (**1**) was reduced to the corresponding dialcohol (**2**) which was converted to the ether **7** through reaction with N-(4-bromobutyl)phthalimide. **7** was converted through an Appel reaction[83] to the dibromo compound **8**, which in turn was reacted with dipicolylamine to give **9**. Finally, hydrazinolysis gave the desired BDPA-acid **10**. The identity of all intermediates and final product was confirmed by ^{1}H NMR and HRMS.

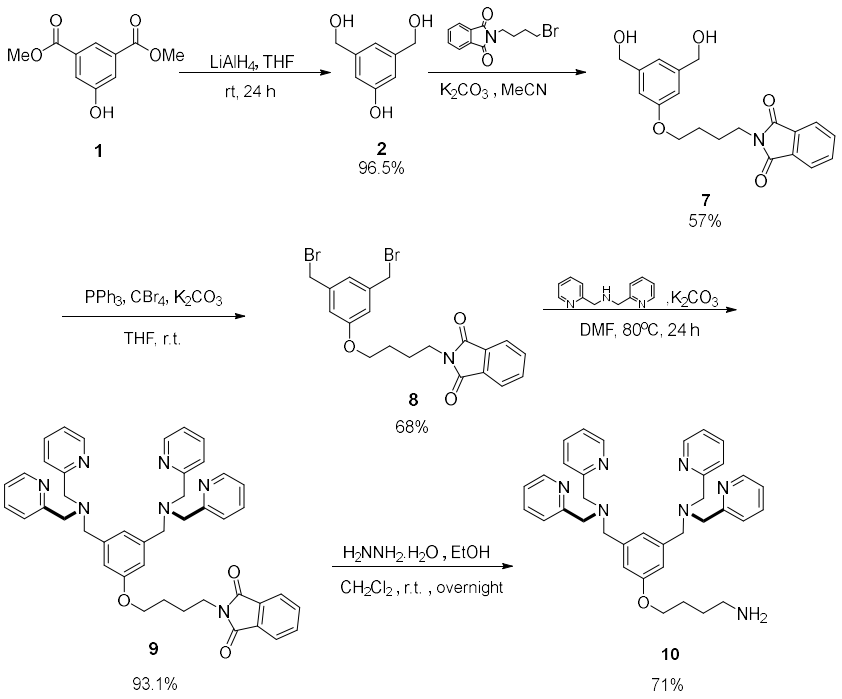

Scheme 3.10. Preparation of BDPA-amine **10**.

3.6 Preparation of BDPA-CMs

3.6.1 Preparation of BDPA-CM-I

BDPA-CM-I was prepared by reacting amine-CMs with pentafluorophenol-activated BDPA-acid **10** (Scheme 3.11).[71] Through CHNS analysis it was estimated that BDPA-CM-I had a BDPA ligand concentration of about 0.123 μmol/g. The FTIR spectrum of BDPA-CM-I exhibits a peak corresponding to the amide carbonyl group at 1654 cm^{-1} and peak at around 766 cm^{-1} is indicative of N-H wag, and sharp peak at around 1570 $cm^{-1}$is indicative of in plane N-H bend. (Figure 3.24).[84]

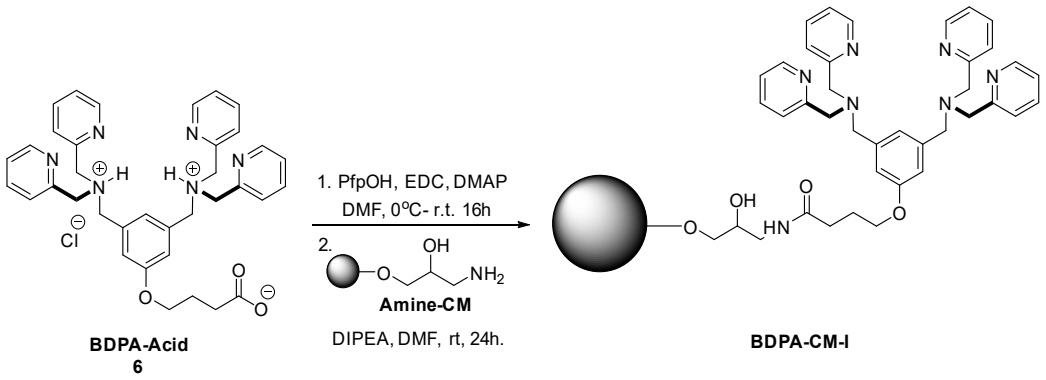

Scheme 3.11. Preparation of BDPA-CM-I.

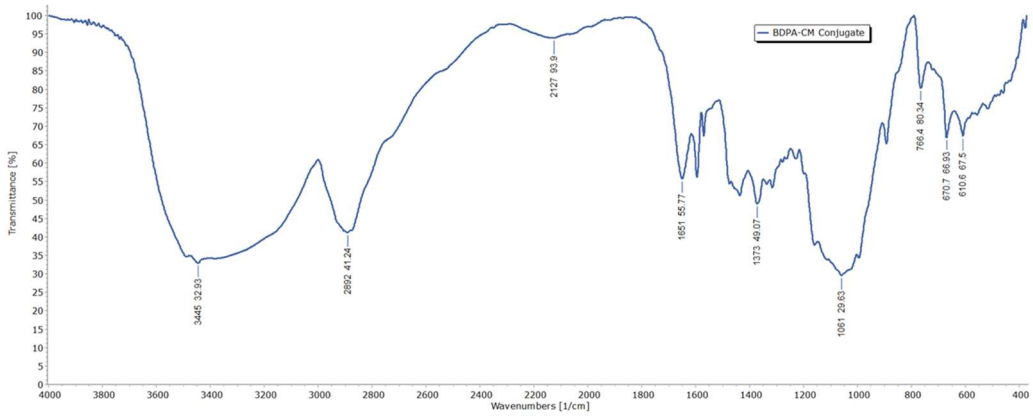

Figure 3.24. FTIR spectrum of BDPA-CM-I.

3.6.2 Preparation of BDPA-CM-II

Bisaldehyde-CM and BDPA-amine ligand **6** were reacted under standard reductive amination conditions to give BDPA-CM-II (Scheme 3.12). Through CHNS analysis it was estimated that BDPA-CM-II had a BDPA ligand concentration of about 0.070 μmol/g. As mentioned before aldehyde peaks in CMs can be observed at 1640 cm^{-1} when hydrated and around 1689 cm^{-1} when dehydrated. After reductive amination, it was observed that this peak disappeared and secondary amine peaks were observed at 758 cm^{-1} for N-H wag, 1157 cm^{-1} for C-N-C asymmetric stretch, and 1593 cm^{-1} for N-H bend (Figure 3.25, upper spectrum).[85]

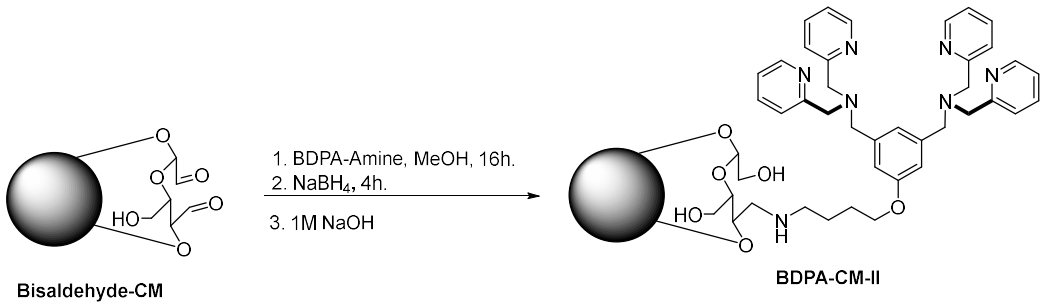

Scheme 3.12. Preparation of BDPA-CM-II.

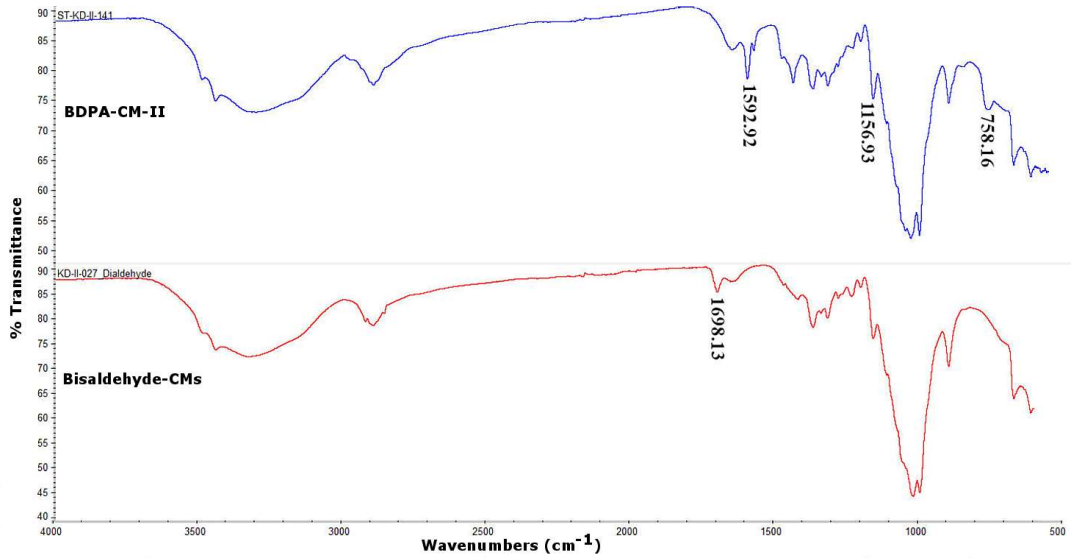

Figure 3.25. FTIR spectra of BDPA-CM-II (upper spectrum) and bisaldehyde-CMs (lower spectrum).

3.6.3 Preparation of BDPA-CM-III

BDPA-CM-III was prepared by reacting BDPA-amine ligand **10** with epoxy-CMs in refluxing acetic acid (Scheme 3.13).[86] Through CHNS analysis it was estimated that BDPA-CM-III had a BDPA ligand concentration of about 0.020 µmol/g. After coupling, secondary amine peaks were observed at 1158 cm^{-1} for C-N-C asymmetric stretch and 1596 cm^{-1} for N-H bend (Figure 3.26, upper spectrum).[85]

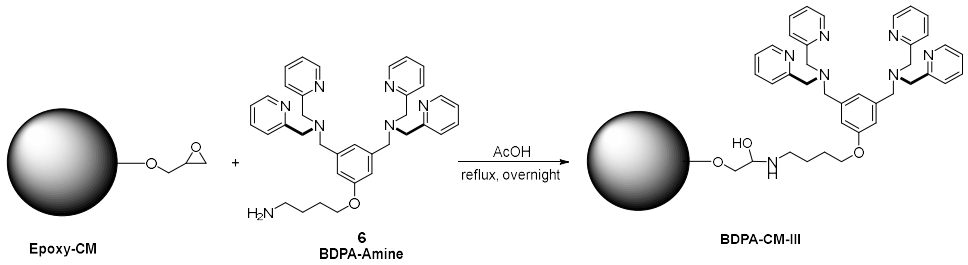

Scheme 3.13. Preparation of BDPA-CM-III.

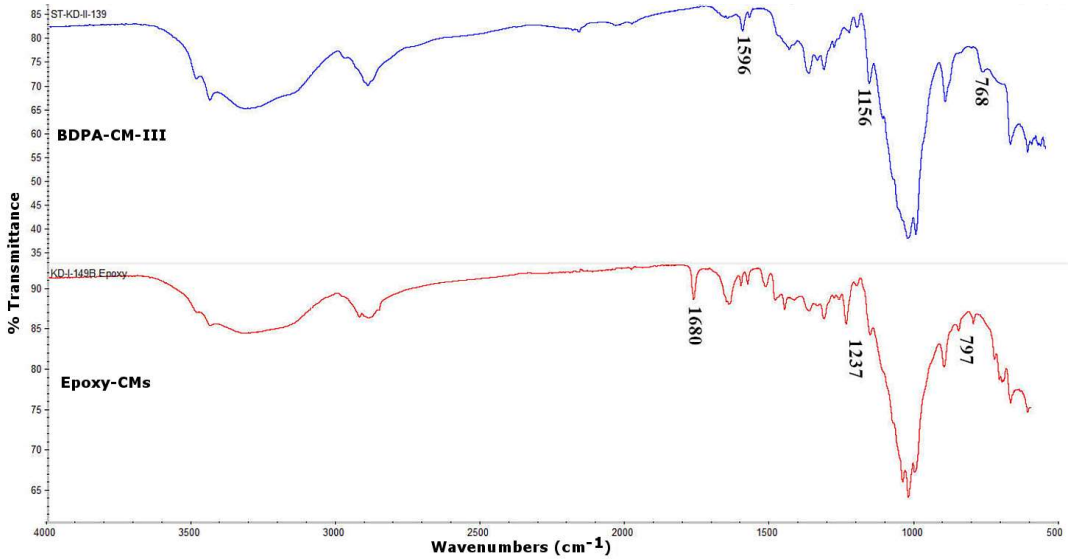

Figure 3.26. FTIR spectra of BDPA-CM-III (upper spectrum) and epoxy-CMs (lower spectrum).

3.7 Investigation of the Affinities of Neutral and Negatively Charged Biomembranes Towards Zn_2BDPA-Complex Bearing CMs

3.7.1 Investigation of the Affinities of Neutral and Negatively Charged Liposomes Towards Various Functionalized Cellulose Microspheres

Liposomes can be used as model membranes to study various biological, biochemical, and biophysical phenomena. In this study, negatively charged liposomes were used as models for bacterial cell membranes and neutral liposomes were used as models for mammalian cell membranes. Investigation of the affinities of these liposomal systems towards various functionalized CMs obtained in this project would then give a measure of their affinities and selectivity towards bacterial cells. The liposomal systems were designed to be fluorescent, thus their sequestration into functionalized CMs could be followed by fluorescence spectroscopy.

3.7.1.1 Liposome Formulation and Preparation

The neutral liposomes used in this study were formulated as DiO/POPC/Cholesterol (2/68/30), where DiO is a lipophilic cyanine dye with a $\lambda_{excitation}$ of 484 nm and a $\lambda_{emission}$ of 501 nm. The negatively charged liposomes used in this study were formulated as DiD/POPG-Na/POPC/Cholesterol (2/10/58/30), where DiD is a lipophilic cyanine dye with a $\lambda_{excitation}$ of 644 nm and a $\lambda_{emission}$ of 663 nm (Figure 3.27). Total lipid concentrations for the stock dispersions of both types of liposomes were 3.32 mM each. The liposomes were prepared through the lipid film hydration/extrusion method, detailed in the experimental section, and summarized in Scheme 3.14. The liposomes obtained were characterized through dynamic light scattering (DLS) and zeta potential measurements. The neutral liposomes had an average diameter of approximately 184 nm and a zeta potential close to zero, whereas the negatively charged liposomes had an average diameter of 145 nm and a zeta potential of -16.7 mV (Figure 3.28).

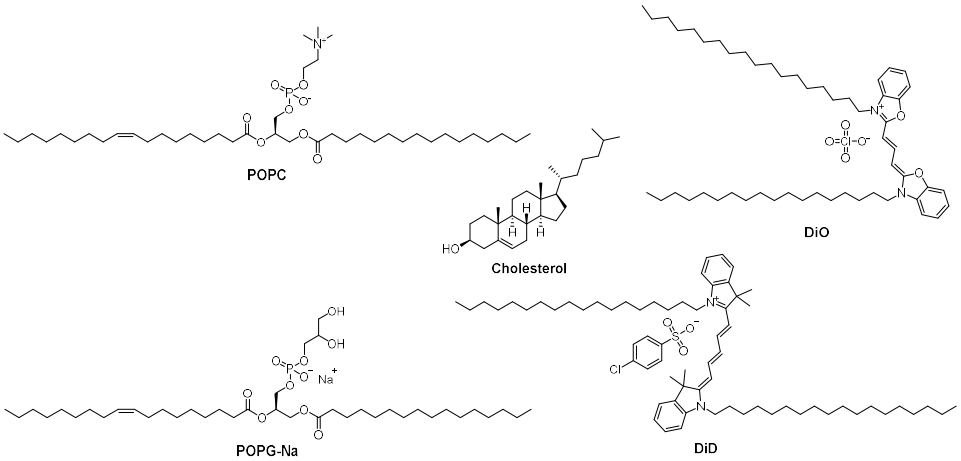

Figure 3.27. Components of the liposomes used in this study.

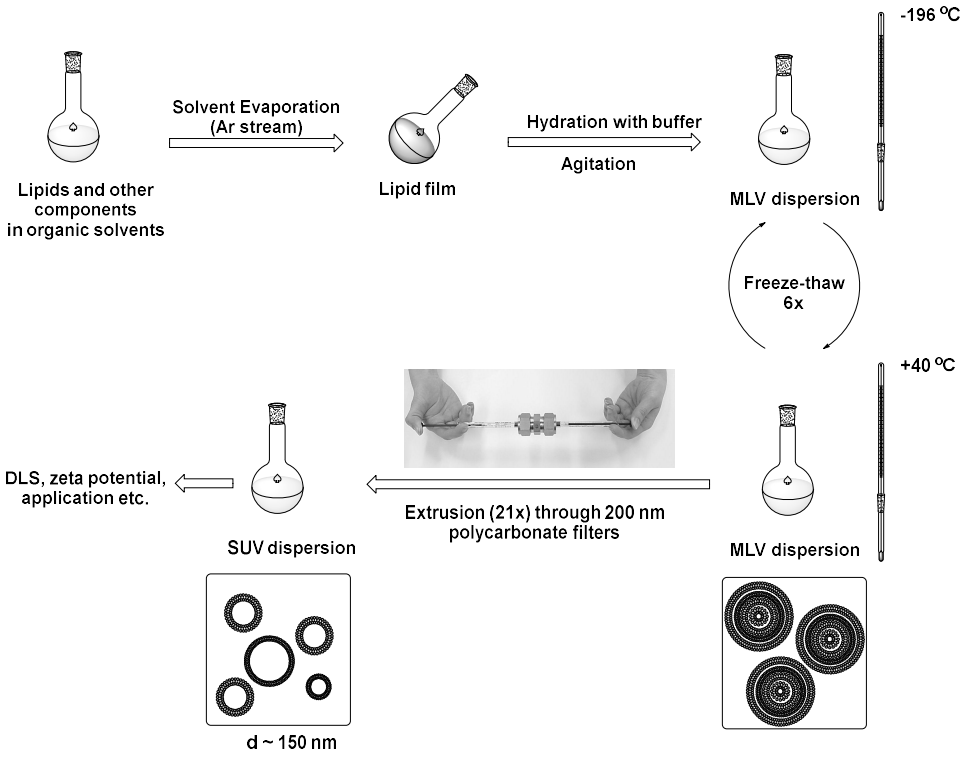

Scheme 3.14. Summary of the process for liposome preparation using the lipid film hydration/extrusion method.

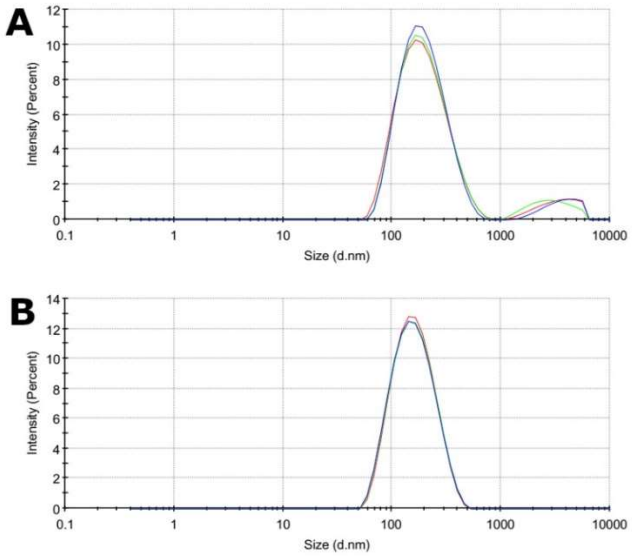

Figure 3.28. Size distribution graphs obtained through dynamic light scattering measurements for neutral (A) and negatively charged (B) liposomes.

3.7.1.2 Calibration Graphs for the Fluorescence of Neutral and Negatively Charged Liposomes

In order to quantify liposome binding affinity and selectivity, it is necessary to construct calibration graphs for the liposomes used in this study. DiO is the lipophilic cyanine dye with a $\lambda_{excitation}$ of 484 nm and a $\lambda_{emission}$ of 501 nm used in the neutral liposomes. DiD is the lipophilic cyanine dye with a $\lambda_{excitation}$ of 644 nm and a $\lambda_{emission}$ of 663 nm used in the negatively charged liposomes. Stock liposomal dispersions were diluted to obtain samples with dye concentrations in the 0.066-0.66 μM range. The fluorescence signal responses for both types of liposomes in this concentration range were found to be linear (Figure 3.29).

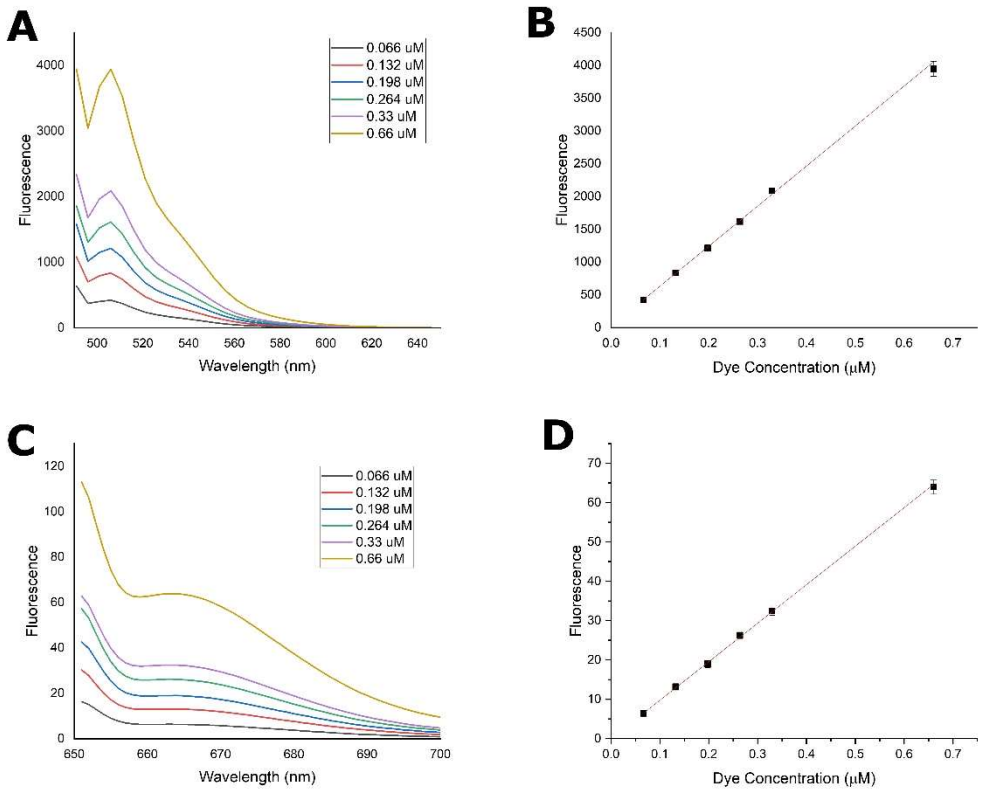

Figure 3.29. Fluorescence spectra and calibration graphs for neutral (Panels A and B) and negatively charged liposomes (Panels C and D) in the 0.066-0.66 μM dye concentration range. For the graph in Panel B: Slope = 6108.70, intercept = 20.74, R^2 = 0.9990. For the graph in Panel D: Slope = 97.96, intercept = -0.0474, R^2 = 0.9996.

3.7.2 Investigation of the Affinities of Neutral and Negatively Charged Liposomes Towards Various Functionalized CMs Through Fluorescence Measurements

The affinities of neutral and negatively charged liposomes towards BDPA-CM-I, BDPA-CM-II, BDPA-CM-III and their respective control BDPA-amine, BDPA-aldehyde, BDPA-epoxide were investigated. To this end functionalized CMs were added to 0.132 μM dye containing liposomal dispersions, incubated, and the supernatants were decanted. The fluorescence intensities of the supernatants at the respective $\lambda_{emission}$ were measured. Fluorescence emissions were normalized. The difference between the original dispersions and the supernatants gave the affinities

and selectivities of the interactions between the liposomes and the functionalized CMs. The results of these experiments are summarized in Figure 3.30.

None of the functionalized CMs had a significant affinity towards neutral liposomes (Figure 3.30, Panel A). BDPA-CM-I and BDPA-CM-III had significantly higher affinities towards negatively charged liposomes compared to their controls, amine-CM and epoxy-CM (Figure 3.30, Panel B). This is due to the interactions between the Zn_2BDPA complexes present on the surfaces of BDPA-CM-I and BDPA-CM-III with the negatively charged phosphate groups of the POPG present in the negatively charged liposome. The control liposomes lack these complexes and thus this mode of interaction with negatively charged liposomes. While BDPA-CM-II had an apparently larger affinity towards negatively charged liposomes compared to its control bisaldehyde-CM, the difference was not statistically significant. This may be due to too low a BPDA ligand concentration in these CMs.

BDPA-CM-I and BDPA-CM-III adsorbed roughly 20% of the negatively charged liposomes in dispersions at 0.132 μM dye (6.6 μM total lipid) concentration while the adsorption of negatively charged liposomes at the same concentration onto their respective controls, amine-CM and epoxy-CM, was not statistically significant. The fact that adsorption of neutral liposomes onto BDPA-CM-I and BDPA-CM-III is not statistically significant whereas adsorption of negatively charged liposomes is statistically significant indicates clear selectivity of these BDPA-CMs towards negatively charged liposomes. BDPA-CM-I and BDPA-CM-III adsorbed similar amounts of liposomes despite having different total BDPA ligand concentrations, indicating that only surface adsorption that is interaction of liposomes with surface-exposed BDPA ligands only plays a significant role in the adsorption process. This would be rational as these CMs are not very porous.

Assuming that the negatively charged liposomes have an average diameter of 144 nm this would correspond to approximately 171000 lipids per liposome.[99] Based on the fluorescence data, the total amount of lipid absorbed onto the BDPA-CMs can be estimated to be 1.06×10^{-10} mol/mg of CM. Therefore, the liposome

binding capacity of BDPA-CMs would be about $3.7x10^8$ liposomes/mg of CM, which would roughly correspond to a binding capacity of 69000 liposomes per single CM particle assuming a CM particle diameter of 62 μm and a bulk cellulose density of 1.5 g/cm^3.

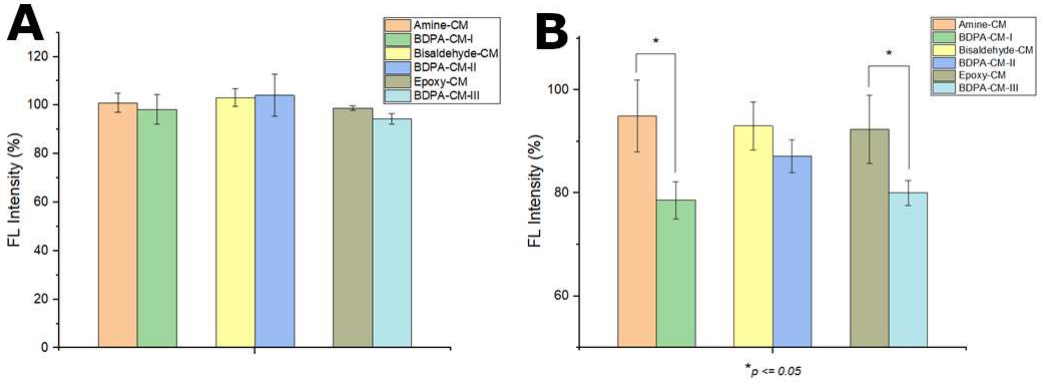

Figure 3.30. Normalized fluorescence intensities for neutral (A) and negatively charged (B) liposomal dispersions after incubation with various functional CMs.

3.7.3 Investigation of the Affinities of Negatively Charged Liposomes Towards Various Functionalized CMs Through Fluorescence Microscopy

The enhanced affinities exhibited by negatively charged liposomes towards BDPA-CM-I and BDPA-CM-III with respect to their controls amine-CMs and epoxy-CMs were further confirmed by fluorescence spectroscopy. After incubation with negatively liposomes the CMs were washed with buffer and examined using brightfield and fluorescence (TX-2 filter) microscopy. The micrographs for BDPA-CM-I and amine-CM are given in Figure 3.31. Comparing the fluorescence micrographs in Panels B and D it is clear that BDPA-CM-I have a much higher affinity towards the negatively charged liposomes compared to amine-CMs. Fluorescence microscopy also revealed that BDPA derivatization among CMs is not uniform, as evidenced by the variation in fluorescence intensities of individual CMs in micrograph D. Similar conclusions can be drawn from the micrographs in Figure 3.33, which are of BDPA-CM-III and epoxy-CMs. Fluorescence spectroscopy

measurements revealed that BDPA-CM-II did not have a statistically significant higher affinity towards negatively charged liposomes compared to their control bisaldehyde-CMs. This observation is confirmed by the fluorescence micrographs in Figure 3.32, where there is no significant difference in fluorescence between panels B and D. Studies are presently underway to improve the BDPA ligand density on BDPA-CM-II.

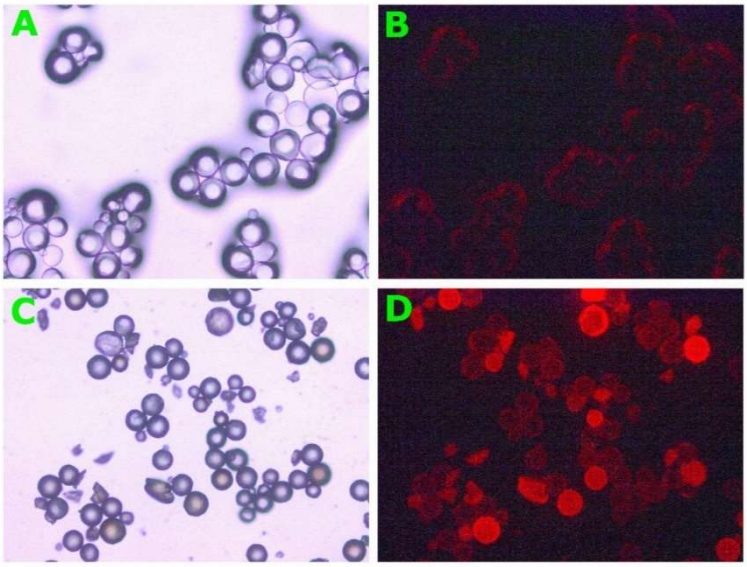

Figure 3.31. Brightfield micrographs (10x) of amine-CM (A) and BDPA-CM-I (C) and fluorescence micrographs (10x, TX-2 filter) of amine-CM (B) and BDPA-CM-I (D) after treatment with negatively charged liposomes and washing.

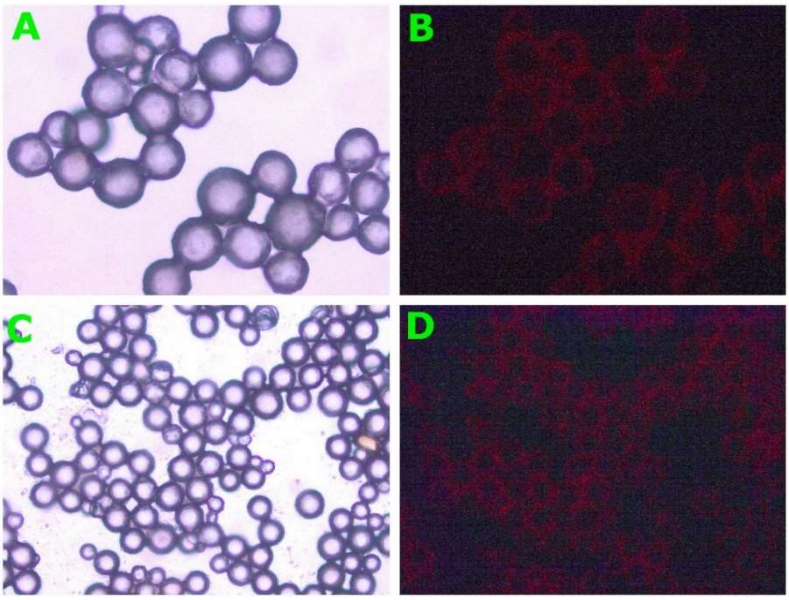

Figure 3.32. Brightfield micrographs of (40x) bisaldehyde-CM (A) and (10x) BDPA-CM-II (C) and fluorescence micrographs of (40x, TX-2 filter) bisaldehyde-CM (B) and (10x, TX-2 filter) BDPA-CM-II (D) after treatment with negatively charged liposomes and washing.

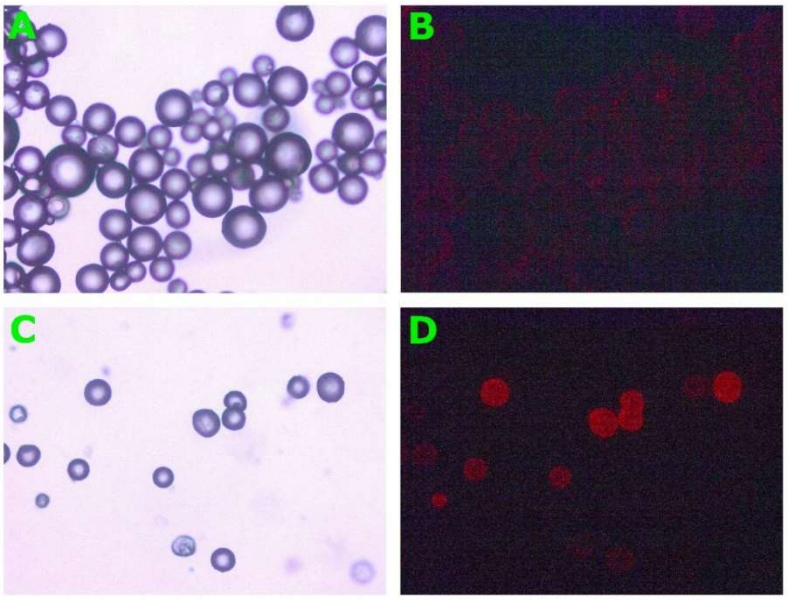

Figure 3.33. Brightfield micrographs (10x) of epoxy-CM (A) and BDPA-CM-III (C) and fluorescence micrographs (10x, TX-2 filter) of epoxy-CM (B) and BDPA-CM-III (D) after treatment with negatively charged liposomes and washing.

3.7.4 Investigation of the Affinities of *Escherichia coli* Cells to Various Functionalized Cellulose Microspheres

The affinity of negatively charged liposomes towards BDPA-CMs provided an impetus to investigate the potential affinity of bacterial cells towards BDPA-CMs. To this end the interaction between GFP-expressing *Escherichia coli* (K12 pSB1C3-GFP) and various functional CMs was investigated using fluorescence microscopy. Aliquots of 5 mg each of the six functional CMs were mixed with 250 μL 10^6 CFU/mL dispersions of *E. coli* cells, incubated, washed, and the CMs were examined using fluorescence microscopy (GFP filter). Brightfield and fluorescence micrographs for BDPA-CM-I and its control amine-CMs are given in Figure 3.34. It is evident that amine-CMs have some affinity towards bacterial cells. Based on the fluorescence intensity the affinity of BDPA-CM-I towards bacterial cells seems to be significantly higher than the control amine-CMs. Considering that the amount of BDPA ligands on BDPA-CM-I is not very high, this level of bacteria binding can be regarded as a testament to the high affinity of Zn_2BDPA complexes towards phosphate containing negatively charged biomembranes.

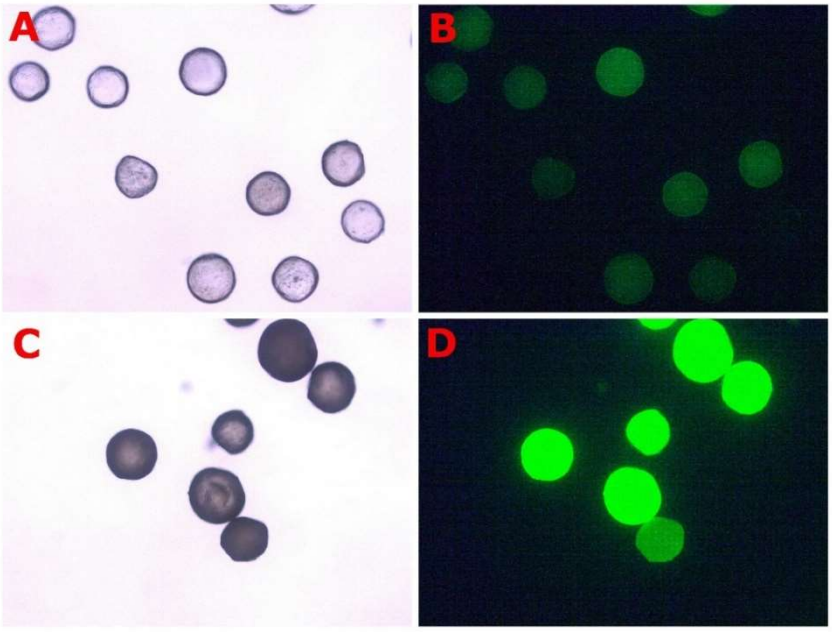

Figure 3.34. Brightfield micrographs (10x) of amine-CM (A) and BDPA-CM-I (C) and fluorescence micrographs (10x, GFP filter) of amine-CM (B) and BDPA-CM-I (D) after treatment with GFP-expressing *E. coli* cells and washing.

Surprisingly BDPA-CM-II, which did not have a significantly higher affinity towards negatively charged liposomes compared to its control bisaldehyde-CMs, exhibited apparently robust binding towards bacterial cells (Figure 3.35, Panel D). The corresponding control bisaldehyde-CMs did not exhibit significant binding of bacterial cells as evidenced in Figure 3.35, Panel B. BDPA-CM-III, as would be expected from the study involving negatively charged liposomes, also exhibited an affinity towards bacterial cells as evidenced in the fluorescence micrograph displayed on Panel D of Figure 3.36. The corresponding control epoxy-CMs, however, did not exhibit significant binding of bacterial cells as evidenced in Figure 3.36, Panel B.

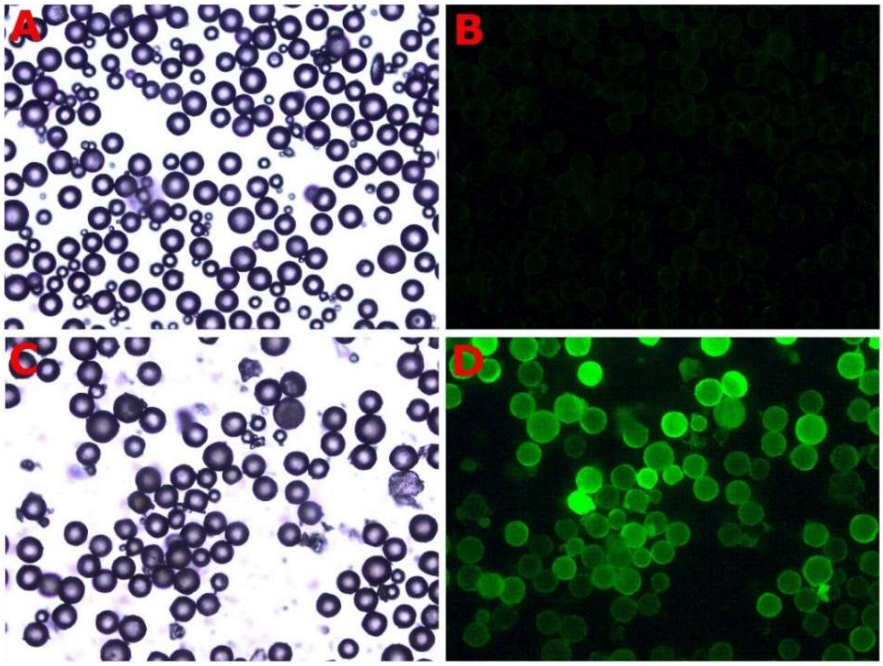

Figure 3.35. Brightfield micrographs (10x) of bisaldehyde-CM (A) and BDPA-CM-II (C) and fluorescence micrographs (10x, GFP filter) of bisaldehyde-CM (B) and BDPA-CM-II (D) after treatment with GFP-expressing *E. coli* cells and washing.

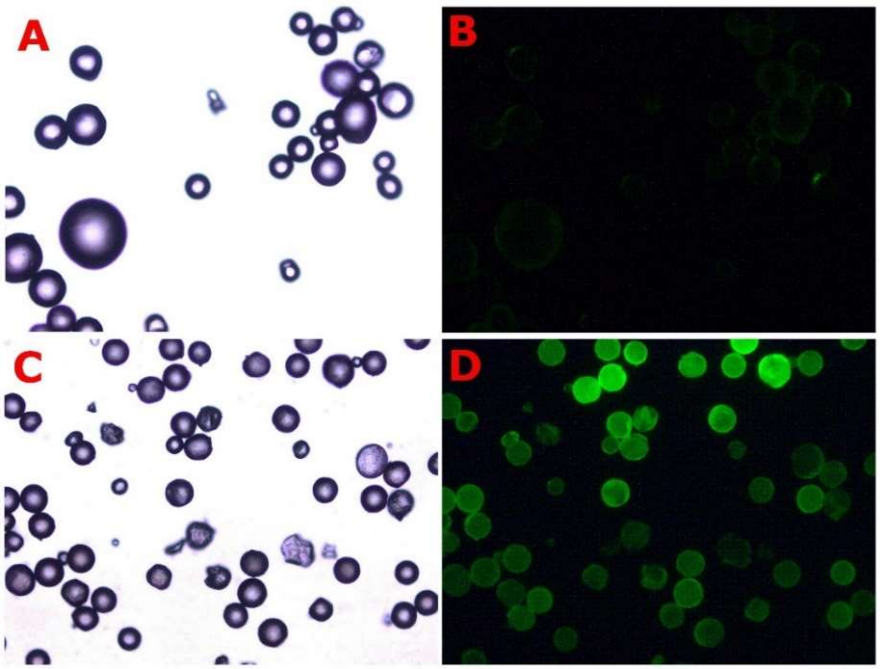

Figure 3.36. Brightfield micrographs (10x) of epoxy-CM (A) and BDPA-CM-III (C) and fluorescence micrographs (10x, GFP filter) of epoxy-CM (B) and BDPA-CM-III (D) after treatment with GFP-expressing *E. coli* cells and washing.

CHAPTER 4

CONCLUSION

In this study a method has been developed for the preparation of viscose solutions from cotton and for the size-controlled production of cellulose microspheres (CMs) based on formation of water-in-oil emulsions of viscose solutions followed by thermal cellulose regeneration. Factors that affect CM size have been identified as viscose droplet size, quantity of surfactant (Span 80), type of surfactant, rotor speed (rpm), and rotor size. CMs with diameters in the 40-700 μm range have been prepared using the method developed in this study and characterized. CMs have been activated with a variety of functional groups including epoxy, amino, cyano, aldehyde, and carboxylic acid groups. Three different BDPA-CM conjugates have been prepared using a variety of chemistries: Pentafluorophenol activation of BDPA-acid (6) followed by reaction with amine-CMs gave BDPA-CM-I, reductive amination of bisaldehyde-CMs with BDPA-amine (10) gave BDPA-CM-II, and reaction of BDPA-amine (10) and epoxy-CMs gave BDPA-CM-III. Formation of these conjugates was confirmed using CHNS and FTIR analysis. The BDPA content of these CMs was found as 0.123 μmol/g, 0.070 μmol/g and 0.020 μmol/g respectively for BDPA-CM-I, BDPA-CM-II, and BDPA-CM-III. Fluorescence spectroscopy and microscopy was used to demonstrate that BDPA-CM-I and BDPA-CM-III were capable of binding significantly more negatively charged liposomes compared to their control amine-CMs and epoxy-CMs. Fluorescence spectroscopy also demonstrated that while BDPA-CM-I and BDPA-CM-III had an affinity towards negatively charged liposomes, they did not bind significantly to neutral liposomes. Finally, fluorescence microscopy was used to demonstrate that BDPA-CM-I, BDPA-CM-II, and BDPA-CM-III were capable of binding to GFP-expressing Escherichia coli cells whereas their respective controls had little or no binding capability to these cells.

Clinical diagnosis of bacteremia, apart from the symptoms displayed by the patients, involves culturing blood to isolate pathogenic bacterial cells, identification of the isolated strains of bacteria, and determination of antibiotic susceptibility of these bacterial strains. Diagnosis using this method takes 2-3 days. Antibiotic treatment upon diagnosis may take 2-3 weeks. Patients may be given broad-spectrum antibiotics before diagnosis. A significant portion of bacteremia patients are lost during diagnosis and treatment. The prognosis for bacteremia patients is-and will become increasingly-worse if antibiotic resistant strains are involved. The need for the rapid diagnosis and treatment of bacteremia is self-evident. Sorbents capable of selectively binding to bacterial cells may aid in the diagnosis and treatment of bacteremia. Analytical scale preconcentration of bacterial cells using these sorbents may facilitate bacterial cell culture and also enable strain identification using rapid techniques like PCR and mass spectroscopy. These sorbents may also be used for the treatment of bacteremia through extracorporeal whole blood filtration where bacterial cells are removed from the whole blood of the patient, reducing bacterial cell load, toxin release, and moderating immune response to bacteremia.

In conclusion, selective sorbents for species with negatively charged biomembranes have been developed in this study. Further development of these materials is likely to lead to effective sorbents for bacterial cells which would have applications in the diagnosis and treatment of bacteremia and in the isolation and preconcentration of bacterial cells from a variety of liquid samples. It is conceivable that materials of this nature could also be used for the isolation and preconcentration of other species with negatively charged biomembranes like circulating tumor cells, viruses, and yeasts.

REFERENCES

1) Bennett Jr, I. L.; Beeson, P. B. Bacteremia. *The Yale Journal of Biology and Medicine* **1954**, *26*, 241-262.
2) Madigan, M. T.; Bender, K. S.; Buckley, D. H.; Sattley, W. M.; Stahl, D. A.; Brock, T. D. *Brock Biology of Microorganisms*. Pearson: New York, **2019**.
3) Hogg, S. Microbial Nutrition and Cultivation. In *Essential Microbiology.* John Wiley & Sons: Chichester, UK, **2005,** 79-90.
4) Bebbington, C.; Yarranton. G. Antibodies for the treatment of bacterial infections: current experience and future prospects. *Curr. Opin. Biotechnol*. **2008**, *19*, 613-619.
5) Rice, D. R.; Plaunt, A. J.; Turkyilmaz, S.; Smith, M.; Wang, Y.; Rusckowski, M.; Smith, B. D. Evaluation of [(111)In]-Labeled Zinc-Dipicolylamine Tracers for SPECT Imaging of Bacterial Infection. *Mol. Imaging. Biol.* **2015**, *17*(2), 204-213.
6) White, A.G.; Fu, N.; Leevy, W.M.; Lee, J.J.; Blasco, M.A.; Smith, B.D. Optical imaging of bacterial infection in living mice using deep-red fluorescent squaraine rotaxane probes. *Bioconjugate Chem.* **2010,** *21*, 1297-1304.
7) Xiao, S.; Abu-Esba, L.; Turkyilmaz, S.; White, A. G.; Smith, B. D. Multivalent Dendritic Molecules as Broad Spectrum Bacteria Agglutination Agents. *Theranostics* **2013**, *3*, 658-666.
8) Turkyilmaz, S.; Rice, D.R.; Palumbo, R.; Smith, B.D. Selective recognition of anionic cell membranes using targeted liposomes coated with zinc (ii)-bis (dipicolylamine) affinity units. *Org. Biomol. Chem.* **2014**, *12*, 5645-5655.
9) Lee, J.J.; Jeong, K.J.; Hashimoto, M.; Kwon, A.H.; Rwei, A.; Shankarappa, S.A.; Tsui, J.H.; Kohane, D.S. Synthetic ligandcoated magnetic nanoparticles for microfluidic bacterial separation from blood. *Nano Letters*. **2013**, *14(1)*, 1-5.

10) Smith D.A.; Nehring S.M. *Bacteremia*. StatPearls Publishing: Treasure Island, FL, **2017**.
11) Thomas, D. L. Recovering from sepsis. https://www.news-medical.net/health/Recovering-from-Sepsis.aspx (Accessed 03.08.2021)
12) Pitt, W.G.; Alizadeh, M.; Husseini, G.A.; McClellan, D.S.; Buchanan, C.M.; Bledsoe, C.G.; Robison, R.A.; Blanco, R.; Roeder, B.L.; Melville, M.; Hunter, A.K. Rapid separation of bacteria from blood—review and outlook. *Biotechnology Progress*. 2016, *32*(4), 823-839.
13) Herrmann, I.K.; Schlegel, A.A.; Graf, R.; Stark, W.J.; Beck-Schimmer, B. Magnetic separation-based blood purification: a promising new approach for the removal of disease-causing compounds? *J. Nanobiotechnology*. **2015**, *13*(1), 49.
14) Lattuada, M.; Ren, Q.; Zuber, F.; Galli, M.; Bohmer, N.; Wichser, A.; Bertazzo, S.; Pier, G.B.; Herrmann, I.K. Theranostic body fluid cleansing: rationally designed magnetic particles enable capturing and detection of bacterial pathogens. *J. Mater. Chem. B* **2016**, *4*(44), 7080-7086.
15) Lee, J.J.; Jeong, K.J.; Hashimoto, M.; Kwon, A.H.; Rwei, A.; Shankarappa, S.A.; Tsui, J.H.; Kohane, D.S. Synthetic ligandcoated magnetic nanoparticles for microfluidic bacterial separation from blood. *Nano Lett.* **2013**, *14*(1), 1-5.
16) Aran, K.; Morales, M.; Sasso, L.A.; Lo, J.; Zheng, M.; Johnston, I.; Kamdar, N.; Ündar, A.; Zahn, J.D. Microfiltration device for continuous, label-free bacteria separation from whole blood for sepsis treatment. *15th International Conference on Miniaturized Systems for Chemistry and Life Sciences MicroTas*. **2011,** *1*, 497-499.
17) Mach, A.J.; Di Carlo, D. Continuous scalable blood filtration device using inertial microfluidics. *Biotechnol. and Bioeng.* **2010**, *107*(2), 302-311.
18) Gericke, M.; Trygg, J.; Fardim, P. Functional cellulose beads: preparation, characterization, and applications. *Chem. Rev.* **2013**, *113*(7), 4812-4836.

19) Wang, S.; Yu, Y. Bioactive Bead Type Cellulosic Adsorbent for Blood Purification. In Cellulose - Medical, Pharmaceutical and Electronic Applications; Van De Ven, T. G. M., Ed.; IntechOpen: London, UK, **2013**, pp 195-214.

20) Weber, V.; Ettenauer, M.; Linsberger, I.; Loth, F.; Thümmler, K.; Feldner, A.; Fischer, S.; Falkenhagen, D. Functionalization and application of cellulose microparticles as adsorbents in extracorporeal blood purification. *Macromol. Symp.* **2010**, *294*(2), 90-95.

21) Kong, D.L.; Chen, C.Z.; Lin, E.F.; Yu, Y.T. Clinical trials of type I and in vitro studies of type II immunoadsorbents for systemic lupus erythematosus therapy. *Artificial Organs* **1998**, 22(8), 644-650.

22) Weber, V.; Linsberger, I.; Ettenauer, M.; Loth, F.; Höyhtyä, M.; Falkenhagen, D. Development of specific adsorbents for human tumor necrosis factor-α: Influence of antibody immobilization on performance and biocompatibility. *Biomacromolecules* **2005**, *6*(4), 1864-1870.

23) Trygg, J.; Fardim, P.; Gericke, M.; Mäkilä, E.; Salonen, J. Physicochemical design of the morphology and ultrastructure of cellulose beads. *J. Carbohydr. Polym.* **2013**, *93*(1), 291-299.

24) Sescousse, R.; Gavillon, R.; Budtova, T. Wet and dry highly porous cellulose beads from cellulose–NaOH–water solutions: influence of the preparation conditions on beads shape and encapsulation of inorganic particles. *J. Mater. Sci.* **2011**, *46*(3), 759-765.

25) Karbstein, H.; Schubert, H. Developments in the continuous mechanical production of oil-in-water macro-emulsions. *Chem. Eng. Process.: Process Intensification* **1995**, *34*(3), 205-211.

26) Maggioris, D.; Goulas, A.; Alexopoulos, A. H.; Chatzi, E. G.; Kiparissides, C. Prediction of particle size distribution in suspension polymerization reactors: effect of turbulence nonhomogeneity. *Chem. Eng. Sci.* **2000**, *55*(20), 4611-4627.

27) Klemm, D.; Heublein, B.; Fink, H. P.; Bohn, A. Cellulose: fascinating biopolymer and sustainable raw material. *Angew. Chem. Int. Ed.* **2005**, *44*(22), 3358-3393.

28) Strunk, P. *Characterization of cellulose pulps and the influence of their properties on the process and production of viscose and cellulose ethers* (Doctoral dissertation, Umeå Universitet) **2012**.

29) Zou, H.; Luo, Q.; Zhou, D. Affinity membrane chromatography for the analysis and purification of proteins. *J. Biochem. Bioph. Methods* **2001**, *49*(1-3), 199-240.

30) McCormick, C. L.; Callais, P. A. Derivatization of cellulose in lithium chloride and *N,N*-dimethylacetamide solutions. *Polymer* **1987**, *28*(13), 2317-2323.

31) Rosenberg, P.; Rom, M.; Janicki, J.; Fardim, P. New cellulose beads from biocelsol solution. *Cellul. Chem. Technol.* **2008**, *42*(7), 293-305.

32) Ushikubo, F. Y.; Cunha, R. L. Stability mechanisms of liquid water-in-oil emulsions. *Food Hydrocolloids* **2014**, *34*, 145-153.

33) Needs, A. *The HLB System: A Time-Saving Guide to Emulsifier Selection*; ICI Americas Inc.: Wilmington, DE, **1987**.

34) Bowen, P. Particle size distribution measurement from millimeters to nanometers and from rods to platelets. *J. Dispersion Sci. Technol.* **2002**, *23*(5), 631-662.

35) Thümmler, K.; Fischer, S.; Feldner, A.; Weber, V.; Ettenauer, M.; Loth, F.; Falkenhagen, D. Preparation and characterization of cellulose microspheres. *Cellulose* **2011**, *18*(1), 135-142.

36) Hentschel, M. L.; Page, N. W. Selection of descriptors for particle shape characterization. *Part. Part. Syst. Char*. **2003**, *20*(1), 25-38.

37) Du, K. F.; Yan, M.; Wang, Q. Y.; Song, H. Preparation and characterization of novel macroporous cellulose beads regenerated from ionic liquid for fast chromatography. *J. Chromatogr. A* **2010**, *1217*(8), 1298-1304.

38) Pinnow, M.; Fink, H. P.; Fanter, C.; Kunze, J. Characterization of highly porous materials from cellulose carbamate. *J. Macromol. Symp.* **2008**, *262*(1), 129-139.

39) Xia, H. F.; Lin, D. Q.; Yao, S. J. Preparation and characterization of macroporous cellulose–tungsten carbide composite beads for expanded bed applications. *J. Chromatogr. A* **2007**, *1175*(1), 55-62.

40) Thünemann, A. F.; Klobes, P.; Wieland, C.; Bruzzano, S. On the nanostructure of micrometer-sized cellulose beads. *Anal. Bioanal. Chem.* **2011**, *401*(4), 1101-1108.

41) Ek, R.; Henriksson, U.; Nyström, C.; Ödberg, L. Pore characterization in cellulose beads from diffusion studies using the spin echo NMR technique. *Powder Technol.* **1994**, *81*(3), 279-286.

42) Webber, B. NMR Looks Deep Inside Nooks and Crannies. *Physics* **2012**, 5, 14. DOI: 10.1103/Physics.5.14

43) Kaster, J. A.; de Oliveira, W.; Glasser, W. G.; Velander, W. H. Optimization of pressure-flow limits, strength, intraparticle transport and dynamic capacity by hydrogel solids content and bead size in cellulose immunosorbents. *J. Chromatogr. A* **1993**, *648*(1), 79-90.

44) Anderson, R. L.; Owens, J. W.; Timms, C. W. The toxicity of purified cellulose in studies with laboratory animals. *Cancer Lett*. **1992**, *63*(2), 83-92.

45) Fang, H.; Wei, J.; Yu, Y. In vivo studies of endotoxin removal by lysine–cellulose adsorbents. *Biomaterials* **2004**, *25*(23), 5433-5440.

46) Gough, B. M. Interaction of wheat starch and epichlorohydrin. *Starch (Stärke)* **1967**, *19*(8), 240-243.

47) Štamberg, J. Bead cellulose. *J. Sep. Purif. Method.* **1988**, *17*(2), 155-183.

48) Tahiri, C.; Vignon, M. R. TEMPO-oxidation of cellulose: Synthesis and characterisation of polyglucuronans. *Cellulose* **2000**, *7*(2), 177-188.

49) Oliveira, W. D.; Glasser, W. G. Hydrogels from polysaccharides. I. Cellulose beads for chromatographic support. *J. Appl. Polym. Sci.* **1996**, *60*(1), 63-73.

50) Gemeiner, P.; Polakovič, M.; Mislovičová, D.; Štefuca, V. Cellulose as a (bio) affinity carrier: properties, design and applications. *J. Chromatogr. B: Biomedical Sciences and Applications* **1998**, *715*(1), 245-271.

51) Vincent, P.; Compoint, J. P.; Fitton, V.; Santarelli, X. Evaluation of Matrex cellufine GH 25. *J. Biochem. Biophys. Methods* **2003**, *56*(1-3), 69-78.

52) Denizli, A.; Pişkin, E. Dye-ligand affinity systems. *J. Biochem. Biophys. Methods* **2001**, *49*(1-3), 391-416.

53) Sharma, R. K.; Agrawal, M.; Marshall, F. Heavy metal contamination of soil and vegetables in suburban areas of Varanasi, India. *Ecotox. Environ. Safety* **2007**, *66*(2), 258-266.

54) Peška, J.; Štamberg, J.; Hradil, J. Chemical transformations of polymers. XIX. Ion exchange derivatives of bead cellulose. *Angewandte Makromolekulare Chemie* **1976**, *53* (1), 73–80.

55) Matejka, Z.; Stamberg J.; Benes, M. J. Ion Exchange Sorbents. *React. Polym.* **1984**, *3*, 33-36.

56) Hirota, M.; Tamura, N.; Saito, T.; Isogai, A. Surface carboxylation of porous regenerated cellulose beads by 4-acetamide-TEMPO/NaClO/$NaClO_2$ system. *Cellulose* **2009**, *16*(5), 841-851.

57) Chesney, A.; Barnwell, P.; Stonehouse, D. F.; Steel, P. G. Amino-derivatised beaded cellulose gels. Novel accessible and biodegradable scavenger resins for solution phase combinatorial synthesis. *Green Chem.* **2000**, *2*(2), 57-62.

58) Englebretsen, D. R.; Harding, D. R. Solid phase peptide synthesis on hydrophilic supports: Part II-Studies using Perloza beaded cellulose. *Int. J. Pept. Prot. Res.* **1992**, *40*(6), 487-496.

59) Englebretsen, D. R.; Harding, D. R. Fmoe SPPS using Perloza™ beaded cellulose. *Int. J. Pept. Prot. Res.* **1994**, *43*(6), 546-554.

60) Chesney, A.; Steel, P. G.; Stonehouse, D. F. High loading cellulose based poly (alkenyl) resins for resin capture applications in halogenation reactions. *J. Comb. Chem.* **2000**, *2*(5), 434-437.

61) Balaxi, M.; Nikolakakis, I.; Malamataris, S. Preparation of porous microcrystalline cellulose pellets by freeze-drying: Effects of wetting liquid and initial freezing conditions. *J. Pharm. Sci.* **2010**, *99*(4), 2104-2113.

62) Volkert, B.; Wolf, B.; Fischer, S.; Li, N.; Lou, C. Application of modified bead cellulose as a carrier of active ingredients. *Macromol. Symp.* **2009**, *280*(1), 130-135.

63) Still, W.C.; Kahn, M.; Mitra, A. Rapid chromatographic technique for preparative separations with moderate resolution. *J. Org. Chem.* **1978**, *43* (14), 2923–2925.

64) ASTM International. *D4243-16 Standard Test Method for Measurement of Average Viscometric Degree of Polymerization of New and Aged Electrical Papers and Boards*. West Conshohocken, PA; ASTM International, **2016**. DOI: https://doi.org/10.1520/D4243-16.

65) Kes, M.; Christensen, B. E. A re-investigation of the Mark–Houwink–Sakurada parameters for cellulose in Cuen: a study based on size-exclusion chromatography combined with multi-angle light scattering and viscometry. *J. Chromatogr. A* **2013**, *1281*, 32-37.

66) Luo, X.; Zhang, L. Creation of Regenerated Cellulose Microspheres with Diameter Ranging from Micron to Millimeter for Chromatography Applications. *J. Chromatogr. A* **2010**, *1217* (38), 5922–5929.

67) Ettenauer, M.; Loth, F.; Thümmler, K.; Fischer, S.; Weber, V.; Falkenhagen, D. Characterization and functionalization of cellulose microbeads for extracorporeal blood purification. *Cellulose* **2011**, *18*(5), 1257-1263.

68) Zhang, L.; Zhang, S.; Dong, F.; Cai, W.; Shan, J.; Zhang, X.; Man, S. Antioxidant activity and in vitro digestibility of dialdehyde starches as influenced by their physical and structural properties. *Food Chemistry* **2014**, *149*, 296-301.

69) Kim, U. J.; Kuga, S. Ion-exchange chromatography by dicarboxyl cellulose gel. *J. Chromatogr. A* **2001**, *919*(1), 29-37.

70) Isogai, A.; Saito, T.; Fukuzumi, H. TEMPO-oxidized cellulose nanofibers. *Nanoscale* **2011**, *3*(1), 71-85.

71) Turkyilmaz, S.; Rice, D. R.; Palumbo, R.; Smith, B. D. Selective recognition of anionic cell membranes using targeted liposomes coated with zinc (ii)-bis (dipicolylamine) affinity units. *Org. Biomol. Chem*. **2014**, *12*(30), 5645-5655.

72) Lakshmi, C.; Hanshaw, R. G.; Smith, B. D. Fluorophore-linked zinc (II) dipicolylamine coordination complexes as sensors for phosphatidylserine-containing membranes. *Tetrahedron* **2004**, *60*(49), 11307-11315.

73) Kes, M.; Christensen, B. E. A re-investigation of the Mark–Houwink–Sakurada parameters for cellulose in Cuen: a study based on size-exclusion chromatography combined with multi-angle light scattering and viscometry. *J. Chromatogr. A* **2013**, *1281*, 32-37.

74) Hamzavi, S. F.; Gerivani, S.; Saeedi, S.; Naghdipari, K.; Shahverdizadeh, G. Preparation and characterization of a novel spherical cellulose–copper (II) oxide composite particles: as a heterogeneous catalyst for the click reaction. *Molecular Diversity* **2020**, *24*(1), 201-209.

75) Wang, D. M.; Hao, G.; Shi, Q. H.; Sun, Y. Fabrication and characterization of superporous cellulose bead for high-speed protein chromatography. *J. Chromatogr. A* **2007**, *1146*(1), 32-40.

76) Sundberg, L.; Porath, J. Preparation of adsorbents for biospecific affinity chromatography: I. Attachment of group-containing ligands to insoluble polymers by means of bifunctional oxiranes. *J. Chromatogr. A* **1974**, *90*(1), 87-98.

77) Yamamoto, M.; Izuhara, Y.; Kakuta, T.; Takizawa, S.; Fujita, A.; Higaki, T.; Miyata, T. Carbonyl stress reduction in peritoneal dialysis fluid: development of a novel high-affinity adsorption bead. *Peritoneal Dialysis International* **2007**, *27*(3), 300-308.

78) Draman, S. F. S.; Daik, R.; El-Sheikh, S. M.; Latif, F. A. Nanocomposites of cellulose-based adhesive and toluenesulfonic acid-doped polypyrrole

prepared via colloidal dispersion. *Journal of Reinforced Plastics and Composites* **2013**, *32*(20), 1553-1560.

79) Zhou, J.; Li, Q.; Song, Y.; Zhang, L.; Lin, X. A Facile Method for the Homogeneous Synthesis of Cyanoethyl Cellulose in Naoh/Urea Aqueous Solutions. *Polymer Chemistry* **2010**, *1*(10), 1662-1668.

80) Dawy, M.; A-AMA Nada. IR and dielectric analysis of cellulose and its derivatives. *Polymer-Plastics Technology and Engineering* **2003**, *42*(4), 643-658.

81) Spedding, H. 628. Infrared Spectra of Periodate-Oxidised Cellulose. *Journal of the Chemical Society (Resumed)* **1960**, 3147-3152.

82) Habibi, Y.; Chanzy, H.; Vignon, M. R. TEMPO-mediated surface oxidation of cellulose whiskers. *Cellulose* **2006**, *13*(6), 679-687.

83) Appel, R. Tertiary Phosphane/Tetrachloromethane, a Versatile Reagent for Chlorination, Dehydration, and P-N Linkage. *Angew. Chem. Int. Ed. Eng.* **1975**, *14*(12), 801-811.

84) Smith, B. C. Organic Nitrogen Compounds, VII: Amides-The Rest of the Story. *Spectroscopy Online.* **2020**. https://www.spectroscopyonline.com/view/organic-nitrogen-compounds-vii-amides-rest-story (Accessed 03.08.2021)

85) Smith, B. C. Organic Nitrogen Compounds III: Secondary and Tertiary Amines. *Spectroscopy Online.* **2019**. https://www.spectroscopyonline.com/view/organic-nitrogen-compounds-iii-secondary-and-tertiary-amines (Accessed 03.08.2021)

86) Li, D.; Wang, J.; Yu, S.; Ye, S.; Zou, W.; Zhang, H.; Chen, J. Highly regioselective ring-opening of epoxides with amines: a metal-and solvent-free protocol for the synthesis of β-amino alcohols. *Chem. Commun.* **2020**, *56*(15), 2256-2259.

87) Milla, C. E. Antibody-based antibacterial agents: An emerging option. *Drugs Future* **2012**, *37*, 33-43.

88) Fox, J. L. Anthrax drug first antibacterial mAb to win approval. *Nat. Biotechnol.* **2013**, *31*, 8.

89) Johnson, G. A., Muthukrishnan, N., Pellois, J. P. Photoinactivation of Gram Positive and Gram Negative Bacteria with the Antimicrobial Peptide (KLAKLAK)(2) Conjugated to the Hydrophilic Photosensitizer Eosin Y. *Bioconjug. Chem.* **2013**, *24 (1)*, 114-23.

90) Sharon, N. Carbohydrates as future anti-adhesion drugs for infectious diseases. *Biochim. Biophys. Acta.* **2006**, *1760*, 527-537.

91) Kell, A. J.; Stewart, G.; Ryan, S.; Peytavi, R.; Boissinot, M.; Huletsky, A.; Bergeron, M. G.; Simard, B. Vancomycin-modified nanoparticles for efficient targeting and preconcentration of Gram-positive and Gram-negative bacteria. *ACS Nano* **2008**, 2, 1777-88.

92) Hamblin, M. R.; O'Donnell, D. A.; Rajagopalan, K.; Michaud, N.; Sherwood, M. E.; Hasan, T. Polycationic photosensitiser conjugates: Effects of chain length and gram classification on the photodynamic inactivation of bacteria. *Journal of Antimicrobial Chemotherapy* **2002**, *49*, 941–951.

93) Helander, I. M.; Halakomi, H. L.; Latva-Kala, K.; Koski, P. Polyethyleneimine is an efficient permeabilizer of gram-negative bacteria. *Microbiology* **1997**, *143*, 3193–3199.

94) Clear, K. J.; Smith, B. D. Synthetic Receptors for Polar Lipids. In *Synthetic Receptors for Biomolecules: Design Principles and Applications.* Smith, B. D., Ed.; Royal Society of Chemistry: Cambridge, UK, **2015**; pp 404-436.

95) Leevy, W. M.; Johnson, J. R.; Lakshmi, C.; Morris, J.; Marquez, M.; Smith, B. D. Selective recognition of bacterial membranes by zinc(II)-coordination complexes. *Chem. Commun.* **2006**, 1595-1597.

96) Ribeiro, M.; Domingues M.; Freire, J.; Santos N.; Castanho M. Translocating the blood-brain barrier using electrostatics. *Frontiers in Cellular Neuroscience* **2012**, *6*, 44. DOI: 10.3389/fncel.2012.00044.

97) Soni, K. A.; Balasubramanian, A. K.; Beskok, A.; Pillai, S. D. Zeta potential of selected bacteria in drinking water when dead, starved, or exposed to minimal and rich culture media. *Current Microbiology* **2008**, *56(1)*, 93-97.
98) Fernandes, H. P.; Cesar, C. L.; de Lourdes Barjas-Castro, M. Electrical properties of the red blood cell membrane and immunohematological investigation. *Rev. Bras. Hematol. Hemoter.* **2011**, *33(4)*, 297-301.
99) Mozafari, M.R.; Mazaheri, E.; Dormiani, K. Simple Equations Pertaining to the Particle Number and Surface Area of Metallic, Polymeric, Lipidic and Vesicular Nanocarriers. *Sci. Pharm.* **2021**, *89*, 15.

APPENDICES

A. ^{1}H NMR Spectra

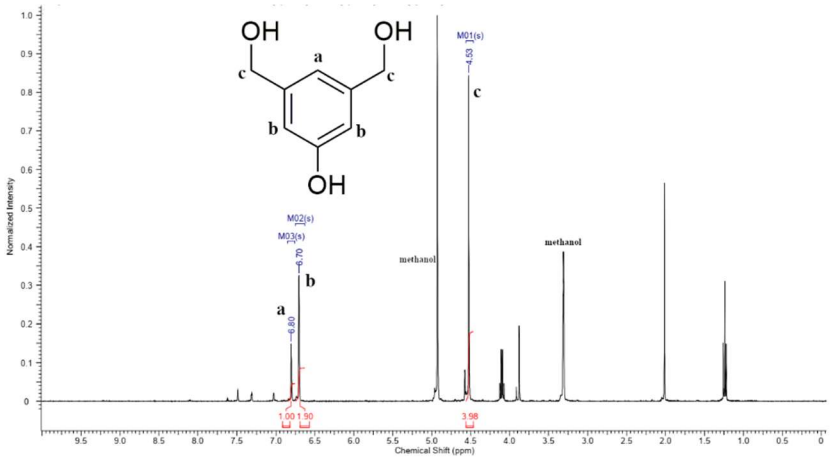

Figure 6.1. ^{1}H NMR spectrum of compound **2**.

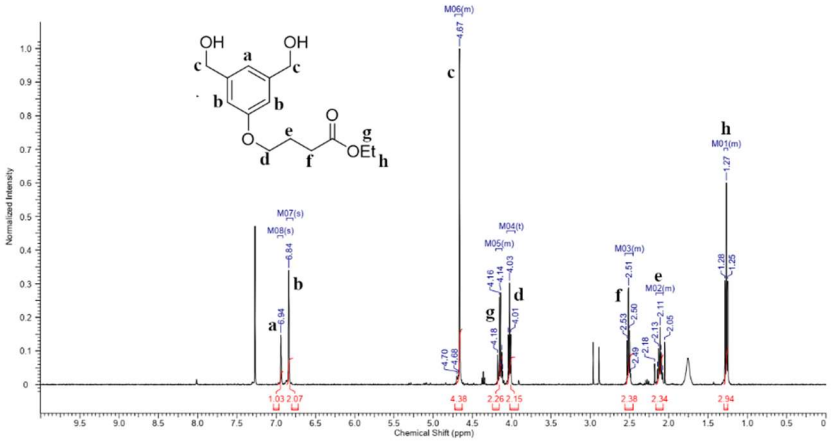

Figure 6.2. ^{1}H NMR spectrum of compound **3**.

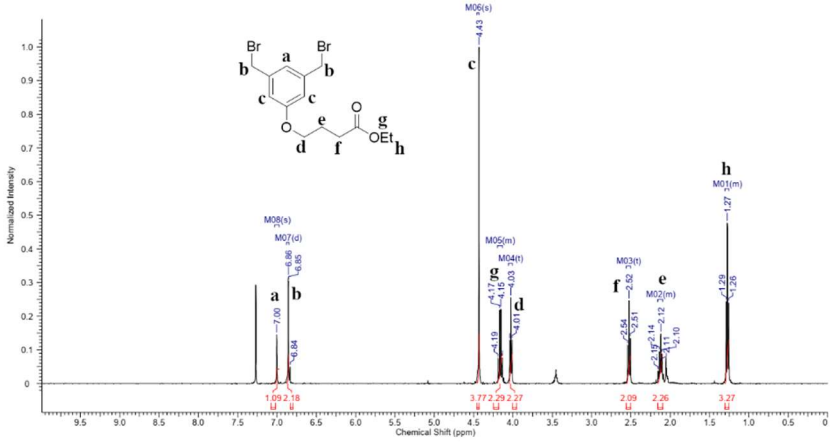

Figure 6.3. ^{1}H NMR spectrum of compound **4**.

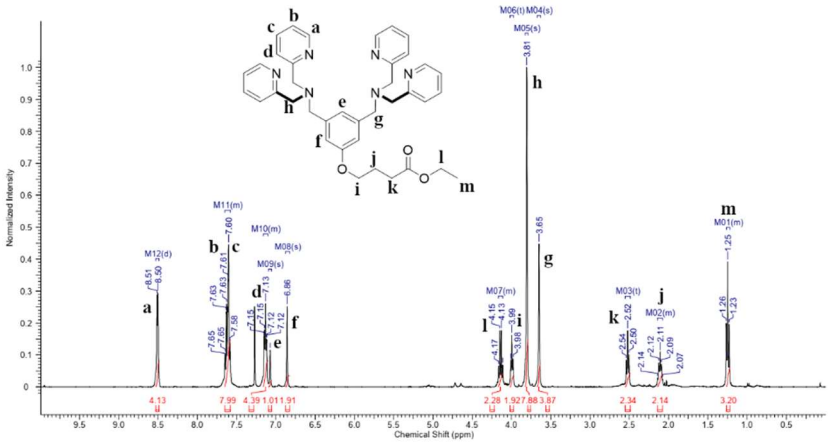

Figure 6.4. ^{1}H NMR spectrum of compound **5**.

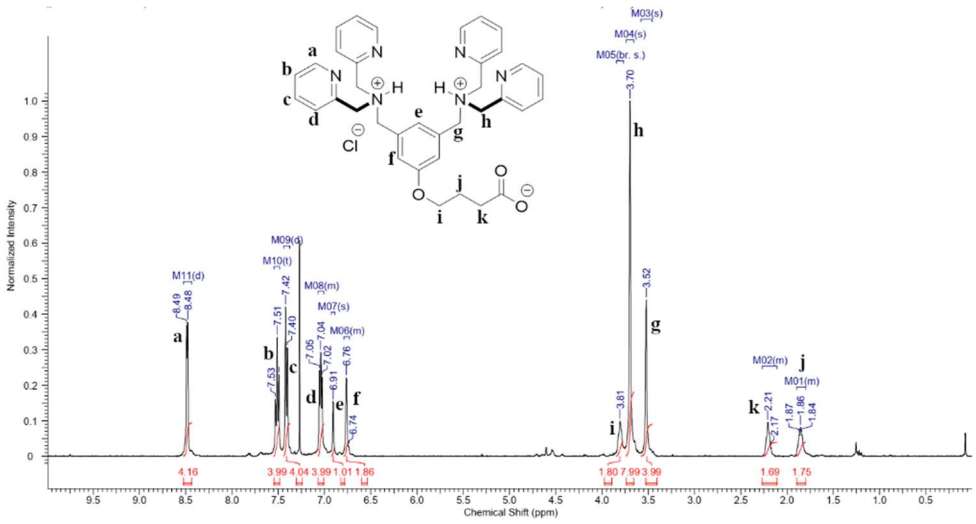

Figure 6.5. ^{1}H NMR spectrum of BDPA-acid **6**.

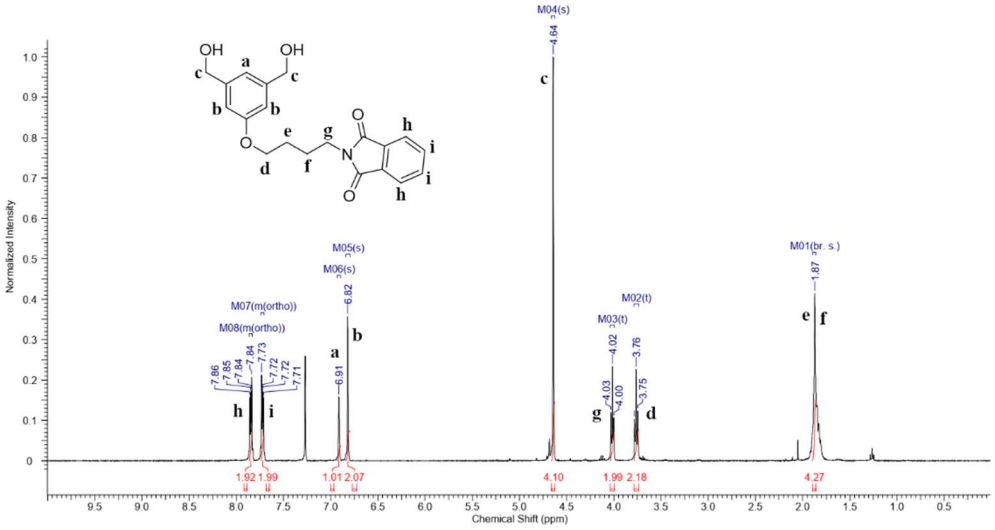

Figure 6.6. ^{1}H NMR spectrum of compound **7**.

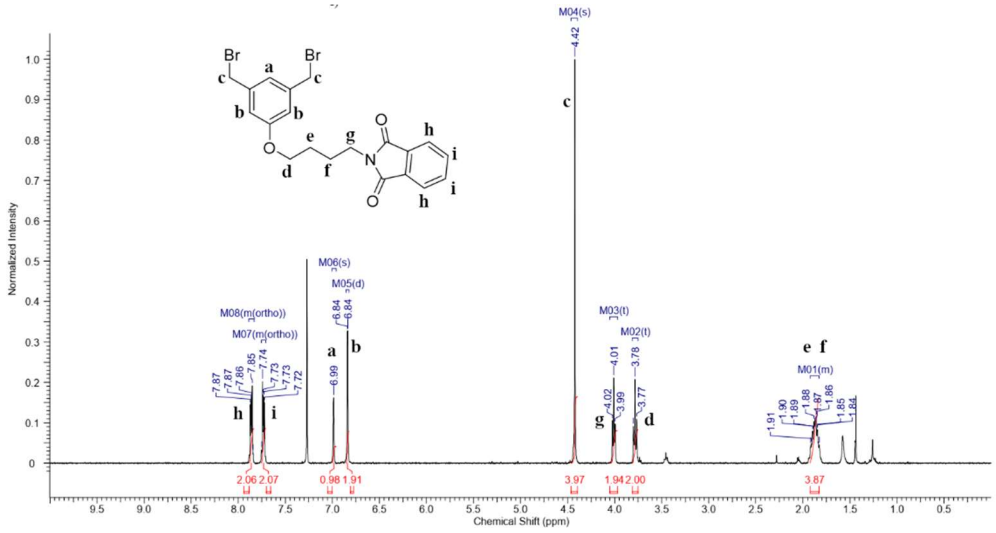

Figure 6.7. [1]H NMR spectrum of compound **8**.

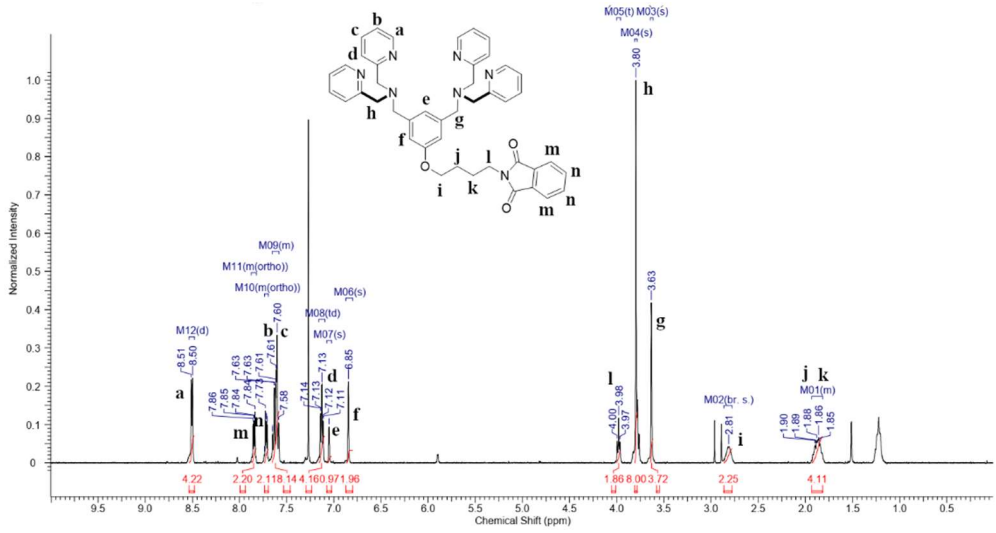

Figure 6.8. [1]H NMR spectrum of compound **9**.

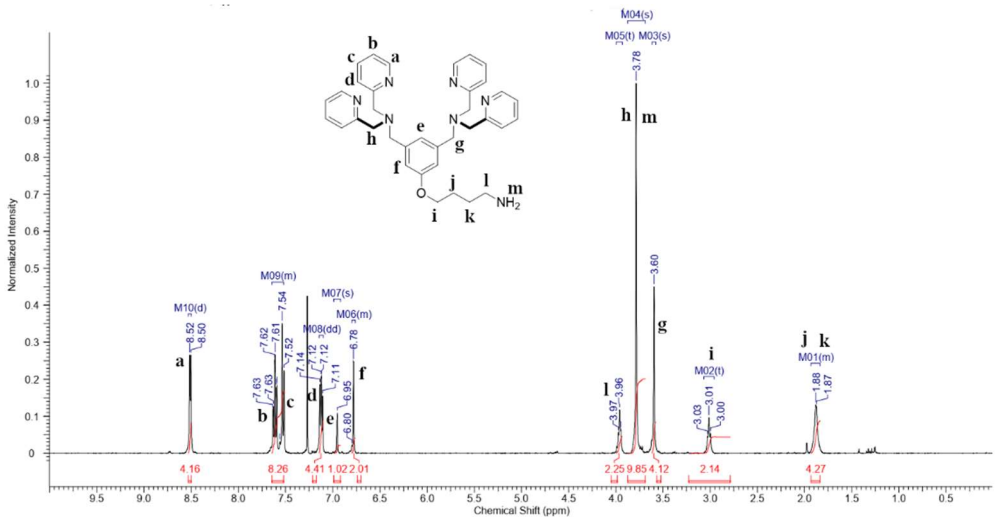

Figure 6.9. ^{1}H NMR spectrum of BDPA-amine **10**.

B. High-Resolution Mass Spectra

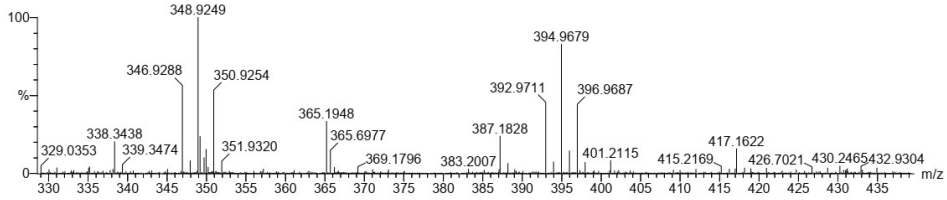

Minimum: -5.5
Maximum: 1000.0 5000.0 1000.0

Mass	Calc. Mass	mDa	PPM	DBE	i-FIT	i-FIT (Norm)	Formula
394.9679	394.9680	-0.1	-0.3	4.5	406.6	0.0	C14 H19 O3 79Br 81Br

Figure 6.10. High-resolution mass spectrum of compound **4**.

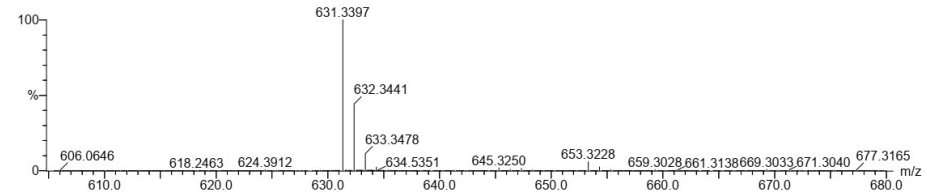

Minimum: -5.5
Maximum: 1000.0 5000.0 1000.0

Mass	Calc. Mass	mDa	PPM	DBE	i-FIT	i-FIT (Norm)	Formula
631.3397	631.3397	0.0	0.0	20.5	575.6	0.0	C38 H43 N6 O3

Figure 6.11. High-resolution mass spectrum of compound **5**.

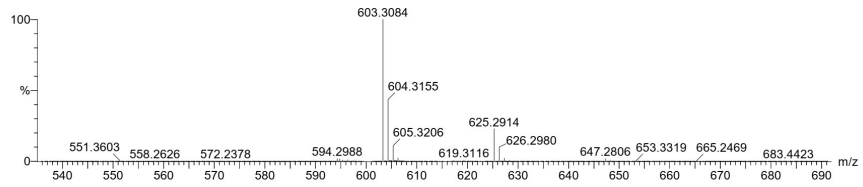

Minimum: -5.5
Maximum: 1000.0 5000.0 1000.0

Mass	Calc. Mass	mDa	PPM	DBE	i-FIT	i-FIT (Norm)	Formula
603.3084	603.3084	0.0	0.0	20.5	575.8	0.0	C36 H39 N6 O3

Figure 6.12. High-resolution mass spectrum of BDPA-acid **6**.

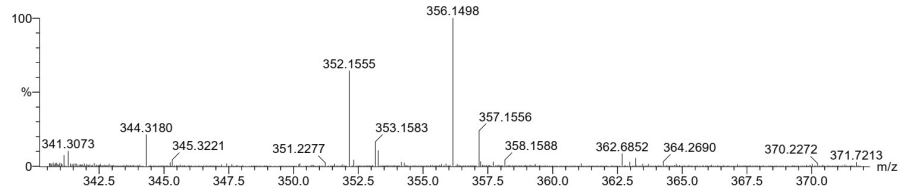

Minimum:				-5.5			
Maximum:		1000.0	5000.0	1000.0			
Mass	Calc. Mass	mDa	PPM	DBE	i-FIT	i-FIT (Norm)	Formula
356.1498	356.1498	0.0	0.0	10.5	304.4	0.0	C20 H22 N O5

Figure 6.13. High-resolution mass spectrum of compound **7**.

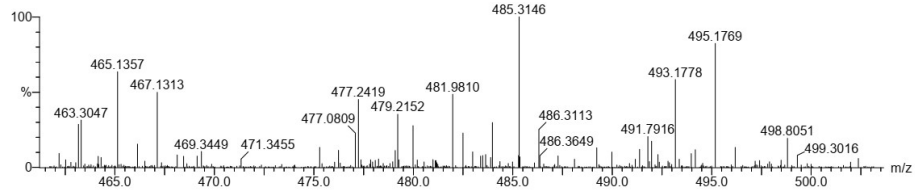

Minimum:				-5.5			
Maximum:		1000.0	5000.0	1000.0			
Mass	Calc. Mass	mDa	PPM	DBE	i-FIT	i-FIT (Norm)	Formula
481.9810	481.9789	2.1	4.4	10.5	186.8	0.0	C20 H20 N O3 79Br 81Br

Figure 6.14. High-resolution mass spectrum of compound **8**.

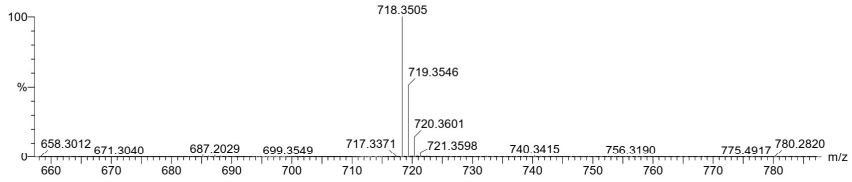

Minimum:				-5.5			
Maximum:		1000.0	5000.0	1000.0			
Mass	Calc. Mass	mDa	PPM	DBE	i-FIT	i-FIT (Norm)	Formula
718.3505	718.3506	-0.1	-0.1	26.5	532.6	0.0	C44 H44 N7 O3

Figure 6.15. High-resolution mass spectrum of compound **9**.

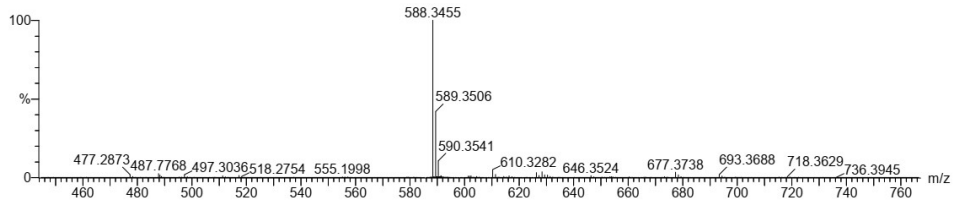

Minimum:				-5.5			
Maximum:		1000.0	5000.0	1000.0			
Mass	Calc. Mass	mDa	PPM	DBE	i-FIT	i-FIT (Norm)	Formula
588.3455	588.3451	0.4	0.7	19.5	460.5	0.0	C36 H42 N7 O

Figure 6.16. High-resolution mass spectrum of BDPA-amine **10**.